



National Library
of Canada

Bibliothèque nationale
du Canada

Canadian Theses Service

Service des thèses canadiennes

Ottawa, Canada
K1A 0N4

NOTICE

The quality of this microform is heavily dependent upon the quality of the original thesis submitted for microfilming. Every effort has been made to ensure the highest quality of reproduction possible.

If pages are missing, contact the university which granted the degree.

Some pages may have indistinct print especially if the original pages were typed with a poor typewriter ribbon or if the university sent us an inferior photocopy.

Previously copyrighted materials (journal articles, published tests, etc.) are not filmed.

Reproduction in full or in part of this microform is governed by the Canadian Copyright Act, R.S.C. 1970, c. C.30.

AVIS

La qualité de cette microforme dépend grandement de la qualité de la thèse soumise au microfilmage. Nous avons tout fait pour assurer une qualité supérieure de reproduction.

Si manque des pages, veuillez communiquer avec l'université qui a conféré le grade.

La qualité d'impression de certaines pages peut laisser à désirer, surtout si les pages originales ont été dactylographiées à l'aide d'un ruban usé ou si l'université nous a fait parvenir une photocopie de qualité inférieure.

Les documents qui font déjà l'objet d'un droit d'auteur (articles de revue, tests publiés, etc.) ne sont pas microfilmés.

La reproduction, même partielle, de cette microforme est soumise à la Loi canadienne sur le droit d'auteur, R.S.C. 1970, c. C.30.

THE UNIVERSITY OF ALBERTA

SEDIMENTATION AND DIAGENESIS OF THE UPPER DEVONIAN KAKISA
FORMATION, TROUT RIVER AREA, N. W. T.

by

DONALD JAMES FYVIE

A THESIS

SUBMITTED TO THE FACULTY OF GRADUATE STUDIES AND RESEARCH
IN PARTIAL FULFILMENT OF THE REQUIREMENTS FOR THE DEGREE
OF MASTER OF SCIENCE

DEPARTMENT OF GEOLOGY

EDMONTON, ALBERTA

SPRING 1988

Permission has been granted to the National Library of Canada to microfilm this thesis and to lend or sell copies of the film.

The author (copyright owner) has reserved other publication rights, and neither the thesis nor extensive extracts from it may be printed or otherwise reproduced without his/her written permission.

L'autorisation a été accordée à la Bibliothèque nationale du Canada de microfilmer cette thèse et de prêter ou de vendre des exemplaires du film.

L'auteur (titulaire du droit d'auteur) se réserve les autres droits de publication; ni la thèse ni de longs extraits de celle-ci ne doivent être imprimés ou autrement reproduits sans son autorisation écrite.

ISBN 0 315-42890 2

THE UNIVERSITY OF ALBERTA

RELEASE FORM

NAME OF AUTHOR DONALD JAMES FYVIE
 TITLE OF THESIS SEDIMENTATION AND DIAGENESIS OF THE
 UPPER DEVONIAN KAKISA FORMATION,
 TROUT RIVER AREA, N. W. T.

DEGREE FOR WHICH THESIS WAS PRESENTED MASTER OF SCIENCE
 YEAR THIS DEGREE GRANTED SPRING 1988

Permission is hereby granted to THE UNIVERSITY OF ALBERTA LIBRARY to reproduce single copies of this thesis and to lend or sell such copies for private, scholarly or scientific research purposes only.

The author reserves other publication rights, and neither the thesis nor extensive extracts from it may be printed or otherwise reproduced without the author's written permission.

(SIGNED) *D. J. Fyvie*

PERMANENT ADDRESS:

*1111 17th St SW
 Calgary, Alberta
 T2T 0A2*

DATED *April 11* 1988

THE UNIVERSITY OF ALBERTA
FACULTY OF GRADUATE STUDIES AND RESEARCH

The undersigned certify that they have read, and recommend to the Faculty of Graduate Studies and Research, for acceptance, a thesis entitled SEDIMENTATION AND DIAGENESIS OF THE UPPER DEVONIAN KAKISA FORMATION, TROUT RIVER AREA, N. W. T. submitted by DONALD JAMES FYVIE in partial fulfilment of the requirements for the degree of MASTER OF SCIENCE.

.....
Supervisor

C. Stelck
.....

~~.....~~
.....

Joseph A. Allan
.....

Date..... *April 11, 1988*

ABSTRACT

The Kakisa Formation, which represents an overall shallowing-upward sequence, was deposited on a depositional margin near the edge of the north northwest-south southeast trending Great Slave Shelf margin during latest Frasnian time. In the Trout River area the Kakisa Formation can be divided into four informal members designated, from bottom to top, A, B, C, and D.

Members A and B are characterized by storm-influenced shelf slope sedimentation. Three shallowing-upward sequences comprise member A while member B is formed of a single deepening-upward sequence. Several small reef mounds occur in the basal part of member B. These grew on an irregular, thin debris flow deposit.

The lower part of member C is formed of an irregular, relatively thick debris flow deposit. This deposit was laid down on the shelf slope. It was overlain by the carbonate bank deposits which form the upper part of member C.

Most of member D was deposited in the restricted lagoon that existed above the member C carbonate bank. Isolated patch reefs grew in this lagoon. The lagoonal deposits are capped by a thin paleosol.

Deposition of the debris deposits that occur at the bases of members B and C significantly modified the depositional regime of the Kakisa Formation. These deposits

were also significant precursors for reef growth. The sudden shallowing and stable substrate they provided promoted reef growth. The type of reef growth that occurred can be related to the thickness of the underlying, precursor debris flow deposit.

The Kakisa Formation underwent a complex diagenetic history which was strongly influenced by eustatic sea level fluctuations. This history included the following events: 1) syndepositional cementation by isopachous calcite in the sea floor diagenetic environment, 2) formation of a paleosol and solution-enlarged vertical fractures in the meteoric diagenetic environment following a relative drop in sea level, 3) precipitation of unzoned blocky, syntaxial rim, and zoned blocky calcite cements in the meteoric environment, and 4) anhedral and saddle dolomite precipitation and pressure solution in the burial diagenetic environment following the resubmergence (which resulted from a relative rise in sea level) and subsequent burial of the Kakisa Formation.

Hydrocarbon migration accompanied pressure solution. However, by this time virtually all of the porosity and permeability in the Kakisa Formation had been destroyed.

ACKNOWLEDGEMENTS

I express my heartfelt thanks to my supervisor, Dr. Brian Jones, for his patience and informed guidance throughout the duration of the study. His encouragement was instrumental in the successful completion of this thesis.

I am indebted to Drs. A. E. H. Pedder (corals), S. G. Pemberton (trace fossils), and C. Singh (palynomorphs) for their aid in fossil identification. Thanks also to B. J. R. Barnett for her excellent work on the figures.

My appreciation is extended to my fellow graduate students, Drs. Q. H. Goodbody, P. S. Mortensen, and F. W. Nentwich, for their valued technical feedback and to Leni Honsaker and Elsie Tsang for their office support. I also acknowledge the members of my thesis committee, Drs. B. D. E. Chatterton, J. S. Nelson, and C. R. Stelck, for their constructive criticisms.

The field work and research for this thesis were funded by grants from the American Association of Petroleum Geologists, the Boreal Institute for Northern Studies, and the Natural Sciences and Engineering Research Council of Canada (Grant number A6090 awarded to Dr. B. Jones). I offer my sincere thanks to these three organizations.

Finally, I would like to acknowledge my parents for their dedication and constant encouragement and Cindy Soderberg for her understanding and support.

Table of Contents

Chapter	Page
I: INTRODUCTION	1
A. PURPOSE OF STUDY	1
B. LOCATION OF STUDY AREA	2
C. METHOD OF STUDY	2
D. STRATIGRAPHY	4
E. PALEOGEOGRAPHY	7
F. PREVIOUS STUDIES	8
G. TERMINOLOGY	9
Introduction	9
Classification Systems	9
Sedimentologic Terms	10
II. SEDIMENTATION	12
A. INTRODUCTION	12
B. MEMBER A	14
Introduction	14
Facies A1: Argillaceous mudstone	14
Facies A2: Nodular bioclastic wackestone	15
Facies A3: Laminated bioclastic wackestone lenses	18
Interrelationship Between Facies	19
Interpretation	20
C. MEMBER B	28
Introduction	28
Facies B1: Coral/echinoderm rudstone	28
Facies B2: Coral bioherms	30
Facies B3: Coral bafflestone patches	30

Facies B4: Nodular bioclastic wackestone32
Facies B5: Argillaceous mudstone33
Facies B6: Laminated bioclastic wackestone lenses33
Interrelationship Between Facies34
Interpretation35
D. MEMBER C44
Introduction44
Facies C1: Coral bafflestone blocks44
Facies C2: Bedded coral/echinoderm rudstone	.45
Facies C3: Argillaceous mudstone47
Facies C4: Massive coral bioherms47
Facies C5: Coral bafflestone48
Facies C6: Coral/stromatoporoid bindstone	...49
Facies C7: Massive coral bindstone50
Facies C8: Tabular stromatoporoid framestone50
Facies C9: Medium grained quartzarenite52
Interrelationship Between Facies53
Interpretation57
E. MEMBER D68
Introduction68
Facies D1: Mottled bioclastic wackestone68
Facies D2: Stromatoporoid/coral bioherms69
Facies D3: Calcareous claystone70
Interrelationship Between Facies71
Interpretation71
F. DEPOSITIONAL HISTORY73

Introduction	73
Depositional Framework	73
Succession of Events	77
Debris Flow Deposition	79
III. DIAGENESIS	82
A. INTRODUCTION	82
B. FRACTURING	83
Introduction	83
Fractures	84
C. SOLUTION	86
Introduction	86
Chemical Dissolution	86
Pressure Solution	88
D. CEMENTATION	90
Introduction	90
Isopachous Calcite Cement	90
Unzoned Blocky Calcite Cement	92
Zoned Blocky Calcite Cement	93
Syntaxial Rim Cement	96
Saddle Dolomite Cement	98
E. REPLACEMENT	100
Introduction	100
Anhedral Dolomite	100
F. DIAGENETIC HISTORY	102
Introduction	102
Diagenetic Framework	103
Succession of Events	103

IV. SUMMARY AND CONCLUSIONS 107
PLATES 110
REFERENCES CITED 131

List of Figures

Figure		Page
1	Location map.....	3
2	Stratigraphic nomenclature in the southwestern N. W. T.	5
3	Schematic type section of the Kakisa Formation.	13
4	Illustration of the eustatic and autocyclic models of cyclic sedimentation.	25
5	Schematic diagram illustrating the facies and lithologic interrelationships in member B.	31
6	Schematic diagram of the facies and lithologic interrelationships in the lower part of member C.	54
7	Schematic facies diagram illustrating the main depositional environments of the Kakisa Formation.	76
8	Flow diagram illustrating the sequence of diagenetic events and environments.	85

List of Plates

Plate	Page
1 Sedimentation: member A	112
2 Sedimentation: members A and B	114
3 Sedimentation: member B	116
4 Sedimentation: member C	118
5 Sedimentation: member C	120
6 Sedimentation: member C	122
7 Sedimentation: member C	124
8 Sedimentation: member D	126
9 Diagenesis: member C ..	128
10 Diagenesis: members A, B, and C ..	130

1. INTRODUCTION

A. PURPOSE OF STUDY

Upper Devonian carbonate sequences contain some of the largest hydrocarbon reservoirs in western Canada. Sedimentary facies and diagenesis are two major influences on the localization and extent of these reservoirs. As a result, sedimentologic and diagenetic studies of Upper Devonian carbonate sequences are of vital importance to the petroleum geologist because these studies can be used to help pinpoint hydrocarbon reservoirs, determine their extent, and predict their lateral continuity.

This study will concentrate on the sedimentation and diagenesis of the Upper Devonian Kakisa Formation. The primary objectives of the study are to: 1) identify and describe the major sedimentologic units that form the Kakisa Formation, 2) determine the depositional environments in which these units formed, 3) reconstruct the depositional history of the formation, 4) identify and describe the major diagenetic features that occur in the rocks of the Kakisa Formation, 5) determine the diagenetic environments in which each feature was formed, and 6) reconstruct the diagenetic history of the formation.

The Kakisa Formation is well suited for a sedimentologic and diagenetic study for several reasons. First, it is well exposed; its exposures are typically laterally continuous and easily accessible. Second, it

contains good reef exposures. Third, it has not been pervasively dolomitized and therefore most of its original fabrics and textures have been preserved. Fourth, it provides an opportunity to examine some of the little studied uppermost Frasnian strata of western Canada. Fifth, it lies immediately beneath the Frasnian/Famennian unconformity and thus is perfectly suited for the study of the diagenetic effects related to subaerial exposure. Sixth, it is one of the most prospective hydrocarbon reservoirs in the upper Mackenzie River area (Law, 1971).

B. LOCATION OF STUDY AREA

The best exposures of the Kakisa Formation occur in the southwestern part of the Northwest Territories, just south of the upper Mackenzie River. The study area includes the type section of the Kakisa Formation, which occurs along Trout River, and the adjacent outcrops. It spans from the region from just west of Trout River eastward to Bouvier River (Fig. 1). Most of the outcrops in this study area are easily accessible from the Mackenzie Highway.

C. METHOD OF STUDY

The field work for the study was carried out during the summers of 1983 and 1984. During this time thirteen sections were measured; six along Trout River, four along the Mackenzie Highway, and one each along Redknife River, Bouvier River, and Wallace Creek (Fig.1). In the field all

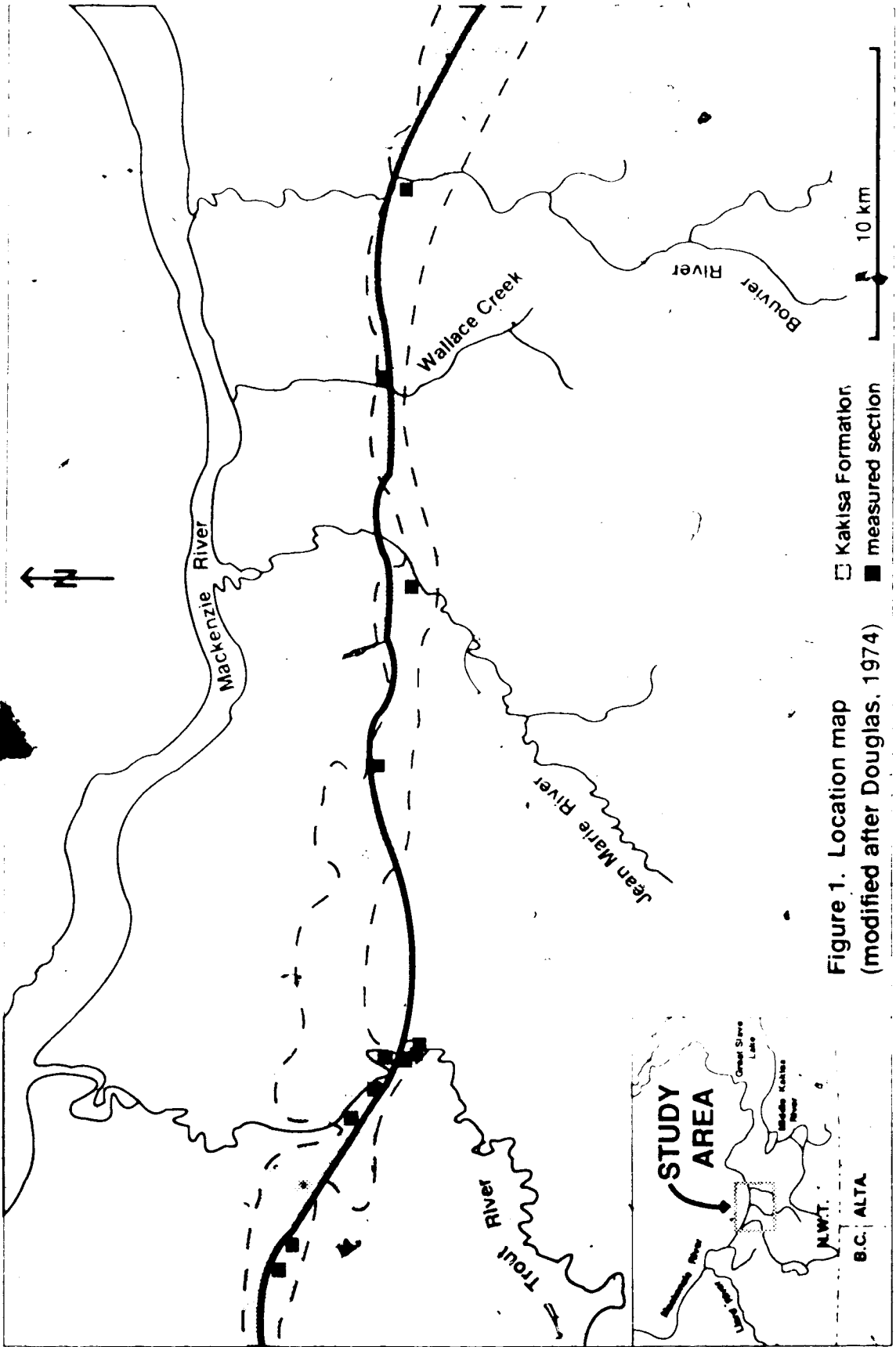


Figure 1. Location map (modified after Douglas, 1974)

□ Kakisa Formation
 ■ measured section

of these sections were subdivided into locally mappable lithologic units, described, sampled, and photographed. In all 179 lithologic and 67 paleontologic samples were collected. All of the lithologic samples were slabbed and polished and 115 thin sections were prepared from the lithologic samples. These thin sections were impregnated with blue epoxy to aid in the identification of original porosity. They were also stained with Alizarin Red-S (Evamy, 1969) to differentiate calcite from dolomite and with potassium ferricyanide (Dickson, 1966) to indicate the presence of ferroan carbonates.

D. STRATIGRAPHY

The Kakisa Formation is latest Frasnian in age (Belyea and McLaren, 1962; McLean, 1982; A. E. H. Pedder, written comm., 1985). It is 57 m thick in its type section where it is composed of green-grey silty/sandy limestones. It contains a diverse fauna of corals, brachiopods, and stromatoporoids.

In the Liard River area (Fig. 2) the Kakisa Formation grades into the grey shales of the Fort Simpson Formation (Belyea and McLaren, 1962; Hills *et al.*, 1981). The Kakisa Formation extends southwestward into northeast British Columbia and northwest Alberta where it maintains a relatively consistent thickness of about 30 m until it reaches the Peace River arch where it becomes increasingly dolomitic and loses its identity as a distinct unit (Belyea

UPPER DEVONIAN	LIARD RIVER AREA	STUDY AREA	MIDDLE KAKISA RIVER
Famennian	Mississippian	Cretaceous	Trout River Formation
	Kotcho Formation	Kotcho Formation	KAKISA FORMATION
	Tetcho Formation	Tetcho Formation	Redknife Formation
	Trout River Formation	Trout River Formation	Tathlina Formation
Frasnian	Fort Simpson Formation	Upper Member Jean Marie Member	Twin Falls Formation
		Fort Simpson Formation	Hay River Formation
			Middle Devonian

Figure 2. Upper Devonian stratigraphic nomenclature in the southwestern N.W.T. (modified after Belyea & McLaren, 1962).

and McLaren, 1962; Hills *et al.*, 1981). North and east of the Trout River area the Kakisa Formation has been removed by pre-Cretaceous erosion (de Wit *et al.*, 1973; Douglas, 1974).

In the study area the Kakisa Formation gradationally overlies the grey-green limey shales and argillaceous limestones of the upper member of the Redknife Formation and is unconformably overlain by the calcareous sandstones of the Trout River Formation (Fig. 2). The Trout River Formation is early Famennian in age while both the Kakisa and Redknife formations are of late Frasnian age (Fig. 2). The contact between the Kakisa and Trout River formations denotes the boundary between the Frasnian and Famennian stages (McLaren, 1959; Belyea and McLaren, 1962; Belyea, 1964; Braun and Lethiers, 1982; Davies, 1986). This boundary is very significant since it coincides with the widespread extinction of the important Devonian reef-building organisms (McLaren, 1970; House, 1975; Copper, 1977). A marked faunal break occurs at Trout River where the fauna of the Trout River Formation differs greatly from that of the Kakisa Formation (Crickmay, 1957; McLaren, 1959; Belyea and McLaren, 1962; McLaren, 1982; Pedder, 1982). Although a variety of mechanisms have been proposed to explain the Frasnian/Famennian extinctions (see McLaren, 1970; Johnson, 1974; House, 1975; Copper, 1977; McLaren, 1982), their cause is still uncertain.

In central Alberta the Kakisa Formation correlates with the Blueridge Member of the Graminia Formation and the upper part of the underlying Calmar Formation (Warren and Stelck, 1956; Belyea, 1964; Davies, 1986) while in the Rocky Mountains of northern Alberta it correlates with the Ronde Member of the Southesk Formation (McLaren and Mountjoy, 1962; McLean, 1982; A. E. H. Pedder, written comm., 1985). The corals of the Kakisa Formation are part of the youngest Devonian coral fauna known in western Canada and correlate well with those of the Ronde Member (McLean, 1982; A. E. H. Pedder, written comm., 1985). According to Pedder (written comm., 1985) the coral fauna of the Kakisa Formation has more genera and species than any other described Upper Devonian coral fauna.

F. PALEOGEOGRAPHY

The Kakisa Formation was deposited on the Great Slave Shelf. This shelf was bounded by the emergent Canadian Shield to the east, the submerged (Belyea, 1971) Tathlina high to the south, and the Mackenzie miogeosyncline to the west (Bassett and Stout, 1967).

The paleogeographic reconstructions of Scotese *et al.* (1986) indicate that during late Devonian time, when the sediments of the Kakisa Formation were being deposited, the Trout River area was situated at approximately 28° north latitude. At that time the Great Slave Shelf was covered by a shallow epicontinental sea and the shelf edge in the Trout

River region had a general north northwest-south southeast trend (Bassett and Stout, 1967; Ziegler, 1967).

Overall sea level was rising during Frasnian time (Vail *et al.*, 1977; Johnson *et al.*, 1985). However, the Frasnian/Famennian boundary roughly corresponds with a marked sea level lowering (Bassett and Stout, 1967; de Wit *et al.*, 1973; Johnson *et al.*, 1985).

F. PREVIOUS STUDIES

To date studies of the Kakisa Formation have concentrated on stratigraphy or paleontology; the sedimentation and the diagenesis of this formation have yet to be delineated. Whittaker (1922, 1923), Crickmay (1953, 1957), and Belyea and McLaren (1962) outlined the stratigraphic position of the Kakisa Formation in their regional studies. Douglas (1974) employed Belyea and McLaren's (1962) stratigraphic nomenclature in his map of the upper Mackenzie River region. Belyea and McLaren's (1962) nomenclature was also adopted for this study (Fig. 2).

Warren and Stelck (1956) and McLaren *et al.* (1962) illustrated many of the fossils from the area. Crickmay (1953, 1957) and Belyea and McLaren (1962) examined brachiopods from the Kakisa Formation, while Stearn (1966) identified some of the stromatoporoids, and Smith (1945) and Pedder (1982, written comm., 1985) the corals. The conodonts have been studied by Apon (1980) and Klapper and Lane

(1985), the ammonoids by House and Pedder (1963), and the ostracods by Braun and Lethiers (1982).

G. TERMINOLOGY

Introduction

There is an abundance of rock classification systems and sedimentologic terms currently in existence in the geologic literature. Therefore, in order to avoid ambiguity and confusion it is essential to outline the classification systems and define the sedimentologic terms used in this study.

Classification Systems

In this study Embry and Klovan's (1971) classification system is used for the carbonates in the sequence while Folk's (1968) classification system is used for the sandstones. Bedding is classified according to Ingram's (1954) scale of stratification thickness while Wentworth's grade scale (1922) is used when referring to particle grain sizes. Crystal size is classified using Folk's (1959) system while crystal shape follows Friedman's (1965) classification and crystal texture is categorized according to Gregg and Sibley (1984). Cement fabrics are referred to using Flügel's (1982) outline while Bathurst's (1975) size divisions are used when referring to neomorphic spar. Choquette and Pray's (1970) classification of pore types and James and

Choquette's (1983a) breakdown of diagenetic environments are adopted in this study.

Sedimentologic Terms

Bioherm: A mound-shaped structure which exhibits a discordant relationship with the surrounding lithologies (Klement, 1967).

Biostrome: A coarsely layered structure composed of skeletal carbonate which grades concordantly into the surrounding lithologies (Klement, 1967).

Reef: A broad non-specific master label for all dense *in situ* accumulations of skeletal carbonate, even where these accumulations did not obviously build a wave-resistant framework (Burchette, 1981).

Carbonate bank: A special type of reef which is sheet-like, composed of tiered biostromes, and lacks lateral facies differentiation (Burchette, 1981).

Carbonate buildup: A specific type of reef which 1) differs in nature to some degree from equivalent deposits and surrounding and overlying rocks, 2) is typically thicker than equivalent carbonates, and 3) probably stood topographically higher than surrounding sediment during some time in its depositional history (Heckel, 1974).

Fair weather wave base: The water depth at which daily wave action ceases to stir the sea floor sediments (after American Geological Institute, 1976).

Storm wave base: The water depth at which storm wave action ceases to stir the sea floor sediments (after American Geological Institute, 1976).

Shelf: A gently sloping, shallowly submerged portion of the continental margin extending from the shore to the region where there is an abrupt increase in sea floor inclination (American Geological Institute, 1976).

Shallowing-upward sequence: A sequence of carbonate deposits in which each unit is deposited in progressively shallower water (James, 1984).

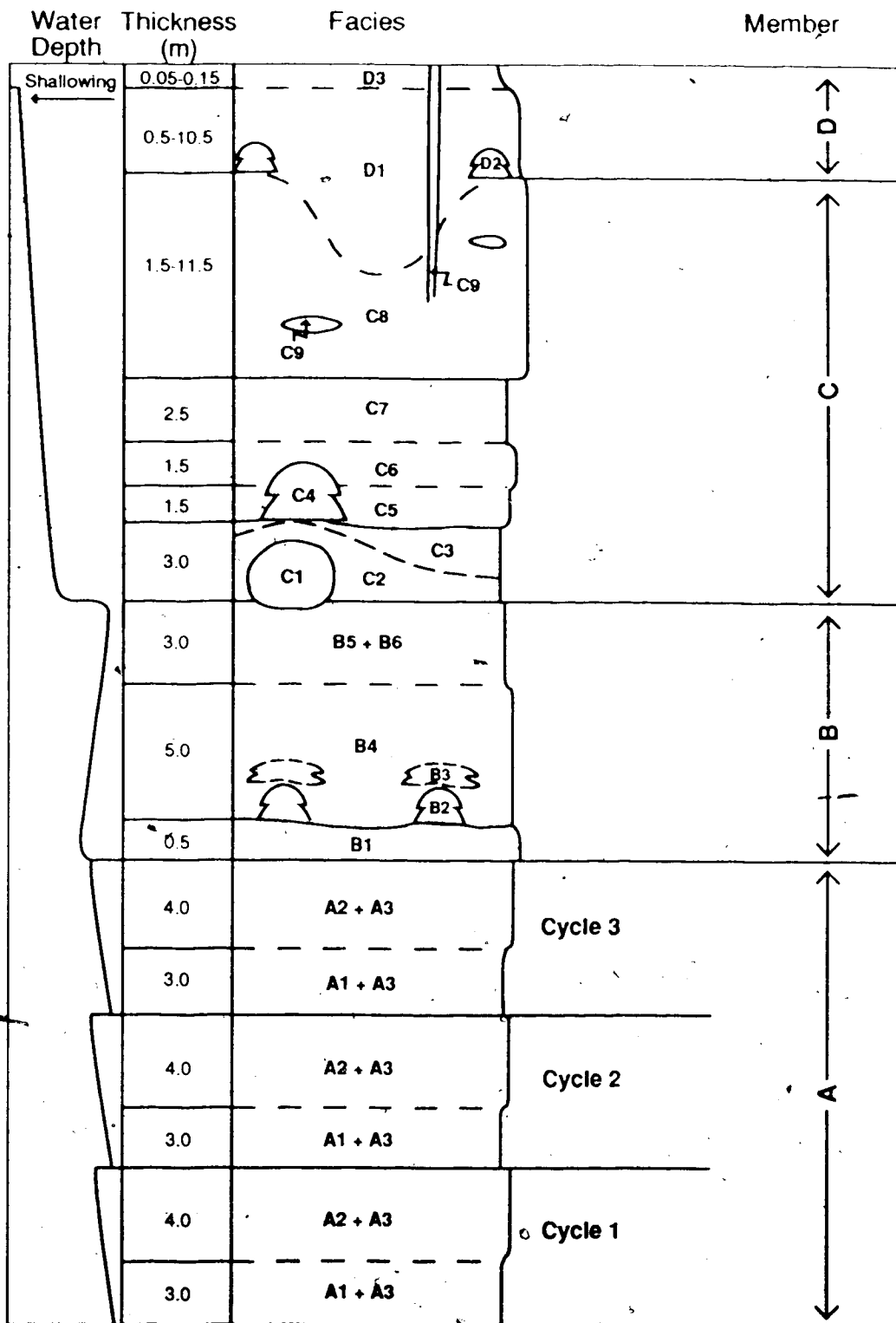
II. SEDIMENTATION

A. INTRODUCTION

There have been many sedimentologic studies of western Canadian Upper Devonian carbonate sequences, particularly those containing reefs (e. g. Klovan, 1964; Murray, 1966; Jenik and Lerbekmo, 1968; Leavitt, 1968; Embry and Klovan, 1971; Jamieson, 1971; McGillivray and Mountjoy, 1975; Wendte and Stoakes, 1982). The abundance of studies is the result of the fact that sedimentary facies commonly exert a marked influence on the localization of hydrocarbon reservoirs in these sequences.

The easily accessible, laterally and vertically continuous exposures of the essentially undolomitized, reef-bearing limestones of the Kakisa Formation are particularly well suited to a detailed sedimentologic study. Unlike subsurface studies, this study is not confined to an irregular distribution of bore holes and drill cores. Also, critical sections of the Kakisa Formation are not covered, eroded, or pervasively dolomitized as is the case with many Upper Devonian outcrops in western Canada.

The Kakisa Formation has been divided into four informal members, designated A, B, C, and D (Fig. 3). As illustrated in Fig. 3, each member has then been further subdivided into facies. In this study the depositional environments of each member are interpreted on the basis of the lithologies, fauna, and sedimentary structures of its



— sharp contact - - gradational contact

Figure 3. Schematic type section of the Kakisa Formation.

constituent facies and the interrelationships between those facies. These interpretations are then used to reconstruct the overall depositional history of the Kakisa Formation.

B. MEMBER A

Introduction

Member A forms the lower part of the Kakisa Formation (Fig. 3). This member is 21 m thick and is best exposed at Trout River, Redknife River, Bouvier River, and Wallace Creek. Additional outcrops occur in roadcuts along the Mackenzie Highway.

Member A is characterized by its relatively sparse but diverse fauna and the common occurrence of thin, sharp-based, planar laminated, laterally discontinuous beds. Its fauna includes brachiopods, solitary corals, dome-shaped massive corals, echinoderms, gastropods, and a diverse ichnofauna. This member is made up of facies A1, A2, and A3 (Fig. 3).

Facies A1: Argillaceous mudstone

Facies A1 is characterized by its medium green weathered color, its sparse fauna, its recessive weathering nature, and its lensoid bedded appearance (Plates 1A, 1B, 2D). It is laterally extensive and has an average thickness of 3.0 m.

Lithology: The argillaceous mudstone is composed of 40% microspar, 25% very fine grained quartz sand, 10% fine grained bioclasts, 10% pseudospar, 10% clays, and 5% finely crystalline anhedral dolomite.

Fauna: Facies A1 contains a very sparse shelly fauna that consists primarily of small solitary corals (average 1.0 cm long, 0.7 cm in diameter). These corals are relatively unabraded and occur in aerially restricted patches (average 0.5 m in diameter) with their long axes parallel to bedding. *Hunanophrentis* sp. nov. is common.

Bedding: The argillaceous mudstone has been totally homogenized by bioturbation and, therefore, does not exhibit bedding.

Facies A2: Nodular bioclastic wackestone

Facies A2 weathers light green-grey, is sparsely fossiliferous, semi-resistant (Plates 1A, 2D), and has a flaggy bedded appearance (Plate 1E). It is laterally extensive and has an average thickness of 4.0 m.

Lithology: The texture of the nodular bioclastic wackestones closely resembles that of the Type I rubbly argillaceous limestones described by Jones *et al.* (1979). This nodular texture is created by elongate lumps of bioclastic wackestone surrounded by a matrix of argillaceous bioclastic wackestone (Plate 1D). The bioclastic wackestone lumps are formed of 40% microspar, 30% fine grained bioclasts, 20% very fine grained quartz sand, 5% pseudospar,

and 5% finely crystalline anhedral dolomite. They generally comprise 70% of the nodular bioclastic wackestone (Plate 10) and average 1.5 cm in length and 0.75 cm in width. Their long axes display a subhorizontal alignment and the matrix displays evidence of differential compaction around them. In addition, microstylolite swarms typically occur around the edges of the lumps. In this section rare lumps display a well defined whorled texture.

Fauna: Facies A2 has a moderately abundant and relatively diverse shelly fauna. This fauna is typically concentrated on bedding planes where it occurs in areally restricted patches. These patches have an irregular outline and an average diameter of 1.0 m. Based on their dominant faunal elements three types of faunal patches can be differentiated: 1) solitary coral patches, 2) brachiopod patches, and 3) mixed fauna patches.

The solitary corals that dominate the solitary coral patches are small (average 7.0 cm long, 1.0 cm in diameter) and unabraded. Rare corals occur in growth position. *Hunanophrentis* sp. nov., *Piceaphyllum* sp., and *Michtophyllum* sp. are common. These patches also contain fragments of branching corals, echinoderms, gastropods, fenestrate bryozoans, and brachiopods.

The brachiopod patches have a less diverse fauna than the solitary coral patches. These patches are composed entirely of brachiopods. These brachiopods are typically unabraded and articulated. *Devonoproductus* sp. and *Atrypa*

dentonensis Stainbrook are common brachiopod species in facies A2. Generally each patch is dominated by one of these two species.

The mixed fauna patches consist of fragmented and abraded branching corals, echinoderms, small solitary corals, fenestrate bryozoans, and gastropods.

Not all of the shelly fauna in facies A2 occurs in patches. Dome-shaped massive corals up to 50 cm in diameter and 20 cm high occur on bedding planes of the nodular bioclastic wackestones (Plate 1F). These corals are unabraded, typically in growth position, and are aligned along a north northwest-south southeast trend (Plate 1F). *Phillipsastrea exigua* sensu Smith 1945 and "*Frechastrea*" sp. nov. are common dome-shaped massive corals in facies A2.

Rare, nearly intact crinoids also occur along the bedding plane surfaces of facies A2 (Plate 2A). These crinoids commonly have most of their stem and calyxes intact (Plate 2A) and have been tentatively identified as *Prinocrinus robustus* (G.C. McIntosh, written comm., 1984).

In addition to its relatively diverse shelly fauna, facies A2 also contains an abundant and diverse ichnofauna (Plate 2B). *Phycodes pedum*, *Cruziana*, *Rusophycus*, and *Planolites beverleyensis* are common ichnotaxa in this lithotype. *Planolites montanus*, *Paleophycus sulcatus*, *Uchrites*, *Skolithos*, *Monomorphicus*, and *Chondrites* are rare. This ichnofaunal assemblage is characteristic of the *Cruziana* ichnofacies.

Bedding: The nodular bioclastic wackestones occur in very thin (average 2.0 cm thick) planar beds that are separated by thin dark green shale partings. These beds have irregular, slightly wavy surfaces, which gives facies A2 its flaggy bedded appearance (Plate 1E).

Facies A3: Laminated bioclastic wackestone lenses

Facies A3 weathers light grey and occurs in resistant, thin, planar laminated, laterally discontinuous lens-shaped beds (Plate 1C, E). These beds are very variable in size and shape.

Lithology: The laminated bioclastic wackestone is formed of 40% pseudospar, 25% fine to medium grained bioclasts, 15% very fine grained quartz sand, 15% microspar, and 5% coarsely crystalline blocky calcite and saddle dolomite cements. The calcite and dolomite cements fill former shelter porosity beneath the larger bioclasts, particularly brachiopods. The planar laminated character is created by the interlayering of laminae of slightly differing quartz sand content.

Fauna: Facies A3 is commonly transected by discrete dwelling burrows of the *Skolithos* ichnofacies (Plate 2C).

Bedding: The lens-shaped beds that comprise facies A3 have sharp basal contacts and slightly gradational upper contacts (Plates 1C, 1E, 2C). Their thickness ranges from 3 to 10 cm and their width from 0.4 to 1.5 m. The thicker beds are also the most laterally extensive and generally have a

trough shape, i.e. a curved, concave-upward base and a relatively flat top (Plate 1E). Section views of these trough-shaped beds indicate that they have an east-west trend, i. e. roughly perpendicular to the shelf edge. Some beds exhibit hummocky cross stratification.

Within each bed, lamination thickness and grain size decreases upwards. Also, elongate argillaceous mudstone lithoclasts and coarser bioclasts commonly occur in the basal parts of the beds forming a lag-type deposit (Plate 2C).

Interrelationship Between Facies

The lens-shaped beds of facies A3 are dispersed throughout the laterally continuous deposits of facies A1 and A2. These beds truncate the argillaceous mudstones of facies A1 and the nodular bioclastic wackestones of facies A2 and typically comprise 70% of the stratigraphic interval occupied by facies A1 and 20% of the facies A2 interval. The difference in weathering prominence between the recessive facies A1 and the resistant facies A3 gives the facies A1 stratigraphic interval a lensoid bedded appearance (Plate 1B).

The facies A3 beds that truncate facies A2 are generally thicker, more laterally extensive, slightly more coarsely grained, and more extensively burrowed than those that truncate facies A1. Hummocky cross stratification in facies A3 generally occurs only where this facies truncates

facies A1.

Facies A2 gradationally overlies facies A1 (Plate 2D). This vertical succession is cyclically repeated three times in member A (Fig. 3; Plates 1A, 2D). At cycle boundaries facies A1 sharply overlies facies A2 (Fig. 3). Each cycle boundary is marked by a laterally extensive, vertically burrowed hardground surface (Plates 1A, 1B).

Interpretation

The relatively diverse fauna that characterizes member A is indicative of deposition in an unrestricted environment. The solitary corals, brachiopods, dome-shaped massive corals, and echinoderms that dominate member A are considered to be indicative of an open marine depositional environment. Since the member A fauna consists primarily of suspension-feeders, waters must have been well circulated in order for sufficient amounts of food to be brought to these organisms and for their feeding surfaces to be kept free of accumulating sediment. The preservation of nearly intact crinoids in facies A2 indicates that, although well circulated, the waters were not of particularly high energy.

The patchy distribution of the shelly fauna in member A implies that the waters were not equally circulated throughout the environment. Wright (1973) attributed patchy distributions of suspension-feeding organisms to the existence of subtle topographic highs on the sea floor at the time of their growth. He maintained that

suspension-feeders preferentially colonized such highs because they were better circulated and less turbid than the topographically lower areas around them.

The fact that the suspension-feeding fauna of facies A2 is more abundant and diverse than that of facies A1 suggests that facies A2 was deposited in shallower, better circulated waters. The specific nature of the coral faunas of each facies confirms this. Dome-shaped massive corals occur in facies A2 while solitary corals dominate facies A1. According to Tsien (1971) and Rożkowska (1980) dome-shaped massive corals are typical of shallower, better circulated environments than solitary corals.

The assignment of the nodular bioclastic wackestones of facies A2 to the *Cruziana* ichnofacies indicates that this facies was deposited in deeper, quieter waters below fair weather wave base and possibly above storm wave base. Ekdale *et al.* (1984) and Frey and Pemberton (1984) claimed that the *Cruziana* ichnofacies is representative of deposition below fair weather wave base under conditions that range from moderate energy waters located above storm wave base to lower energy waters located below storm wave base.

In addition, nodular limestones such as those that comprise facies A2 commonly occur in the shelf slope environment, i.e. downslope of the shelf margin, below fair weather wave base (Cook and Mullins, 1983; McIlreath and James, 1984). The moderate to low energy conditions commonly associated with shelf slope depositional environments

correspond well with the depositional conditions suggested for facies A2 by its shelly fauna and its ichnofauna.

The sharp bases and the presence of shelter porosity in the lens-shaped beds of facies A3 indicates that these beds were deposited rapidly. Kriesa (1981) maintained that sharp basal contacts and shelter porosity are characteristic of rapidly deposited sediment. The lag-type deposits at their bases and the manner in which these beds truncate the adjacent limestones suggests an erosive depositional mechanism for these laterally discontinuous beds. The upward decrease in lamination thickness and bioclast size in each bed is indicative of deposition by a single, waning high energy episode (Reineck and Singh, 1972; Kriesa, 1981). Planar lamination results from deposition by a fluctuating current (Harms *et al.*, 1982).

Storm deposits are generally assumed to have been laid down rapidly by erosive, waning, high energy, fluctuating flows (Cant, 1980; Dott and Bourgeois, 1982; Swift *et al.*, 1983; Walker, 1984). This suggests that the lens-shaped beds of facies A3 were deposited by storms. The hummocky cross stratification exhibited by some of the lens-shaped beds is also evidence of this type of deposition. Hummocky cross stratification is typical of storm deposition (Hamblin and Walker, 1979; Dott and Bourgeois, 1982; Walker, 1984). In addition, hummocky cross stratification is considered to have formed above storm wave base and below fair weather wave base (Hamblin and Walker, 1979; Dott and Bourgeois,

1982; Walker, 1984). The occurrence of facies A3 storm deposits in both facies A1 and A2 indicates that both of these facies were deposited above storm wave base. Furthermore, the occurrence of hummocky cross stratification in the storm beds that truncate facies A1 suggests that this facies was deposited below fair weather wave base while the confinement of facies A2 to the *Cruziana* ichnofacies indicates that it too was deposited below fair weather wave base.

A closer examination of the storm deposits suggests that the lens-shaped beds that occur in facies A2 were deposited in a shallower, more proximal depositional environment than those that occur in facies A1. Kriesa (1981) asserted that the thickness of storm deposits decreases with increasing depositional depth. This suggests that the thicker lens-shaped beds of facies A2 were laid down in a shallower depositional environment than the thinner lens-shaped beds of facies A1. This interpretation is consistent with that made from the shelly fauna in these two facies. The coarser bioclast size as well as the greater number of *Skolithos*-type burrows in the lens-shaped beds of facies A2 also supports this suggestion. Pemberton and Frey (1984) suggested that the abundance of *Skolithos* burrows decreases with increasing depositional depth and distality.

Thus, member A was deposited above storm wave base and below fair weather wave base in a storm-influenced shelf slope environment, facies A1 having been deposited in deeper

waters than facies A2. The fact that facies A2 gradationally overlies facies A1 in each of the three cycles present in member A indicates that gradual shallowing took place during the deposition of each of these cycles. Hence, each cycle represents a shallowing-upward sequence.

Shallowing-upward sequences are formed when the rate of carbonate accumulation exceeds the rate of relative sea level rise (James, 1984). Thus, it is likely that the shallowing-upward sequence that comprises each cycle was terminated when the rate of carbonate accumulation no longer exceeded the rate of relative sea level rise; either due to a decrease in the rate of carbonate accumulation or an increase in the rate of sea level rise.

The cause of cyclicity on member A is more difficult to determine. Cyclicity in carbonate sequences has been the topic of much debate. Wilkinson (1982) and James (1984) have provided excellent summaries of current viewpoints on this topic. These authors pointed out that there are basically two end-member models that have been used to explain cyclicity, the eustatic model and the autocyclic model (Fig. 4). Both models can be used to produce virtually identical looking sequences.

In the eustatic model the rate of carbonate accumulation is constant while the rate of relative sea level rise increases episodically. During periods of relatively constant sea level rise the rate of carbonate accumulation exceeds the rate of sea level rise and a

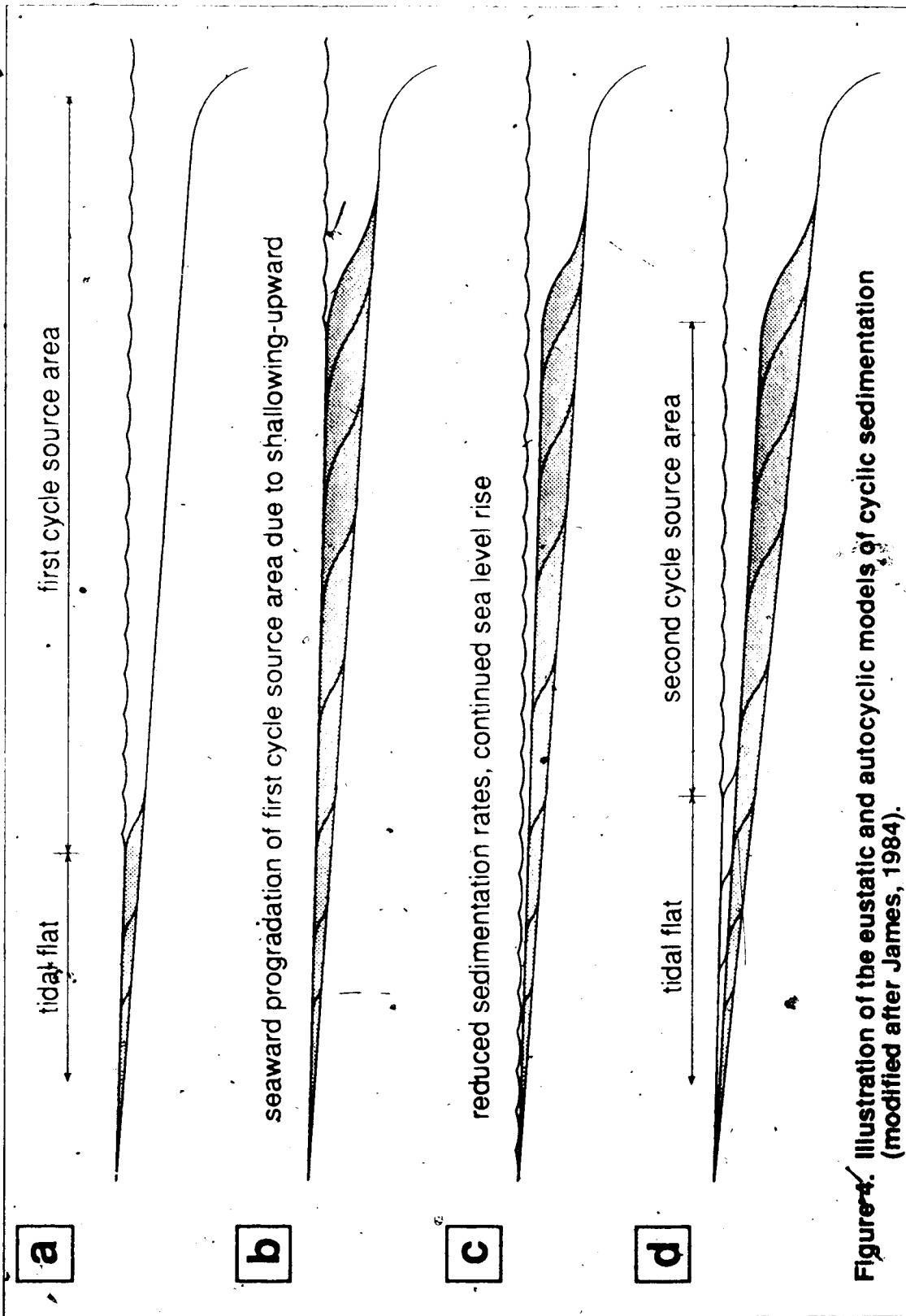


Figure 4. Illustration of the eustatic and autocyclic models of cyclic sedimentation (modified after James, 1984).

shallowing-upward sequence is formed (Fig. 4a and 4b). However, following an episode of rapid sea level rise the rate of carbonate accumulation is greatly reduced (Fig. 4c). Eventually sea level stabilizes and the rate of carbonate accumulation again exceeds the rate of sea level rise causing the initiation of another shallowing-upward sequence (Fig. 4c). Goodwin and Anderson (1985) incorporated this model in their explanation of punctuated aggradational sequences.

In the autocyclic model the rate of sea level rise is constant while the rate of carbonate accumulation varies. This model relies on the assumption that there is a certain optimum water depth that is conducive to maximum rates of carbonate accumulation. James (1984) referred to this region as the source area (Fig. 4). With the seaward progradation that accompanies shallowing-upward the carbonate sequence approaches the shelf edge and the size of the source area gets progressively smaller (Fig. 4b). Eventually the source area becomes too deep or too small and the rate of carbonate accumulation is greatly reduced (Fig. 4c). Sea level will continue to rise, however, and soon the shelf will be resubmerged and a new shoreward source area will be established (Fig. 4d). This will lead to the initiation of another shallowing-upward sequence.

Both models involve a period where the rate of carbonate accumulation is greatly reduced. It was likely during these periods that the laterally extensive

hardgrounds that occur at each member A cycle boundary were formed. Shinn (1969) maintained that hardgrounds are formed in stable, permeable sediments during periods of relatively slow rates of sedimentation.

By examining member A alone it is difficult to ascertain which model is best suited to explain its cyclicity. Yet, the relatively constant thickness of each cycle suggests a uniformity that would not be expected from episodic eustatic sea level rises. By examining members B and C a better estimate can be made of the cause of member A cyclicity. Ironically, it is the lack of cyclicity in these two members that yields the necessary clues.

The deepening-upward sequence of member B suggests a continuous sea level rise during its deposition. This observation corresponds best with the autocyclic model as this model requires that sea level is rising at a relatively constant rate. In this case the rate of accumulation of the member B limestones was exceeded by the rate of sea level rise. Furthermore, the reef of member C does not show any evidence for the occurrence of the rapid sea level rises required by the eustatic model during its growth. Instead it exhibits a continuous sequence of upward shallowing which, according to Kendall and Schlager (1981), Wilkinson (1982), James and Mountjoy (1983), and James (1984), is typically a response to sea level rise.

Thus, although the evidence is far from definitive, it appears that the autocyclic model of sedimentation is best

needed to explain the cyclic deposition of member A.

C. MEMBER B

Introduction

Member B, which is 8.5 m thick, is well exposed at Trout River. It can be recognized by the occurrence of a thick, laterally extensive bed of coral/echinoderm rudstone at its base overlain by several small dome-shaped coral bioherms (Fig. 3). Lithologically its upper part resembles member A.

Member B can be divided into six facies, designated B1 through B6 (Fig. 3).

Facies B1: Coral/echinoderm rudstone

Facies B1 weathers orange-grey and can be recognized by its massive, resistant weathering character, its poorly sorted, coarse grained texture, its bioclastic composition, and its lateral extensiveness (Plate 2F). Its thickness is variable but averages 0.5 m. Its base is sharp and planar (Plate 2D) while its upper surface is irregular and hummocky. At Trout River lithofacies B1 can be traced for approximately 1.0 km in a northwest-southeast direction (i. e. subparallel to the shelf edge). Its lateral extensiveness subparallel to the shelf edge intimates that this facies has a sheet-like morphology.

Lithology: The coral/echinoderm rudstone is formed of low profile, massive corals, which range up to 4.0 cm in height and 20 cm in width (Plate 2F), set in a matrix of coarse grained, poorly sorted bioclastic packstone (Plates 2E, 3A). The massive corals typically form 20% of the rudstone (Plate 2F). They are slightly abraded, commonly overturned, and have a subhorizontal alignment (Plate 2F). The coarse grained bioclastic packstone matrix is composed of 55% coarse grained bioclasts, 25% coarsely crystalline blocky calcite cement, 10% mudstone, 5% coarsely crystalline saddle dolomite cement, and 5% elongate mudstone lithoclasts which range up to 2.0 cm in length and 1.5 cm in width (Plate 3A). The coarsely crystalline blocky calcite occurs as syntaxial rim cement around echinoderm bioclasts and fills shelter and interparticle pore space. The coarsely crystalline saddle dolomite cement also occurs in shelter and interparticle pore space.

Fauna: The bioclasts in the packstone matrix are primarily echinoderm fragments with lesser amounts of fenestrate bryozoans, branching corals and brachiopods (Plates 2E, 3A).

Bedding: Facies B1 is massive. However, the subhorizontal alignment of the massive corals gives this facies a crude planar bedded appearance.

Facies B2: Coral bioherms

Facies B2 consists of several small, green-grey, dome shaped coral bioherms (Plate 3C, 3D). These bioherms have a maximum height of 0.7 m and width of 1.5 m. At Trout River the facies B2 bioherms are aligned along a well defined north-northwest-south-southeast trend (Plate 3C).

Typically the bioherms are composed of two lithologies: 1) a basal coral bafflestone and 2) an overlying layer of coral bindstone (Fig. 5). The coral bafflestone, which forms the thickest part of each bioherm, is dominated by the delicate branching coral *Phaceltophyllum tructense*. The coral bindstone is made up of a combination of *Phaceltophyllum tructense* and low profile massive corals. These massive corals have an average height of 5 cm and width of 35 cm. The corals in the bafflestone and the bindstone are surrounded by a matrix of grey-brown mudstone.

Facies B3: Coral bafflestone patches

Facies B3 weathers medium green-grey and can be recognized by the abundant occurrence of branching coral colonies in growth position (Plate 3E). This facies is 0.5 m thick and occurs in areally restricted patches (Fig. 5).

Lithology: The coral bafflestone is formed primarily of vertically stacked colonies of branching corals surrounded by a green-grey mudstone matrix. Rare large, dome-shaped, massive corals can also occur in this facies (Plate 3B).

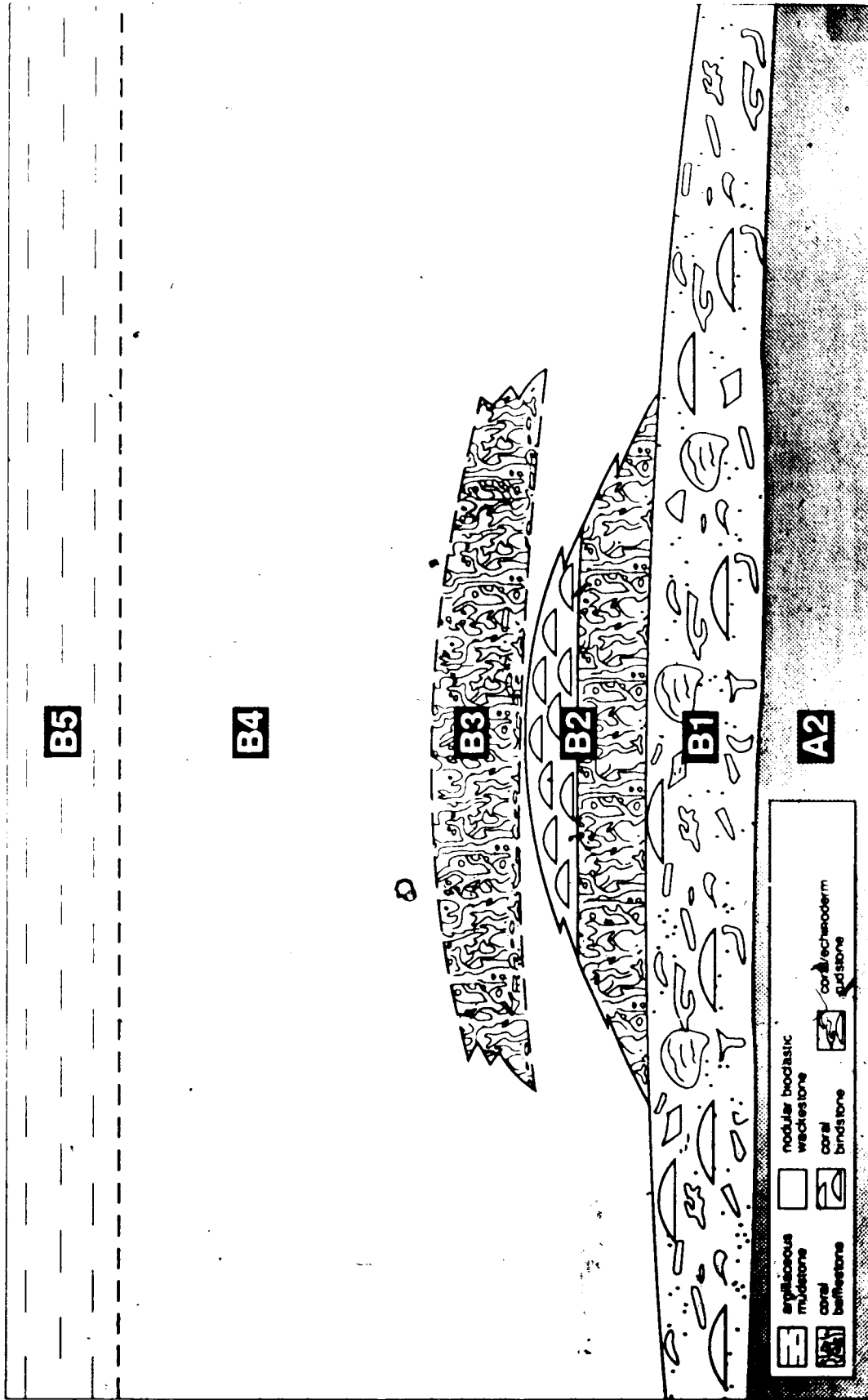


Figure 5. Schematic diagram illustrating the facies and lithologic interrelationships in member B.

Fauna: *Phaceltophyllum tructense* is the dominant branching coral (Plate 3E). Its colonies have an average height of 7 cm and width of 60 cm. The large dome-shaped massive corals, on the other hand, range up to 18 cm high and 55 cm wide (Plate 3B).

Bedding: Well defined bedding is absent in this facies.

Facies B4: Nodular bioclastic wackestone

Facies B4 closely resembles facies A2. For this reason only the differences between these two facies will be discussed.

Facies B4 is 5.0 m thick and, hence, is 1.0 m thicker than facies A2. The main difference between facies B4 and A2, however, is in their faunas. As in facies A2, the shelly fauna of facies B4 occurs on bedding planes in areally restricted patches. The brachiopod patches of facies A2 occur in facies B4. Mixed fauna patches also occur in facies B4 yet the make up of these patches is different from those in facies A2. The abraded and fragmented fauna of the facies B4 mixed fauna patches is composed primarily of branching corals and fenestrate bryozoans with fewer echinoderm fragments, massive corals, brachiopods, solitary corals, and gastropods. This contrasts with the less diverse fauna of facies A2 mixed fauna patches which are made up of branching corals, echinoderms, solitary corals, and gastropods. The solitary coral patches, nearly intact crinoids, and dome-shaped massive corals of facies A2 were not found in

facies B4. Like facies A2, the ichnofauna of facies B4 is representative of the *Cruziana* ichnofacies. However, this ichnofauna is not as abundant or diverse as that of facies A2. *Teichichnus rectus*, *Phycodes pedum*, *Paleophycus sulcatus* are the most common ichnotaxa in facies B4.

Facies B5: Argillaceous mudstone

Since facies B5 is very similar to facies A1 only the differences between these two facies will be described.

The main difference between facies B5 and A1 is in their shelly fauna. The shelly fauna of facies B5 is more abundant and diverse than that of facies A1. In addition to solitary corals, the argillaceous mudstones of facies B5 contain aurally restricted patches of brachiopods and branching coral colonies of *Phacellophyllum tructense*. Rare dome-shaped massive corals (up to 8.0 cm high and 30 cm wide) also occur in this facies.

Facies B6: Laminated bioclastic wackestone lenses

Facies B6 is very similar to facies A3. For this reason only the differences between these two facies will be discussed.

The main difference is that the lens-shaped beds of facies B6 are generally thinner (average 2.5 cm thick) and less laterally extensive than those of facies A3. In addition, the facies B6 beds do not exhibit a trough-shaped morphology.

Interrelationship Between Facies

Unlike member A, the facies that comprise member B are not cyclically repeated and are not always stacked in layers. The coral/echinoderm rudstones of facies B1 occur at the base of member B. Its base truncates fossils in the upper part of member A (Plate 2E). The coral bioherms of facies B2 directly overlie these rudstones (Fig. 5). The bioherms are typically located on top of hummocks on the irregular, hummocky upper surface of facies B1. The facies B3 coral bafflestone patches occur above the bioherms (Fig. 5; Plate 3D).

The facies B4 nodular bioclastic wackestones occur in a variety of stratigraphic positions. The lower part of this facies (approximately 1.0 m thick) occurs between the facies B2 bioherms and the coral bafflestone patches of facies B3 while the upper part (approximately 4.0 m thick) occurs stratigraphically above facies B3 (Fig. 5). The nodular bioclastic wackestones of facies B4 interfinger laterally with the bioherms and the facies B3 coral bafflestones (Fig. 5; Plate 3D). Where facies B4 overlies facies B3 these two facies are in gradational contact (Fig. 5). Unlike facies A2, which facies B4 closely resembles, facies B4 is not truncated by lens-shaped beds. This may be because lens-shaped beds truly do not truncate facies B4 or it may be that these beds were not detected as a result of the raggedy nature of the facies B4 outcrops.

Facies B5 represents a return to the vertical stacking of facies. This facies gradationally overlies facies B4 (Fig. 5). The lens-shaped beds of facies B6 truncate the argillaceous mudstones of facies B5 and commonly comprise 65% of the facies B5 interval.

Interpretation

There are some distinct lithological similarities between members A and B. For example, facies B4 resembles facies A2, facies B5 resembles facies A1, and facies B6 resembles facies A3. These resemblances imply that the depositional environment of member B was similar to the shelf slope environment of member A. Therefore, much could be learned about the deposition of member B by comparing it to member A.

However, there are several important differences between these two members. First, member B has a more abundant and diverse fauna than member A. Second, member A does not contain coral bioherms. Third, member B does not exhibit cyclically repeated depositional sequences. Fourth, member A does not contain laterally extensive, coarse grained bioclastic deposits. These differences suggest differences between the depositional environments of members A and B. Thus, the differences between these two members must also be considered when interpreting member B deposition.

The truncation of fossils in the underlying member A beds by the basal contact of facies B1 and the occurrence of lithoclasts in its matrix suggests that erosion accompanied its deposition. Rapid deposition of this facies is indicated by its sharp basal contact and the presence of shelter porosity in its matrix. According to Kriesa (1981) shelter porosity and sharp basal contacts result from rapid deposition. Its homogeneity implies that the entire facies was deposited by one event. Thus, the coral/echinoderm rudstone has some similarities to the storm deposits of member A. The coarser grained texture and greater thickness of facies B1, however, indicates that it was laid down by a higher energy event than the member A storm deposits. In addition, the lateral extensiveness of facies B1 implies that this event had a more widespread effect than the member A storms. The lack of bedding or grading in the coral/echinoderm rudstone suggests that unlike most storms this widespread, high energy erosive event was not fluctuating or waning.

The lack of inverse or normal grading as well as the absence of well developed Bouma sequences in the rudstone indicates that it was not deposited by either a grain flow or a turbidity current. Its thickness also implies that grain flow was not a viable depositional mechanism for facies B1. Lowe (1976) suggested that grain flows are typically less than 5.0 cm thick. However, the thickness of facies B1 is in the range of debris flow deposits. Cook and

Mullins (1983) claimed that debris flow deposits range from centimeters to tens of meters in thickness. Moreover, most of the other features of the coral/echinoderm rudstone can be explained by debris flow deposition. Sheet-like morphology, poor sorting, lack of bedding and grading, wide variety of slightly abraded bioclast types, and subhorizontal alignment of elongate clasts (massive corals in the case of facies B1) are all characteristic of debris flow deposits (Cook *et al.*, 1972; Middleton and Hampton, 1973; Davies, 1977; Crevello and Schlager, 1980; Cook and Mullins, 1983). In addition, sharp, planar bases and irregular, hummocky upper surfaces, such as those displayed by facies B1 are typical of debris flow deposits (Cook, *et al.*, 1972; Davies, 1977). In fact, facies B1 resembles the finer rudite debris flow sheet of Cook *et al.* (1972).

Nonetheless, the clasts in a debris flow are generally thought to be supported during transport by a cohesive mud matrix (Cook *et al.*, 1972; Middleton and Hampton, 1973; Cook and Mullins, 1983) yet the coral/echinoderm rudstone of facies B1 contains only 10% mud matrix. However, Rodine and Johnson (1976) concluded that debris flows can occur in sediments with as little as 5% mud matrix. Hence, facies B1 is interpreted to have been deposited by a debris flow. In fact, the facies B1 rudstones resemble the finer rudite sheets that Cook *et al.* (1972) interpreted as debris flow deposits. Carbonate debris flow deposits are typical of the shelf slope environment (Cook *et al.*, 1972; Davies, 1977;

Enos and Moore, 1983; Cook and Mullins, 1983; McIlreath and James, 1984).

The small coral bioherms of facies B2 closely resemble the reef mounds described by James (1983). Their domal shape and internal vertical layering are both typical of the reef mounds described by James (1983). He maintained that reef mounds generally exhibit three stages of growth: 1) a basal bioclastic pile formed of muddy sediment with abundant bioclastic debris and no binding or baffling organisms, 2) a bafflestone core which consists of delicate to dendroid forms with upright growth habits in a mudstone matrix and makes up the thickest part of the reef mound, and 3) a mound cap which is composed of a thin layer of encrusting or lamellar forms. The facies B2 coral bioherms display all three growth stages. The coral bafflestone comprises the bafflestone core, the coral bindstone represents the mound cap, and the coral/echinoderm rudstone of facies B1 makes up the basal bioclastic pile.

Reef mounds have been widely documented in the literature (e.g. Wilson, 1975; Mountjoy and Jull, 1978; Burchette, 1981; Mountjoy and Riding, 1981; James, 1983; Machel, 1983; Krause, 1984) yet the reasons for their initiation, localization, and termination of their growth are still poorly understood (James, 1983; Machel, 1983). The larger oil-bearing 'pinnacle reefs' of the Upper Devonian Nisku Formation have been diagnosed as reef mounds (Machel, 1983; Krause, 1984). As a result a good understanding of

reef mound growth and initiation can have significant economic implications.

In the past, reef mound studies have generally been hampered by several factors including incomplete exposures, inaccessible exposures, and extensive dolomitization. The reef mounds of facies B2 do not suffer from any of these difficulties; they are entirely exposed, easily accessible, and virtually undolomitized. Thus, although much smaller than their Nisku cousins, these reef mounds provide an excellent opportunity to attempt to answer some of the problems surrounding the initiation, localization, and termination of reef mound growth.

Reef mounds are generally considered to have grown in a shelf slope environment (Wilson, 1975; Mountjoy and Jull, 1978; Mountjoy and Riding, 1981; James, 1983; James and Mountjoy, 1983; Machel, 1983; Krause, 1984).

According to Mountjoy and Jull (1978) and Mountjoy and Riding (1981) reef mounds required stable substrates and sufficient water agitation in order to thrive. Thus, in order to initiate the growth of the facies B2 reef mounds these two conditions had to be satisfied. The stable substrate was provided by the coral/echinoderm rudstone of facies B1. The necessary water agitation was created as a result of the rapid deposition of this rudstone. Its rapid deposition would have resulted in the sudden elevation of the sea floor which would have caused a relative shallowing in the area and a resultant increase in water circulation.

Hence, rapid deposition of the debris flow deposits of facies B1 was critical to reef mound initiation.

Variations in substrate topography was the controlling factor with regards to the localization of the facies B2 reef mounds. These reef mounds grew on hummocks that existed on the upper surface of facies B1. As a result of their subtle topographic elevation these hummocks were better circulated than the surrounding swales.

Causes of facies B2 reef mound termination are more difficult to determine. James (1983) referred to reef mounds as incomplete reefs because they only comprised the first two stages of the four stages of reef development outlined by Walker and Alberstadt (1975). He suggested that one of the reasons reef mounds did not develop the third and fourth stages is that their depositional environment was not conducive to the growth of the large metazoans (e.g. tabular and massive stromatoporoids) typical of these last two stages. In the case of the facies B2 reef mounds the waters were probably too deep and poorly circulated to permit the growth of these large metazoans. This is supported by the observation that these reef mounds are composed of a low diversity coral assemblage which suggests a stressed environment. To suspension-feeding corals the most crippling stress would probably have been lack of a current strong enough to supply large quantities of food. Also, the delicate morphology exhibited by the branching corals in the facies B2 reef mounds is thought to have been an adaptation

to growth in a low energy environment.

According to James (1983) the most pronounced upward building towards sea level is done by the large metazoans during the third stage of reef development. Since this stage was not developed in the facies B2 reef mounds it appears that they did not have the intrinsic ability to keep pace with rising sea level and, therefore, were particularly susceptible to drowning. The sudden relative shallowing created by the deposition of facies B1 was apparently not sufficient enough to sustain the growth of large metazoans and, therefore, the facies B2 bioherms were not able to keep pace with rising sea level. The insufficient shallowing probably resulted from the thinness of facies B1. This observation is supported by the fact that the facies B2 reef mounds colonized only the topographically highest parts of facies B1, probably because these were the only areas that met the water circulation requirements of reef mound growth.

Following the termination of reef mound growth the branching and dome-shaped corals of facies B3 grew in patches above the drowned facies B2 reef mounds. It appears that the waters were still sufficiently shallow and well enough circulated above the reef mounds to allow the growth of these coral patches.

Facies B3 deposition was both accompanied and succeeded by the deposition of facies B4. This is indicated by the fact that facies B4 interfingers laterally and gradationally overlies facies B3. Facies B4 deposition also accompanied

reef mound growth as is illustrated by the manner in which this facies interfingers laterally with the facies B2 reef mounds.

The sparseness of its fauna in comparison with that of both facies B2 and B3 suggests that facies B4 was deposited in deeper, more poorly circulated waters than the other two facies. Such conditions would have existed between the reef mounds of facies B2 and the coral patches of facies B3. Evidently these conditions also existed over the entire area after the deposition of facies B2 and B3. This is demonstrated by the manner in which facies B4 overlies as well as flanks facies B3. Thus, it is probable that, as with the facies B2 reef mounds, deposition of facies B3 was terminated as the result of drowning. The gradational manner in which facies B4 overlies facies B3 implies that this drowning was a gradual process rather than a sudden one.

The assignment of facies B4 to the *Cruziana* ichnofacies as well as its close lithologic and faunal resemblance to facies A2 indicates that it was deposited in a depositional environment similar to that of facies A2. The lack of observed lens-shaped beds of planar laminated bioclastic wackestone intimates either that, unlike facies A2, facies B4 was deposited below storm wave base or that storm influence was not as pervasive on the shelf slope during the deposition of facies B4. However, as previously noted, lens-shaped beds of the planar laminated bioclastic wackestone may have been present but difficult to detect due

to the ragged nature of the facies B4 outcrops.

Facies B4 deposition was followed by the deposition of facies B5. The close resemblance of facies B5 and A1 suggests that they were both deposited in the same environment, i. e. a storm influenced shelf slope. Since facies A2 was deposited in a shallower part of the shelf slope than facies A1 then by analogy it can be implied that facies B4 was also deposited in a shallower part of the shelf slope environment than facies B5.

Thus, like member A, member B was deposited in a storm influenced shelf slope environment. However, member B is not divisible into three cyclically repeated shallowing upward sequences. Instead, member B deposition can be divided into two parts, a sudden shallowing followed by a gradual deepening. The deposition of the facies B1 debris flow deposits resulted in a sudden shallowing in the shelf slope environment of member A. This shallowing and the stable substrate provided by the facies B1 debris flow deposits fostered the growth of the facies B2 reef mounds. However, the shallowing was not large enough in magnitude to promote complete reef growth and eventually rising sea level overtook reef mound growth and these incomplete reefs were drowned. This drowning was followed by the gradual return to the shelf slope conditions typical of member A.

D. MEMBER C

Introduction

Member C is best exposed at Trout River where it is between 10 m and 20 m thick. Supplementary exposures occur west of Trout River along the Mackenzie Highway. In addition, lithologies similar to some of those of member C were observed just east of the study area at Middle Kakisa River (Belyea and McLaren, 1962; B. Jones, pers. comm., 1985). This member can readily be distinguished by the occurrence of a bedded coral/echinoderm rudstone at its base and by its abundant and diverse fauna which consists of dome shaped massive corals, low profile massive corals, water stromatoporoids, tabular stromatoporoids, branching corals, solitary corals, brachiopods, gastropods, and spiral nautiloids.

Member C is formed of nine facies, designated C1 through C9 (Fig. 3).

Facies C1: Coral bafflestone blocks

Facies C1 weathers medium green-grey and can be recognized by its occurrence in discrete, semi-resistant blocks (Plates 4, 5A). These blocks are up to 2.0 m high and 3.0 m wide. They have concave-upward bases and have been rotated so that their internal bedding dips at a relatively high angle (Plate 4).

Lithology: The coral bafflestone that comprises the blocks of facies C1 is formed primarily of branching corals which occur in growth position. These corals are generally less delicate and occur in denser colonies than the branching corals in either member A or member B. Large dome-shaped massive corals (up to 35 cm high and 75 cm wide) also occur (Plate 4). The corals of this facies are surrounded by a matrix of light orange-green dolomitic mudstone.

Fauna: Facies C1 contains a very diverse coral fauna. "*Disphyllum*" sp., *Phacellophyllum tructense*, and *Cladopora* sp. are common branching corals while *Phillipsastrea exigua* sensu Smith 1945, *Chuanbeiphyllum vesiculosum* Smith, *Smithicyathus cinctus* (Smith), and *Hexagonaria caurus* (Smith) are common dome-shaped massive corals in facies C1.

Bedding: Very thin planar bedding occurs locally in facies C1 (Plate 4). These beds were lithified early as they are undeformed and they typically acted as the substrate for the growth of branching corals.

Facies C2: Bedded coral/echinoderm rudstone

Facies C2 is characterized by its light orange-green weathered color, its very poorly sorted, coarse grained to granular texture, its bioclastic composition, its irregular planar bedding, and its semi-resistant weathering nature (Plates 4, 5B). It has a variable thickness that ranges up to 3 m (Plate 5C). This facies is generally laterally

continuous in the type section of the Kakisa Formation. However, in places it can be laterally discontinuous (Plate 5C).

Lithology: The bedded coral/echinoderm rudstone of facies C2 is composed of low profile massive corals (maximum 2.0 cm high and 8.0 cm wide) set in a matrix of poorly sorted, very coarse grained bioclastic packstone (Plate 5B). The massive corals, which typically form 30% of the rudstone, have a subhorizontal alignment. They are only slightly abraded and commonly overturned. The bioclastic packstone matrix (Plate 5B) is formed of 55% bioclasts, which range from coarse grained to granular in size, 30% dolomitic mudstone, 10% coarsely crystalline blocky calcite and saddle dolomite cements, and 5% dolomitic mudstone lithoclasts. Some of the coarsely crystalline calcite cement occurs as thin syntaxial overgrowths around echinoderm bioclasts. The rest of the calcite and dolomite cement fills interparticle and shelter pore space. The mudstone is generally concentrated in small patches and thin partings. Up to half of this mudstone has been replaced by fine to medium crystalline anhedral dolomite.

Fauna: *Phillipsastrea exigua*^o sensu Smith 1945 and "*Frechastrea*" sp. nov. are common massive corals in facies C2. The bioclasts in the bioclastic packstone matrix are predominantly echinoderms with fewer branching corals, fenestrate bryozoans, and brachiopods (Plate 5B). Relatively intact colonies of delicate branching corals can occur

floating in the bioclastic matrix.

Bedding: Facies C2 displays thin (average 4.0 cm thick) planar bedding (Plate 4). This bedding is defined by alternating clast-supported and clast-dispersed layers. The clast-supported layers are more resistant to weathering than the clast-dispersed layers. This makes the bedding in facies C2 easy to recognize in the field (Plate 4).

Facies C3: Argillaceous mudstone

Facies C3 is easily recognized by its medium green weathered color, its recessive weathering character (Plate 5C), and lack of identifiable fossils. It is laterally discontinuous in the type section of the Kakisa Formation and has a very variable thickness that ranges up to 1.5 m.

Lithology: The argillaceous mudstone that comprises facies C3 is formed of 50% finely crystalline anhedral dolomite, 25% very fine grained quartz sand, 20% clays, and 5% fine grained bioclasts.

Fauna: No identifiable fossils were found in this facies.

Bedding: Homogenization by bioturbation has obliterated any original sedimentary structures that may have been present in facies C3.

Facies C4: Massive coral bioherms

Facies C4 consists of irregular dome-shaped bioherms that have a maximum height of 3.0 m (Plate 5C). They are

formed primarily of dome-shaped massive corals (average 5.0 cm high and 15 cm wide) set in a matrix of medium green bioclastic wackestone (Plate 6C). The massive corals are in growth position and can comprise up to 50% of the bioherms (Plate 6C). The massive corals *Phillipsastrea exigua* sensu Smith 1945 and "*Frechastrea*" sp. nov. have been identified from these bioherms. Rare wafer stromatoporoids (average 1.0 mm thick and 15 cm wide) also occur.

Facies C5: Coral bafflestone

Facies C5 weathers medium green and can be recognized by the abundant occurrence of branching corals in growth position (Plate 6A). This facies is 1.5 m thick, semi-recessive, and is laterally discontinuous (Plate 5C).

Lithology: The coral bafflestone is formed primarily of stacked colonies of branching corals with fewer numbers of medium sized solitary corals (average 3.0 cm long and 1.5 cm in diameter). Both types of corals occur in growth position and are surrounded by a medium green dolomitic mudstone matrix (Plate 6A).

Fauna: The delicate coral *Phacellophyllum tructense* is the most common branching coral while *Hunanophrentis* sp. nov. and *Piceaphyllum* sp. are common solitary corals.

Bedding: Well defined bedding is absent in this facies.

Facies C6: Coral/stromatoporoid bindstone

Facies C6 weathers medium green and can be identified by the abundant occurrence of low profile massive corals and wafer stromatoporoids in growth position (Plate 6B, 6C). This facies is 1.5 m thick, semi-resistant, and can be laterally continuous in its upper part.

Lithology: Low profile massive corals (average 2.0 cm high and 10 cm wide) and wafer stromatoporoids (average 1.0 mm thick and 20 cm wide) are the most common binders in this facies (Plate 6B, 6C). Tabular stromatoporoids (average 3.0 cm thick and 15 cm wide) and branching corals can also occur in facies C6. The massive corals, wafer stromatoporoids, and tabular stromatoporoids typically occur in growth position (Plate 6B, 6C) while the long axes of the branching corals exhibit a subhorizontal alignment, probably due to post-depositional compaction. The corals and stromatoporoids in this facies are surrounded by a matrix of medium green dolomitic bioclastic wackestone (Plate 6B, 6C).

Fauna: *Phillipsastrea exigua* sensu Smith 1945 and "*Frechastrea*" sp. nov. are common massive corals while *Phacellophyllum tructense* is the most common branching coral in facies C6.

Bedding: The occurrence of low profile massive corals, wafer stromatoporoids, and tabular stromatoporoids in growth position gives facies C6 a coarsely layered texture (Plate 6B).

Facies C7: Massive coral bindstone

Facies C7 is characterized by its orange-brown weathered color, its rubbly, semi-recessive weathering character (Plate 7A), and its abundant massive coral content. This facies is 2.5 m thick and is laterally continuous (Plate 7A).

Lithology: Massive corals dominate facies C7. The massive corals in the lower part of the facies have a low profile (average 2 cm high and 20 cm wide) and occur in growth position. In the upper part of facies C7 the massive corals, which are larger (up to 10 cm high and 40 cm wide) than those in the lower part, are dome-shaped and can be overturned. Facies C7 has a matrix of argillaceous dolomitic bioclastic wackestone. This matrix can comprise over half of facies C7 which gives this facies its semi-recessive weathering character.

Fauna: *Phillipsastrea exigua* sensu Smith 1945 and "*Frechastrea*" sp. nov. are common massive corals in facies C7.

Bedding: Whether they are in growth position or overturned the long axes of the massive corals have a horizontal orientation. This gives facies C7 a coarsely layered texture.

Facies C8: Tabular stromatoporoid framestone

Facies C8 can be recognized by its light brown-grey weathered color, its resistant, massive weathering character

(Plate 7A), and its content of abundant tabular stromatoporoids in growth position (Plate 7D). This facies has a very variable thickness and is laterally continuous (Plate 7A). At Trout River the thickness of facies C8 ranges from 1.5 to 11.5 m (average 5.0 m). The thickness changes are relatively abrupt (Plate 7A). In one extreme example its thickness increases from 1.5 m to 11.0 m over a lateral distance of 50 m. These thickness variations give this facies a very undulatory upper surface.

Facies C8 had the highest primary porosity of all the facies in the Kakisa Formation. This porosity was primarily growth-framework porosity and typically comprised 35% of the facies. Channel porosity and vuggy porosity were also well developed, commonly adding an additional 15% porosity to facies C8. Unfortunately in the Trout River area the porosity has been occluded by various types of carbonate cement and quartzarenite (Plates 7B, 7C, 9D).

Lithology: Tabular stromatoporoids comprise up to 70% of facies C8. These tabular stromatoporoids are stacked in layers (Plate 7D) and their thickness ranges from 0.5 to 12.0 cm (average 2.5 cm). Brachiopods, gastropods, and spiral nautiloids also occur in this facies. These fossils are set in a medium green bioclastic wackestone. The bioclastic wackestone occurs in lenses that average 8.0 cm in thickness and 45 cm in width and occur locally between stromatoporoid layers. The brachiopods, gastropods, and spiral nautiloids are generally concentrated in the upper

part of each lens.

A striking feature of the tabular stromatoporoid framestone is the occurrence of thin (average 2.0 mm thick) bands of ivory colored isopachous calcite cement (Plate 9D). These bands typically occur adjacent to the tabular stromatoporoids but are also dispersed throughout the rest of the tabular stromatoporoid framestone.

Fauna: The stromatoporoids *Strictostroma maclareni*, *Trupetostroma hayense*, and *Hermatostroma maillieuxi* (Lecompte) have been identified from this part of the Kakisa Formation (Stearn, 1966). *Cranaena* sp., *Gypidula* sp., *Theodossia scupulorum* and *Atrypa* sp. are common brachiopods in facies C3.

Bedding: The stacking of the tabular stromatoporoids in the tabular stromatoporoid framestone gives facies C8 a coarsely layered texture (Plate 7D).

Facies C9: Medium grained quartzarenite

Facies C9 can be identified by its siliciclastic composition and its light brown weathered color. It is semi-resistant and fills either cavities or vertical fractures in the upper part of the Kakisa Formation (Plate 7B, 7C).

Lithology: The medium grained quartzarenite has 5% interparticle porosity and is formed of 60% medium grained subangular quartz sand, 25% medium crystalline blocky calcite and dolomite cements, 4% fine grained bioclasts, 3%

small lithoclasts, 2% bitumen, and 1% glauconite. The calcite and dolomite cements fill intergranular pore space. The lithoclasts are composed of bioclastic wackestone that displays a clotted texture and commonly contains ostracods and calcispheres. These lithoclasts closely resemble the medium brown bioclastic wackestones of facies D1. The bitumen occurs in relatively equant fine grained blebs. Larger black fragments (up to 3.0 cm long and 1.5 cm wide) resembling charcoal occur rarely (Plate 7B). The medium grained quartzarenite that fills cavities commonly exhibits thin, parallel, undulatory laminations. The laminated character is created by slight variations in grain size. Conversely, the quartzarenite that fills the vertical fractures does not exhibit bedding.

Fauna: The medium grained quartzarenite contains a well preserved fauna of typical Upper Devonian marine spores (C. Singh, written comm., 1985). *Leiotriletes* sp., *Acinosporites* sp., *Stenozonotriletes* sp., *Archaeozonotriletes variabilis*, and *Cymbosporites* sp. are common spores. The medium grained quartzarenites of the overlying Trout River Formation also contain a similarly well preserved fauna of typical Upper Devonian marine spores (C. Singh, written comm., 1985).

Interrelationship Between Facies

The lower part of member C is formed of a complex lateral and vertical interrelationship of six facies, facies C1-C6 (Fig. 6). The base of this member is composed of two

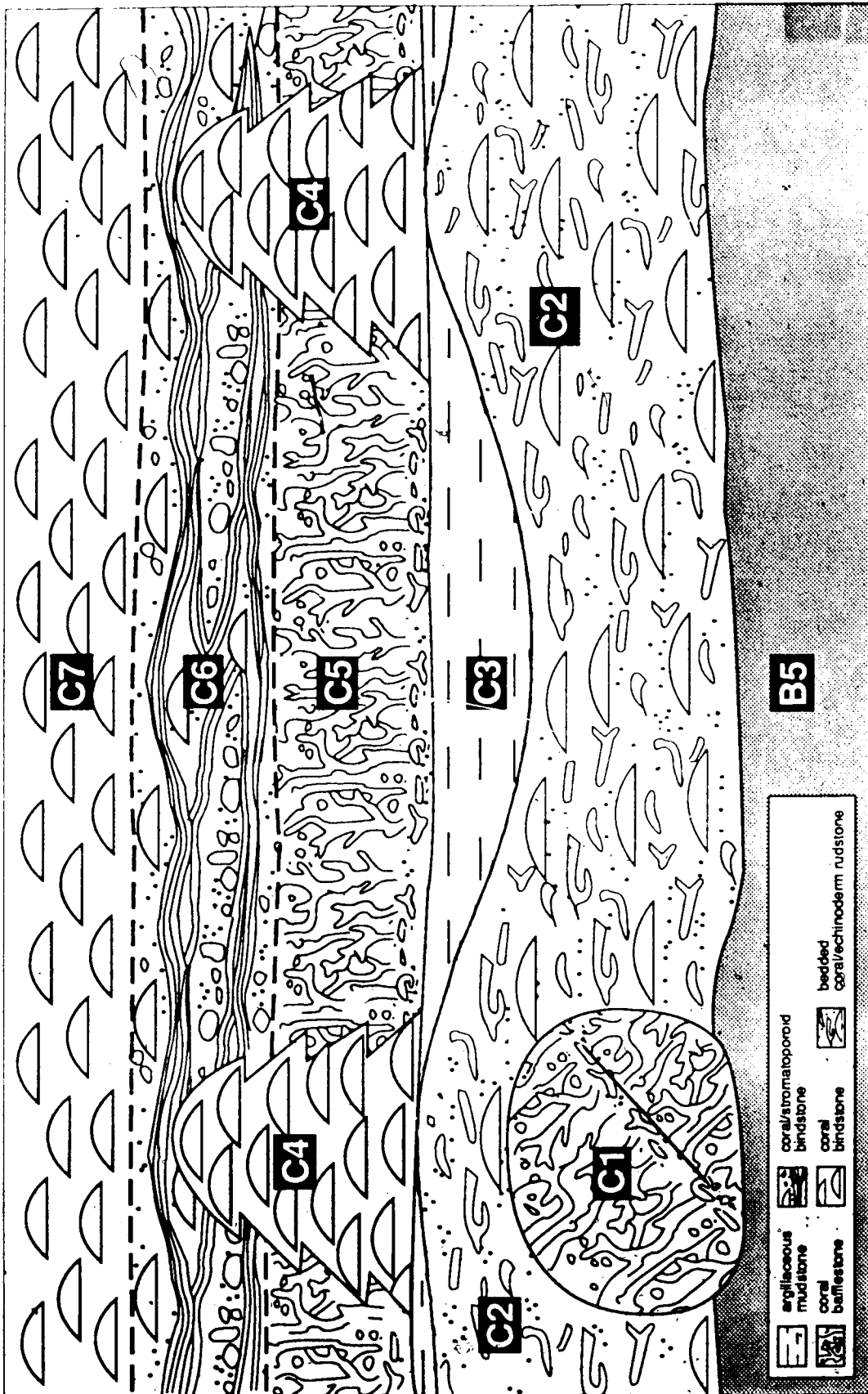


Figure 6. Schematic diagram of the facies and lithologic interrelationships in the lower part of member C.

facies, the coral bafflestone blocks of facies C1 and the bedded coral/echinoderm rudstone of facies C2. The facies C1 blocks are typically overlain and flanked by the rudstones of facies C2 (Fig. 6). Together these two facies form a single unit which is termed unit C1/C2. This unit has an irregular thickness and an erosive basal contact which truncates the upper part of member B (Fig. 6; Plate 4). Its irregular thickness gives this unit an undulatory upper surface.

At Trout River unit C1/C2 is laterally continuous in a north-south direction (i. e. subparallel to the shelf edge). In this direction unit C1/C2 is overlain by the argillaceous mudstones of facies C3 (Fig. 6). However, to the west (i. e. in a seaward direction) this unit terminates abruptly against the facies C3 mudstones. Therefore, to the west facies C3 forms the base of member C.

Based on these observations unit C1/C2 is interpreted to be a sheet-like deposit that is laterally extensive in a north-south direction (i. e. subparallel to the shelf edge) but terminates abruptly into facies C3 in a westward (i. e. seaward) direction. The rare, laterally discontinuous exposures of the unit C1/C2 sheet indicates that this unit has an irregular, ragged western edge. The undulatory upper surface of unit C1/C2 is interpreted to be hummocky in three dimensions.

The massive coral bioherms of facies C4 occur rarely in member C. When they do occur, these bioherms overlie the

thickest (i. e. topographically highest) parts of unit C1 C2 (Fig. 6; Plate 5C).

The coral bafflestones of facies C5 and the coral stromatoporoid bindstones of facies C6 occur between the facies C4 bioherms (Fig. 6). Facies C6 gradationally overlies facies C5 (Fig. 6). Both of these facies interfinger laterally with the bioherms of facies C4 (Fig. 6; Plate 6C). Where they do not reach their maximum height facies C6 can also overlie the bioherms (Fig. 6).

Facies C7 is the first truly laterally extensive facies in member C. The massive coral bindstones of this facies generally gradationally overlie the facies C6 bindstones. However, where the underlying bioherms of facies C4 do reach their maximum height facies C7 overlies facies C4. The facies C8 tabular stromatoporoid framestones directly overlie facies C7 (Plate 7A).

The medium grained quartzarenites of facies C9 fill cavities and vertical fractures in the framestones of facies C8 (Plate 7B, C). The cavities in facies C8 are generally lens-shaped and occur between tabular stromatoporoid layers (Plate 7B). The medium grained quartzarenites in these cavities commonly wrap around the stromatoporoids and can contain stromatoporoid fragments (Plate 7B). The vertical fractures in facies C8 typically show evidence of solution enlargement.

Interpretation

The fact that member C has a more abundant and diverse fauna than that of either member A or member B suggests that it was deposited in shallower, better circulated waters than the other two members. The manner in which the basal contact of unit C1/C2 truncates the upper part of member B implies that the deposition of member C was initiated by an erosive event.

Unit C1/C2 represents an allochthonous deposit derived from a shallower environment than any of the deposits of members A and B. This is indicated by the nature of the exotic fauna that comprises this unit. The coral fauna in unit C1/C2 is much less delicate and more diverse than that of members A and B. In fact, facies C1 has the most robust and diverse coral assemblage of any facies in the Kakisa Formation. This suggests that the corals of this unit grew in shallower, better circulated waters than those of members A and B. In addition, echinoderm fragments are much more common in unit C1/C2 than they are in any of the facies in either member A or member B.

The early lithified beds of facies C1 and the occurrence of this facies in discrete blocks indicates that these blocks were lithified prior to their allochthonous deposition. Early lithification is typical of original deposition in shallow, well-circulated waters (Cook *et al.*, 1972; Bathurst, 1975; Hopkins, 1977; James and Choquette, 1983b).

The significant lime mud content, poor sorting, wide variety of slightly abraded bioclast types, subhorizontal elongate clasts (massive corals in this case), and rotated blocks of unit C1/C2 are all characteristics possessed by debris flow deposits (Cook *et al.*, 1972; Middleton and Hampton, 1973; Davies, 1977; Crevello and Schlager, 1980; Cook and Mullins, 1983). In fact, the rafting-type transportation typical of a debris flow (Middleton and Hampton, 1973) is probably the only mechanism that could have deposited the delicate intact branching corals of facies C2 without breaking them. Debris flow deposition would also explain the abrupt westward termination of unit C1/C2. According to Middleton and Hampton (1973) the terminus of a debris flow deposit is typically abrupt. Furthermore, unit C1/C2 resembles the megabreccia sheets of Cook *et al.* (1972) which have been interpreted as debris flow deposits by these authors. However, unlike facies C2 of unit C1/C2, debris flow deposits generally do not display bedding (Cook *et al.*, 1972; Middleton and Hampton, 1973; Crevello and Schlager, 1980; Cook and Mullins, 1983). Thus, a typical debris flow could not have deposited unit C1/C2. Instead a more complex depositional mechanism must have been responsible for the deposition of this unit.

To delineate this depositional mechanism the cause of the planar bedding in facies C2 must be identified. Hein (1982) determined that bedding defined by alternating clast-supported and clast-dispersed layers of coarse grained

sediment resulted from deposition by pulsating flows. Thus, facies C2 was probably deposited by a pulsating flow. In addition, the bedding of facies C2 resembles the composite bedding of Hendry (1973). He used a process known as progressive liquefaction to explain planar composite bedding. By this process a mass of sediment is liquefied and moved downslope in stages. The uppermost part of the sediment mass has the least confining pressure and therefore will liquefy first. After that part of the sediment mass has been moved downslope, the uppermost part of the remaining sediment will be liquefied and flow downslope. This process will continue until all of the sediment mass has been liquefied and moved downslope. The result is the creation of a pulsating flow (Hendry, 1973). Thus, unit C1/C2 was probably deposited by a pulsating debris flow which caused by progressive liquefaction.

The total homogenization of facies C3 by bioturbation indicates that it was deposited slowly in a low energy environment (Ekdale *et al.*, 1984; Pemberton and Frey, 1984). A low energy depositional environment was probably established above the thinner parts of unit C1/C2. In these areas waters were probably relatively deep and quiet, resembling the shelf slope conditions that typified the area prior to the deposition of unit C1/C2.

The rapid deposition of unit C1/C2 resulted in a sudden shallowing in the area, particularly above the thickest parts of this unit. This sudden shallowing was very similar

to that created by the deposition of the facies B1 debris flow deposits. As with facies B1, the debris flow deposits of unit C1/C2 provided a stable substrate for bioherm growth. The massive coral bioherms of facies C4 colonized the thickest, topographically highest parts of unit C1/C2.

At the same time as the facies C4 bioherms were growing the coral bafflestone of facies C5 was being deposited in the slightly deeper, more poorly circulated waters that existed above facies C3. The synchronous deposition of facies C4 and C5 is indicated by the interfingering relationship between these two facies.

By analogy with Hubbard and Pocock's (1972) study of the growth habits of modern corals, the branching corals that dominate facies C5 are assumed to have grown in deeper, quieter waters than the massive corals that dominate facies C4. Hubbard and Pocock (1972) concluded that sediment rejection by coral polyps and structural resistance to current energy are two of the most important factors in determining growth form variation in recent corals. They maintained that the structurally resistant domal, massive morphology is developed in corals that thrived in well circulated waters where accumulating sediment is most effectively removed from their relatively flat feeding surfaces. Sediment was less likely to accumulate on the feeding surfaces of branching corals with their open structure. Hence, these structurally weaker corals thrived in quieter, more poorly circulated waters than the domal,

massive corals. These findings have been confirmed by James (1983) who claimed that a delicate branching morphology in reef-building skeletal metazoans is more indicative of growth in quieter waters than a domal, massive morphology.

Facies C5 deposition was succeeded by deposition of the coral/stromatoporoid bindstone of facies C6. The interfingering contact between facies C6 and facies C4 illustrates that these two facies were deposited at the same time. As with facies C5, facies C6 was deposited in the deeper, more poorly circulated waters that existed between the facies C4 bioherms. Facies C6 consists of flat-topped filter-feeding organisms such as low profile massive corals. These organisms required more current energy to clear accumulating sediment off of their feeding surfaces than the branching corals of facies C5. Thus, facies C6 was probably deposited in a shallower, better circulated environment than the underlying facies C5. However, since the low profile massive corals and the wafer stromatoporoids of facies C6 were more delicate than the dome-shaped massive corals that dominate the facies C4 bioherms it is probable that facies C6 was deposited in slightly deeper, lower energy waters than facies C4.

Like the massive corals of facies C4 and C6, the massive corals of facies C7 required good water circulation to keep their feeding surfaces clean. The fact that facies C7 is more laterally extensive than facies C4 and C6 implies that this good water circulation was more pervasive during

the deposition of facies C7 than it was during facies C4 and C6 deposition.

The upward increase in size and change from low profile to dome-shaped that the massive corals of facies C7 exhibit is indicative of deposition in an environment of increasing energy and shallowness. According to Tsien (1971), Rożkowska (1980), and James (1983), organisms with a dome-shaped morphology typically grew in more turbulent waters than those with a lower profile morphology. Also, the increase in size presumably made the massive corals more resistant to current energy.

The fact that many of the corals in the upper part of the massive coral bindstone of facies C7 are overturned implies that the waters were turbulent and that the turbulence was relatively constant. This suggests deposition at or above fair weather wave base. Thus, facies C7 marks the upwards growth of member C through fair weather wave base.

The tabular stromatoporoid framestone of facies C8 was deposited in even shallower waters than the upper part of facies C7. This is indicated by the dominant fauna of these two facies. Klovan (1964), Leavitt (1968), and Embry and Klovan (1971) determined that during Upper Devonian time tabular stromatoporoids grew in shallower waters than massive corals. Thus, the tabular stromatoporoid-dominated facies C8 was deposited in shallower waters than the massive coral-dominated facies C7.

In facies C8, the brachiopods, gastropods, and spiral nautiloids that are set in the upper part of the medium green bioclastic wackestone lenses probably grew on the substrate provided by the bioclastic wackestone. The intact nature of these fossils suggests a low energy depositional environment. Such low energy conditions probably existed in the sheltered depressions on the upper surface of the tabular stromatoporoid framestone as it grew upward, stromatoporoid layer by stromatoporoid layer.

The medium grained quartzarenite of facies C9 was emplaced after the tabular stromatoporoid framestone was deposited. This is indicated by the manner in which the quartzarenite fills fractures in the framestone and the way the lens-shaped beds of facies C9 wrap around the tabular stromatoporoids and contain stromatoporoid fragments. The parallel laminations in the lens-shaped beds intimate that these beds were emplaced by fluctuating flows.

The typical Upper Devonian marine spores contained in the medium grained quartzarenites of both facies C9 and the lowermost part of the Trout River Formation along with the marked lithological similarity between these two quartzarenites (both are medium grained, glauconitic, have carbonate cements, and contain the same percentage of quartz sand) cannot be treated as a mere coincidence. Their stratigraphic proximity suggests that the medium grained quartzarenites of facies C9 were derived from the lowermost part of the Trout River Formation.

The lack of evidence of pre-depositional lithification in the facies C9 quartzarenites as well as the parallel laminations in the lens-shaped beds illustrates that these quartzarenites were not lithified prior to their emplacement. Thus, it is assumed that they were emplaced during the deposition of the lowermost part of the Trout River Formation. The evidence of solution enlargement in some of the vertical fractures suggests that some sort of fluid undersaturated in calcium carbonate passed through the fractures before quartzarenite emplacement.

The precise mechanism of facies C9 emplacement is uncertain. The lateral extensiveness of the tabular stromatoporoids gives the tabular stromatoporoid framestone of facies C8 poor vertical permeability. Hence, it is unlikely that the quartzarenites of the lens-shaped beds settled into the lenticular cavities from above. It is assumed, therefore, that the quartzarenites entered facies C8 via the vertical fractures that transect this facies and then spread laterally into the lenticular cavities. The presence of facies D1 derived lithoclasts in the medium grained quartzarenites indicates that these quartzarenites moved through facies D1 on their way down to facies C8.

The dense *in situ* nature of the skeletal carbonates that comprise facies C4 through facies C8 suggests that these five facies represent a reef. The vertical succession of facies that comprise the member C reef is indicative of shallowing upward. The fauna that dominates each successive

facies is representative of deposition in progressively shallower, better circulated waters. The gradational contacts between these facies implies that each progressively shallower water fauna gradually replaced the underlying deeper water fauna. Thus, the upward shallowing was a gradual rather than an episodic process.

The progressive replacement of one community of reef-building organisms by another is known as ecological succession. Walker and Alberstadt (1975) maintained that ecological succession took place in reefs throughout the Paleozoic and Mesozoic. They asserted that in most cases four separate zones of reef growth can be identified: 1) the stabilization zone, 2) the colonization zone, 3) the diversification zone, and 4) the domination zone. The stabilization zone is typically made up of stabilized accumulations of skeletal sand, Pelmatozoans and echinoderms are common components of these sands in the Paleozoic and Mesozoic (James, 1983). The colonization zone represents the initial colonization of the skeletal sand substrate by reef-building organisms. This zone is characterized by massive or, more commonly, branching growth forms. In the diversification zone both the diversity and the variety of growth forms of the reef-building organisms increases greatly. According to James (1983) the diversification zone is where the most pronounced upward building towards sea level occurs. The domination zone is identified by the occurrence of only a few taxa with only one growth habit,

generally massive or lamellar. Most reefs show the effect of fair weather wave base in this zone (James, 1983). As will be illustrated, the member C reef exhibits well developed stabilization, colonization, and domination zones and a poorly developed diversification zone.

Unit C1/C2 represents the stabilization zone of Walker and Alberstadt (1975). The accumulations of bioclastic sand which dominate this unit (the coral/echinoderm rudstones of facies C2) are typical of the stabilization zone.

The composition of the colonization zone varies laterally in member C because the thickness of the stabilization zone (unit C1/C2) varies laterally. The bioherms of facies C4 formed the colonization zone where the stabilization zone was thickest. Where the stabilization was thinner, the colonization zone was composed of a combination of the facies C5 coral bafflestone and the overlying coral/stromatoporoid bindstone of facies C6. In some cases, where the facies C4 bioherms did not achieve their maximum thickness, the facies C6 coral/stromatoporoid bindstone also replaced the massive coral bioherms.

Facies C6 marks the end of the colonization zone and probably represents a poorly developed diversification zone.

The massive coral bindstone of facies C7 and the tabular stromatoporoid framestone of facies C8 together comprise the domination zone of Walker and Alberstadt (1975). The restriction of the fauna in these two facies to a few taxa with one dominant growth habit (tabular), plus

the evidence of the effects of fair weather wave base illustrated by facies C7 are characteristics typical of the domination zone.

The lack of exposure of lateral equivalents of facies C4-C8 in the study area makes it difficult to determine which type of reef these five facies represent, a carbonate buildup or a carbonate bank. However, the occurrence of tabular stromatoporoid framestones similar to those of facies C8 west of Trout River and as far east as Middle Kakisa River suggests that the member C reef was fairly laterally extensive in an east-west direction (i. e. perpendicular to the shelf edge). This combined with the coarsely layered texture and laterally extensive nature of facies C5-C8 in a north-south direction (i. e. subparallel to the shelf edge) implies that the member C reef most closely resembles a carbonate bank.

Thus, like member B, member C deposition can be divided into two main parts. The first part consists of the rapid deposition of the unit C1/C2 debris flow deposits while the second part is formed of the carbonate bank deposits of facies C3-C8. Deposition of the member C debris flow deposits caused a sudden shallowing in the deep shelf environment of member B. This shallowing along with the occurrence of a stable substrate promoted the growth of the member C carbonate bank.

E. MEMBER D

Introduction

Member D crops out at Trout River where its thickness ranges from 0.5 m to 10.5 m. It can be recognized by its medium brown weathering color, its blocky to rubbly weathering character (Plate 8A), and its relatively sparse and restricted fauna. Its fauna is primarily made up of *Amphipora*, calcispheres, ostracods, and gastropods with fewer branching corals, tabular stromatoporoids, and dome-shaped massive corals.

Three unique facies comprise member D, designated D1, D2, and D3. The medium grained quartzarenites of facies C9 also occur in member D.

Facies D1: Mottled bioclastic wackestone

Facies D1 can be identified by its distinct medium brown weathering color, its blocky to rubbly, semi-resistant weathering character, and its sparse fauna (Plate 8A). The weathering character changes upwards in this facies from blocky to rubbly (Plate 8A). Facies D1 has a variable thickness that ranges from 0.5 to 10.5 m in the type section and is laterally continuous.

Lithology: The mottled bioclastic wackestone (Plate 8B) is formed of 40% pseudospar, 30% microspar, 15% fine grained bioclasts, 10% coarsely crystalline blocky calcite cement, and 5% peloids. The pseudospar and microspar dominate

separate parts in the bioclastic wackestone. This gives this lithology a clotted texture on a microscopic scale. The blocky calcite cement fills fractures and occludes intraskeletal porosity.

Fauna: Calcispheres, ostracods, and gastropods are the most common bioclasts in the bioclastic wackestone.

Amphipora and the branching coral *Alveolites* are fairly common in facies D1. Rare thin tabular stromatoporoids (average 1.5 cm thick), wafer stromatoporoids, and the branching coral *Cladopora* sp. occur in the basal part of this facies (Plate 8B), especially where it is thickest. Dome-shaped massive corals (average 4.0 cm high and 10 cm wide) are sparsely distributed in the upper part of facies D1.

Bedding: Where facies D1 is thickest its lower part displays thin (average 7.0 cm thick) planar bedding. Elsewhere primary bedding is not identifiable due to its blocky and rubbly weathering character.

Facies D2: Stromatoporoid/coral bioherms

Facies D2 consists of several small stromatoporoid/coral bioherms (Plate 8C). These bioherms exhibit a variety of morphologies from tabular (average 0.4 m thick and 4.0 m wide) to domal (average 0.8 m thick and 2.3 m-wide). They are formed primarily of tabular stromatoporoids (average 2.0 cm thick) with fewer dome-shaped massive corals (average 20 cm high and 35 cm

wide). Common massive corals are *Wapitiophyllum vallatum* McLean and Pedder, "*Frechastrea*" sp. nov., *Smithicyathus* *infectus* (Smith), and "*Hexagonana*" sp. nov.

Facies D3: Calcareous claystone

Facies D3 can be recognized by its light grey-green weathered color, its rubbly, recessive weathering character, and its lack of megafossils (Plate 8D). This facies ranges between 5 and 15 cm thick and is laterally continuous in the type section.

Lithology: Facies D3 is a medium green poorly indurated calcareous claystone. Its lower part contains rounded fragments of the medium brown mottled bioclastic wackestone of facies D1.

Fauna: Megafossils are absent in this facies but it does contain an abundant and diverse fauna of Upper Devonian spores which is devoid of marine acritarchs (C. Singh, written comm., 1985). *Hystricosporites* sp., *Lophozonotriletes* sp., *Dibolisporites echinaceus*, *Dictyotriletes* sp., *Verruciretusispora* sp., *Phyllotheocotriletes rotundus*, *Apiculiretusispora apsoga*, *Archaeozonotriletes variabilis*, *Dibolisporites* sp., *Chelinospora* sp., *Knoxisporites* sp., and *Contagisporites optivus* are common spores.

Bedding: Facies D3 does not possess well defined bedding although irregular orange subhorizontal bands (average 1.0 cm thick) do occur.

Interrelationship Between Facies

The mottled bioclastic wackestones of facies D1 form most of member D (approximately 80%). This facies gradationally overlies the tabular stromatoporoid framestone of facies C8. The irregular thickness of facies C8 gives facies D1 an undulatory basal contact on a large scale. Facies D1 is thickest where the underlying tabular stromatoporoid framestone is thinnest.

The facies D2 stromatoporoid/coral bioherms are sparsely distributed in member D. They occur above the thicker parts of facies C8 and are overlain by facies D1.

The calcereous claystone of facies D3 gradationally overlies facies D1 and is in turn sharply overlain by the quartzarenites of the lowermost part of the Trout River Formation (Plate 8D). The contact between facies D3 and the Trout River Formation is slightly undulatory (Plate 8E).

Facies C9 fills vertical fractures that truncate facies D1, D2, and D3. The quartzarenite-filled fractures in member D are typically more irregular and difficult to observe in the field than those that occur in the upper part of member C. The difficulty in observing these fractures is caused by the rubbly weathering nature of member D.

Interpretation

The *Amphipora*, calcisphere, ostracod, and gastropod fauna of facies D1 is indicative of the restricted water circulation and increased salinity typical of a lagoonal

environment (Klován, 1964; Murray, 1966; Jenik and Lerbekmo, 1968; Leavitt, 1968; Jamieson, 1971; Machielse, 1972). It is likely that these conditions existed above the upper surface of the member C carbonate bank. The shallowness of the water above the carbonate bank combined with the irregular nature of its upper surface was probably enough to create the restricted conditions necessary for the deposition of facies D1.

The stromatoporoid/coral bioherms of facies D2 grew in the better circulated waters that were present above the thicks in facies C8. These bioherms are reminiscent of the patch reefs that occur in the lagoons of modern carbonate environments.

Facies D3 with its claystone lithology, green and orange color, poor induration, and lack of bedding resembles the paleosols described by Ruhe *et al.* (1961), Walls *et al.* (1975), and Prather (1984). Also, the irregular, rubbly nature of its basal contact and its content of rounded lithoclasts from the underlying sediments are two characteristics possessed by the paleosols described by Prather (1984). Furthermore, the stratigraphic location of facies D3 at the top of the Frasnian Stage correlates with a major eustatic drop in sea level (see Johnson *et al.*, 1985). According to Kendall and Schlager (1981) only a small drop in sea level is required to subaerially expose a carbonate shelf causing karst and/or soil development and the subsequent formation of an unconformity in the geologic

record. The Frasnian/Famennian boundary is generally regarded as an unconformity (e.g. Bassett and Stout, 1967; Law, 1971; Davies, 1987).

In addition to the facies D3 paleosol, other lithological evidence of subaerial exposure is present in the upper part of the Kakisa Formation. The solution enlarged vertical fractures of facies C8, the clotted texture, peloids, and brown color of the facies D1 bioclastic wackestones are all features commonly associated with subaerial exposure (James, 1972; Walls *et al.*, 1975; Harrison, 1977; Kahle, 1977, 1978; Esteban and Klappa, 1983; James and Choquette, 1984; Prather, 1984).

F. DEPOSITIONAL HISTORY

Introduction

The reconstruction of the depositional history of the Kakisa Formation will be done in four stages. First, the depositional framework of the formation will be outlined. Second, the sequence of events responsible for the deposition of the formation will be discussed. Third, the importance of debris flow deposition to the depositional history of the Kakisa Formation will be discussed.

Depositional Framework

The depositional framework of the Kakisa Formation refers to the more regional geological features that

affected Kakisa deposition. In order to understand the details of its deposition it is essential to be familiar with the depositional framework of the Kakisa Formation.

The Kakisa Formation represents an overall shallowing-upward sequence. This is indicated by the fact that its deposition was initiated below fair weather wave base in a shelf slope environment and was terminated above fair weather wave base in a restricted lagoonal environment.

The phenomenon of shallowing-upward is typical of many carbonate sequences and occurs during sea level rises (Kendall and Schlager, 1981; Wilkinson, 1982; James and Mountjoy, 1983; James, 1984). In their sea level curve for the Devonian Johnson *et al.* (1985) documented the occurrence of a relative sea level rise during late Frasnian time. They maintained that this rise was restricted to the Lower *triangularis* conodont zone. The limestones of the Kakisa Formation were deposited during this rise.

During the deposition of the Kakisa Formation the shoreline in the area had a general north northwest-south southeast trend. This trend is indicated by the north northwest-south southeast alignment of both the dome-shaped massive corals in facies A2 and the reef mounds of facies B2. This alignment was probably caused by the presence of a similar trending current at the time of massive coral and reef mound growth. That current would have provided food to the dome-shaped massive corals and the reef mounds. Currents of this type have been widely documented in modern and

ancient carbonate environments where they have generally been demonstrated to parallel shoreline (for a summary see Cook and Mullins, 1983). In addition, this trend corresponds with that of the shelf margin illustrated on the paleogeographic maps of Bassett and Stout (1967) and Ziegler (1967).

The Kakisa Formation is interpreted to have formed on a depositional margin (Fig. 7) similar to that outlined by James and Mountjoy (1983) and McIlreath and James (1984). This margin would have dipped at a low angle to the west southwest (i. e. perpendicular to the shelf edge and in a seaward direction). The argillaceous and moderately fossiliferous limestones of facies A1, A2, B4, and B5 were deposited on the shelf slope of this margin (Fig. 7). These facies represent background hemipelagic slope deposition. The facies A3 and B6 storm deposits and the debris flow deposits of facies B1 and unit C1/C2 were also deposited on the shelf slope (Fig. 7). The reef mounds of facies B2 grew on the shelf slope, just downslope of the shelf margin (Fig. 7). The carbonate bank of facies C4-C8 began its growth on the shelf slope and grew upwards to form the shelf margin (Fig. 7). The lagoonal deposits of member D were deposited just shoreward of the shelf margin; the facies D2 patch reefs growing above the thicker accumulations of the underlying carbonate bank (Fig. 7). Both facies C9 and D3 accumulated after the cessation of Kakisa deposition and therefore were not included in Figure 7.

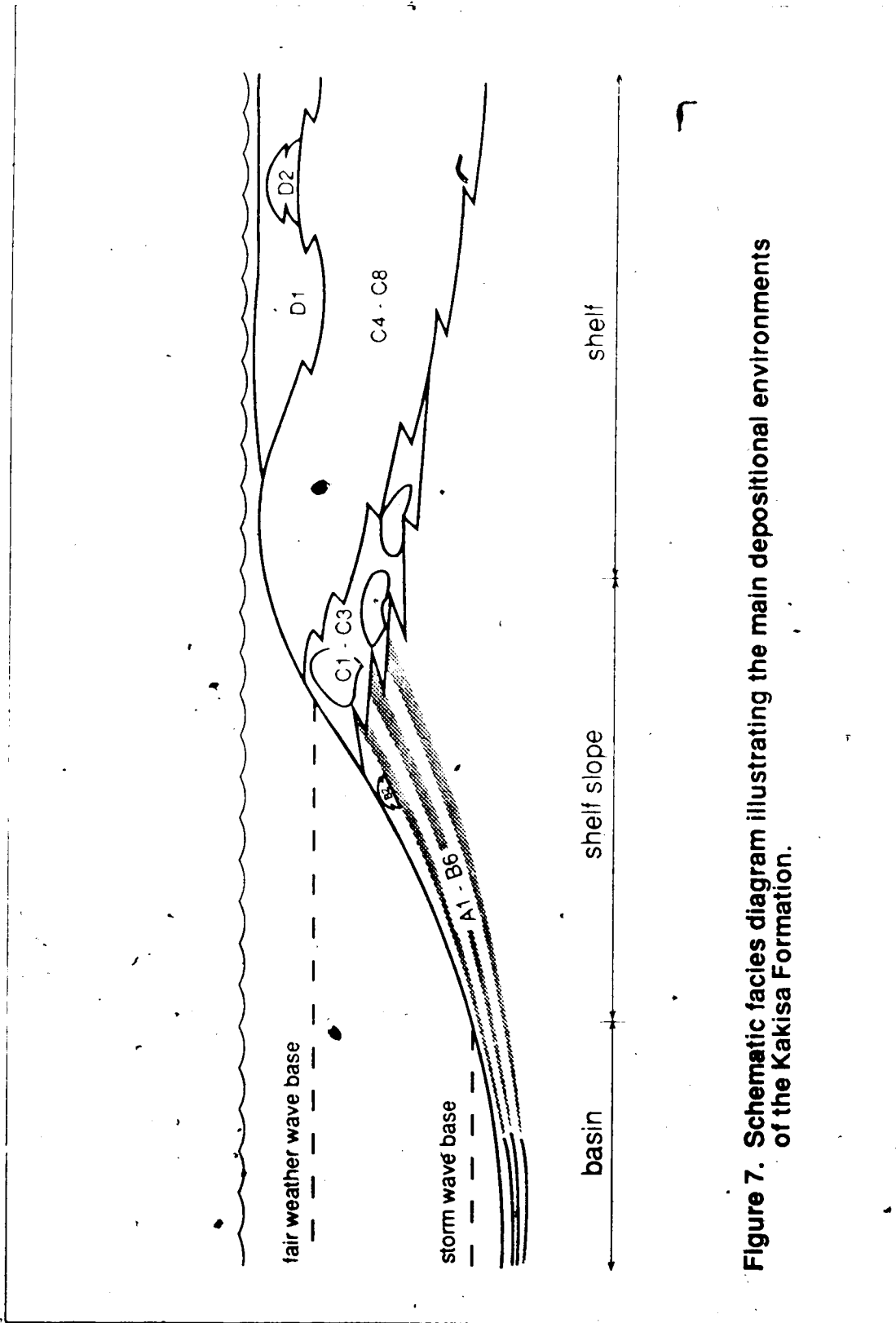


Figure 7. Schematic facies diagram illustrating the main depositional environments of the Kakisa Formation.

Succession of Events

Now that we are familiar with the depositional framework of the Kakisa Formation we are better equipped to understand the succession of events responsible for Kakisa deposition. Deposition of the Kakisa Formation began with the cyclically repeated deposition of the shelf slope limestones of member A (Fig. 3). Each of the three cycles that comprise this member represents a discrete shallowing-upward sequence (Fig. 3).

The sudden influx of the debris flow deposits of facies B1 marked the cessation of member A deposition and the initiation of member B sedimentation. The rapid deposition of this facies created a relative shallowing in the area (Fig. 3). This relative shallowing resulted in an increase in water circulation sufficient enough to promote the growth of the facies B2 reef mounds. Based on the thinness (average 0.5 m) of the coral/echinoderm rudstones of facies B1 the amount of relative shallowing necessary to initiate mound growth was probably not great. Perhaps equally important to reef mound initiation was the stable substrate provided by these rudstones.

The rate of relative sea level rise gradually overtook the sudden shallowing created by the deposition of facies B1 and a deepening-upward sequence of shelf slope lithologies was laid down above the reef mounds (Fig. 3). This deepening-upward resulted in the re-establishment of shelf slope conditions similar to those that existed during the

deposition of member A. However, deposition of the debris flow deposits of unit C1/C2 caused another sudden shallowing in the area (Fig. 3). The greater thickness of unit C1/C2 suggests that this unit fostered a more marked relative shallowing than the debris flow deposits of facies B1.

Growth of the member C carbonate bank was initiated in the shallow waters above the debris flow deposits of unit C1/C2 (Fig. 3). The precise mode of initiation varied laterally and was dependant on the relative thicknesses of the underlying debris flow deposits. The bank is composed of a single shallowing-upward sequence (Fig. 3).

Conditions of restricted water circulation and increased salinity were developed above the member C carbonate bank and the restricted limestones of member D were deposited in this environment.

Deposition of the Kakisa Formation ceased following a sea level drop that subaerially exposed the upper part of the formation (Fig. 3). The paleosol that comprises facies D3 was formed following this drop in sea level as were the solution-enlarged vertical fractures that truncate member D and the upper part of member C.

A sea level rise then resubmerged the Kakisa Formation (Fig. 3). Johnson *et al.*'s (1985) sea level curve portrays this rise as being of a relatively large magnitude. This rise was followed by the deposition of the marine quartzarenites of the lower part of the Trout River Formation. Some of these quartzarenites filtered down into

cavities in the member C carbonate bank through the solution-enlarged vertical fractures.

Debris Flow Deposition

The two debris flow deposits (facies B1 and unit C1/C2) that occur in the Kakisa Formation are particularly important to the depositional history of the formation for two reasons. First, these deposits drastically altered the depositional regime in existence prior to their deposition. In the case of facies B1, the sudden shallowing created by the deposition of this debris flow deposit changed the depositional regime from one characterized by the cyclic deposition of shallowing-upward sequences to one characterized by the deposition of a single deepening-upward sequence (Fig. 3). In the case of unit C1/C2, the sudden shallowing resulting from the deposition of this debris flow deposit caused the existing deepening-upward depositional regime to change to one characterized by the deposition of a single shallowing-upward sequence (Fig. 3).

Second, the two debris flow deposits are important from an economic standpoint. In both cases these deposits are responsible for the growth of reefs in the Kakisa Formation as they provided the sudden shallowing and subsequent improved water circulation as well as the stable substrate necessary for reef initiation. In western Canada Upper Devonian carbonate buildups can form very prolific hydrocarbon reservoirs. In addition, debris flow deposits

can also form excellent hydrocarbon reservoirs (Cook and Mullins, 1983). Hence, if the explorationist understands debris flow deposition he is better equipped to search for two types of hydrocarbon reservoirs in the subsurface.

Furthermore, the type of reef initiated was controlled by the thickness of the precursor debris flow deposit. The thicker unit C1/C2 debris flow deposits created a greater relative shallowing and a greater, more widespread improvement in water circulation than the thinner facies B1 deposits. As a result a more laterally extensive complete reef was initiated above unit C1/C2 while isolated incomplete reefs (reef mounds) were initiated above facies B1.

According to Davies (1977), Kendall and Schlager (1981), James and Mountjoy (1983), Bosellini (1984), and Mullins *et al.* (1986) sediment gravity flow deposition commonly accompanies periods of shelf progradation. In the case of the Kakisa Formation the deposition of unit C1/C2 debris flow deposits was followed by the west southwestward progradation of the member C carbonate bank into the Trout River area.

The composition of the debris flow deposits suggests that they were derived from the area just seaward of the prograding member C carbonate bank. The facies B1 and unit C1/C2 debris flow deposits are composed primarily of massive corals, echinoderms, bryozoans, branching corals, and brachiopods. This type of faunal assemblage thrived in

moderately turbulent waters which typically existed just downslope of Upper Devonian reefs (Klován, 1966; Murray, 1966; Jeník and Lerbekmo, 1968; Leavitt, 1968; Jamieson, 1971). This agrees with McIlreath and James' (1984) suggestion that sediment gravity flow deposits on the shelf slope are derived from the unstable accumulations of lime sand and gravel that build up near the shelf margin.

Despite their importance to the depositional history of the Kakisa Formation, the mechanism responsible for the debris flow deposits of facies B1 and unit C1/C2 is unknown. Several possibilities exist including: fault movement, earthquake shocks, tsunamis, and gravity acting on oversteepened shelf slopes. Whatever the mechanism responsible for the generation of the unit C1/C2 debris flow it must have been of high enough energy to dislocate the large pre-lithified blocks of facies C1. Cook *et al.* (1972) favored an earthquake shocks for the initiation of the debris flows responsible for the deposition of the megabreccia and finer rudite sheets they described from the Canadian Rocky Mountains. Hendry (1973) also proposed an earthquake as the generating mechanism for the debris flow deposits he described from Quebec.

III. DIAGENESIS

A. INTRODUCTION

Interest in the Upper Devonian carbonate sequences of western Canada has resulted from the desire to better understand the nature of the prolific hydrocarbon reservoirs contained in these sequences. Earlier studies of Upper Devonian carbonates concentrated on various aspects of stratigraphy, sedimentology, and paleontology (e. g. Klovan, 1964; Murray, 1966; Stearn, 1966; Jenik and Lerbekmo, 1968; Leavitt, 1968; Embry and Klovan, 1971; Jamieson, 1971; Machielse, 1972). However, many of the more recent studies have concentrated on the diagenesis of these sequences (e. g. Havard and Oldershaw, 1976; Walls *et al.*, 1979; Mattes and Mountjoy, 1980; Wong and Oldershaw, 1981; Walls and Burrowes, 1985; Machel and Mountjoy, 1987). The increasing emphasis on diagenesis has resulted from the desire to better understand the processes responsible for the creation and destruction of porosity in Upper Devonian carbonate reservoirs and hence, predict the occurrence of good reservoirs.

At one time parts of the Kakisa Formation, especially facies C8, exhibited excellent porosity. However, as a result of diagenesis virtually all of this porosity has been occluded. In this chapter the major diagenetic features of the Kakisa Formation will be discussed. Four main processes were important in the diagenesis of the Kakisa Formation: 1)

fracturing, 2) dissolution, 3) cementation, and 4) replacement. These processes were responsible for generating a variety of diagenetic features. Eight diagenetic features will be discussed: 1) chemical solution features, 2) pressure solution features, 3) isopachous calcite cement, 4) unzoned blocky calcite cement, 5) zoned blocky calcite cement, 6) syntaxial rim cement, 7) saddle dolomite, and 8) anhedral dolomite. The timing and mechanism of formation of each feature will be determined in this chapter. This information will then be integrated to help reconstruct the diagenetic history of the Kakisa Formation.

B. FRACTURING

Introduction

Although it could be argued that fracturing is not truly a diagenetic process, fracturing is important to the diagenesis of the Kakisa Formation because the fractures acted as conduits for the diagenetic fluids. Fractures also created the greatest amount of secondary porosity in the formation. Furthermore, since fractures commonly truncate, are modified, or are filled by various diagenetic fabrics they can be used to help determine the relative timing of formation of those fabrics.

Fractures

Description: Fractures are common throughout the Kakisa Formation. They have a dominant vertical to subvertical orientation. Fractures are best developed in facies C8 and D2 but are also common, but not as well defined, in the rubbly weathering limestones of facies D1 (Plates 7C, 8A, 8B, 8C, 9A, 9B, and 9D). These fractures range up to 3 cm in width and 20 cm in length and typically have been enlarged by chemical dissolution.

Timing of formation: The solution enlargement of the fractures in facies C8 and D2 indicates that chemical dissolution followed fracturing (Fig. 8). The wider fractures are typically filled by medium grained quartzarenites (Plate 7C), which were derived from the overlying Trout River Formation, while the smaller fractures can be filled with one or more of the following: unbedded blocky calcite (Plate 9A, 9D), zoned blocky calcite, saddle dolomite, or medium grained quartzarenite. The fact that fractures in facies C8 commonly truncate the isopachous calcite cement (Plate 9D) demonstrates that fracturing succeeded isopachous calcite cementation (Fig. 8).

Mechanism of formation: The vertical to subvertical orientation of the fractures suggests that they were formed by tensional forces. These fractures probably represent joints formed while the Kakisa limestones were subaerially exposed. Solution-enlarged joints are typical of subaerially exposed limestones (Esteban and Klappa, 1983; V. P. Wright,

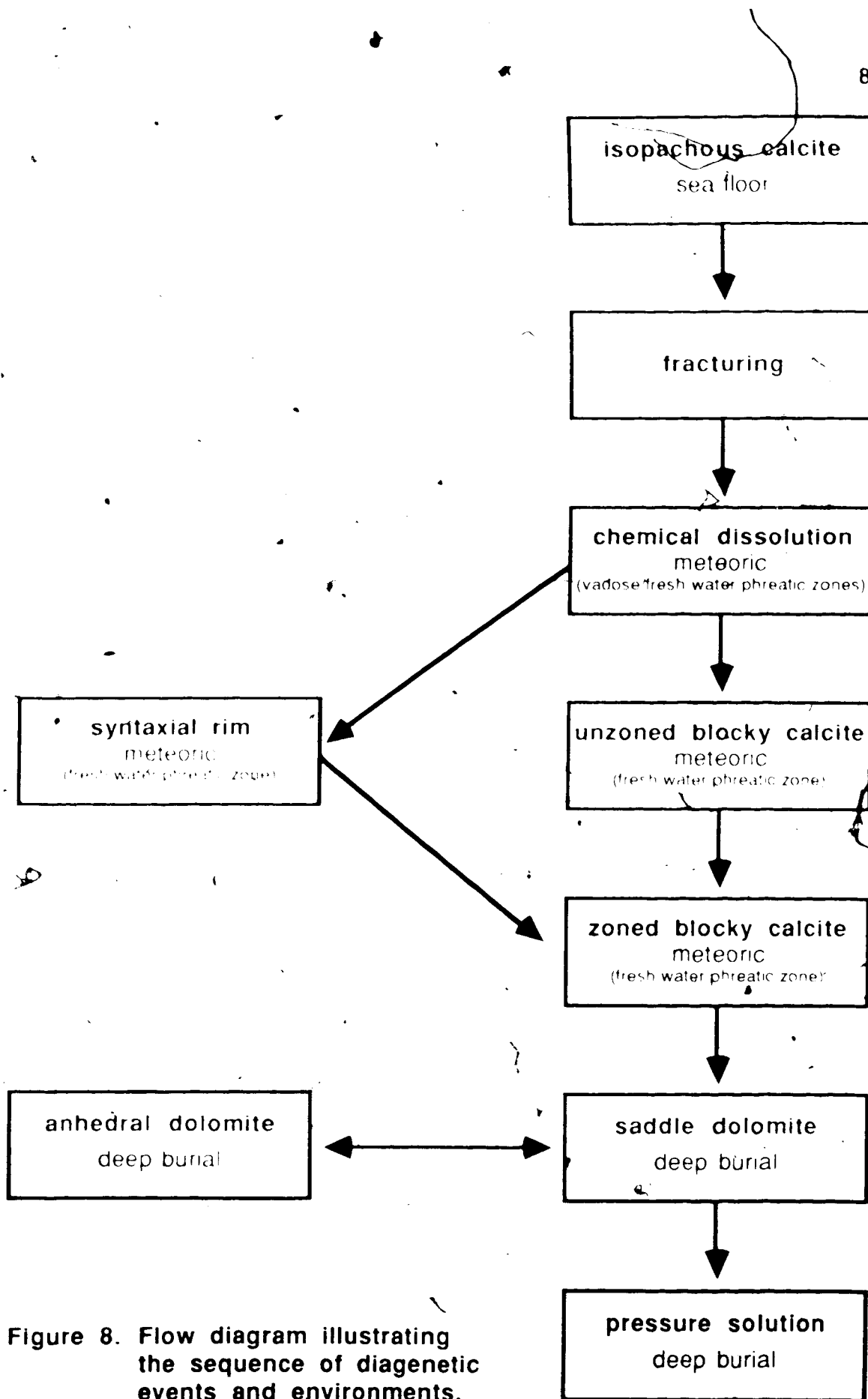


Figure 8. Flow diagram illustrating the sequence of diagenetic events and environments.

pers. comm., 1987). Vertical joints probably form in response to the lateral unloading that occurs once the limestones have been removed from the buoyant forces of sea water (V. P. Wright, pers. comm., 1987). The confinement of the fractures to the upper part of the Kakisa Formation further suggests that subaerial exposure was responsible for their generation.

C. SOLUTION

Introduction

Solution is responsible for the removal of carbonate from the Kakisa Formation. Two types of carbonate solution occurred in the Kakisa Formation: 1) chemical dissolution, and 2) pressure solution. Chemical dissolution features are much less common than pressure solution features. Yet, next to fracturing, chemical dissolution was responsible for the generation of the most secondary porosity in the Kakisa Formation.

Chemical Dissolution

Description: The effects of chemical dissolution are most apparent in facies C8 and D2 where it created channel and some vuggy porosity. The channel porosity was produced through solution-enlargement of fractures. These fractures can range up to centimeters in width. Vugs are relatively rare in the Kakisa Formation.

Timing of formation: Chemical dissolution preceded the precipitation of unzoned blocky calcite cement, zoned blocky calcite cement, and saddle dolomite (Fig. 8). This is indicated by the fact that these cements can fill or partly fill the solution-enlarged fractures and vugs in facies C8. Chemical dissolution also predated deposition of the medium grained quartzarenites of the Trout River Formation as is illustrated by the occurrence of these quartzarenites in many of the solution-enlarged fractures.

Mechanism of formation: Chemical dissolution occurs in diagenetic environments where pore fluids are undersaturated with respect to calcium carbonate; meteoric water being the most common such fluid (Longman, 1980; Flügel, 1982; James and Choquette, 1984). Pore fluids are most likely to be undersaturated in the vadose zone of the meteoric diagenetic environment (Longman, 1980; Esteban and Klappa, 1983). However, chemical dissolution can also take place in the fresh water phreatic zone of the meteoric diagenetic environment (Longman, 1980; Flügel, 1982; Esteban and Klappa, 1983; James and Choquette, 1984). According to Longman (1980) and Flügel (1982) this is particularly common where fractures or some other form of permeability pathway has allowed meteoric waters to pass from the vadose zone into the fresh water phreatic zone before these waters had a chance to become saturated with respect to calcium carbonate. In addition, Runnels (1969) has demonstrated that chemical dissolution can occur in the mixed water zone while

Druckman and Moore (1985) have documented chemical dissolution in the deep burial environment. Thus, it is possible for chemical dissolution to occur in four different diagenetic regimes.

The confinement of the chemical dissolution features to the upper part of the Kakisa Formation suggests that chemical dissolution took place in the vadose and/or the fresh water phreatic zones. Much of the chemical dissolution occurred along fractures which formed following the subaerial exposure of the Kakisa Formation. This subaerial exposure would have allowed the formation of a meteoric diagenetic environment. Thus, it is assumed that chemical solution occurred in the meteoric diagenetic environment, either in the vadose zone and/or the fresh water phreatic zone.

Pressure Solution

Description: Stylolites and microstylolite swarms are the most common pressure solution features in the Kakisa Formation. Both of these features occur parallel or subparallel to bedding. The stylolites have an amplitude of up to 4.0 mm and occur most commonly in the tabular stromatoporoid framestone of facies C8 (Plates 9B, 9C) and the stromatoporoid/coral bioherms of facies D2. Bitumen is commonly concentrated along these stylolites (Plate 9C). Microstylolite swarms, whose amplitude ranges up to 0.4 mm, are more widespread. They occur in the clay-rich matrices of

facies A1, A2, B4, B5, C1, C2, C3, C4, C5, C6, C7, and D1.

Timing of formation: The stylolites in facies C8 can occur between the zoned blocky calcite cement and its substrate as well as between the saddle dolomite cement and its substrate (Plate 9C). They also cut through unzoned blocky calcite, zoned blocky calcite, and saddle dolomite. This suggests that stylolitization post-dated the precipitation of all three of these cements (Fig. 8). In addition, stylolites can cut across the solution-enlarged fractures of facies C8. The common concentration of bitumen along the stylolites suggests that hydrocarbon migration accompanied stylolite formation in the Kakisa Formation.

Mechanism of formation: Pressure solution results from selective solution at grain contacts that have been excessively stressed by overburden or tectonic stresses (Bathurst, 1975). Wanless (1979) claimed that stylolites result from sutured-seam solution and occur in carbonates that are both structurally resistant to stress and contain little clay or platy silt. Conversely, he suggested that microstylolite swarms are the product of nonsutured-seam solution in carbonates that contain significant amounts of clay or platy silt. This would explain the preferential occurrence of stylolites in the structurally resistant, clay- and platy silt-poor limestones of facies C8 and D2, and the common occurrence of microstylolite swarms in the clay-rich limestones of facies A1, A2, B4, B5, C1, C2, C3, C4, C5, C6, C7, and D1.

D. CEMENTATION

Introduction

Cementation is the filling of pore space by chemically precipitated authigenic minerals (Bathurst, 1975). Therefore, unlike solution, cementation is responsible for the net addition of carbonate to the Kakisa Formation. Cementation accounts for the greatest amount of porosity destruction in the Kakisa Formation.

Based on the criteria outlined by Bathurst (1975, p. 417-19) cement can be identified by the presence of several or all of the following features: 1) sharp crystal contact with its substrate, 2) lack of relict structures, 3) plane intercrystalline boundaries, 4) a regular vectoral increase in crystal size away from its substrate, 5) a high percentage of enfacial junctions between crystals, and 6) the occurrence of two generations of crystal growth. Five varieties of cement occur in the rocks of the Kakisa Formation: 1) isopachous calcite, 2) unzoned blocky calcite, 3) zoned blocky calcite, 4) syntaxial rim and 5) saddle dolomite.

Isopachous Calcite Cement

Description: The isopachous calcite (Plate 9D, 9E) is restricted to facies C8 where it occurs in thin bands (average 2 mm thick) and can occlude up to 35% of the growth-framework interparticle, and intraparticle porosity.

The growth framework porosity has an irregular distribution in facies C8 but is most commonly located between layers of stromatopora. The intraparticle porosity generally occurs within brachiopods and gastropods while the interparticle porosity typically occurs between these fossils. The isopachous calcite cement lines the walls of this pore space.

Timing of formation: The isopachous calcite lines the pore walls which implies that it is an early phase cement. This cement is commonly truncated by the vertical fractures that transect facies C8 (Plate 9D) suggesting that it was precipitated before fracturing occurred (Fig. 8).

Mechanism of formation: Isopachous calcite cement is common in Upper Devonian reefs (e. g. Krebs, 1969; McGillivray and Mountjoy, 1975; Walls *et al.*, 1979; Burchette, 1981; Wong and Oldershaw, 1981; Walls and Burrowes, 1985). It resembles the syndepositional calcite cement of modern reefs described by Schroeder (1972), James *et al.* (1976), and MacIntyre (1977). Like its modern counterpart, the isopachous calcite cement of ancient carbonates is interpreted as a syndepositional precipitate formed under high energy conditions in the sea floor diagenetic environment (Krebs, 1969; Walls *et al.*, 1979; Longman, 1980; James and Choquette 1983b; Walls and Burrowes, 1985). The high energy conditions would have caused large volumes of sea water to be pumped through the pores of the rock and, hence, foster precipitation of the

isopachous calcite cement in these pores. Thus, the isopachous calcite of facies C8 was probably precipitated syndepositionally in the sea floor diagenetic environment. This concurs with the earlier observation that it was probably an early phase cement.

Unzoned Blocky Calcite Cement

Description: The unzoned blocky calcite (Plates 9A, 10C) generally occurs in mosaics of very coarse crystals (0.03-4.5 mm diameter) which are either white or clear in hand sample (Plate 9D). This cement is most common in facies C8 where it typically occludes 30% of the porosity. It fills or partly fills growth-framework (Plate 9D), channel (Plate 9A, 9D), interparticle, and intraparticle porosity in this facies. Unzoned blocky calcite cement is also distributed throughout the other facies of the Kakisa Formation where it fills shelter, interparticle, and intraparticle porosity.

Timing of formation: In facies C8 unzoned blocky calcite commonly fills or partly fills the center of pores whose walls are lined by isopachous calcite (Plate 9D). In addition, zoned blocky calcite (discussed in more detail in the next section) can occur in the center of pores lined by isopachous calcite and/or unzoned blocky calcite. This cement stratigraphic relationship suggests that the isopachous calcite was precipitated prior to the unzoned blocky calcite and that the zoned blocky calcite was precipitated after the unzoned blocky calcite (Fig. 8).

Also, the filling of the channel pores in facies C8 by the unzoned blocky calcite (Plate 9A) illustrates that this cement was precipitated after fracturing and chemical dissolution (Fig. 8).

Mechanism of formation: The very coarse texture of the unzoned blocky calcite probably reflects a slow rate of crystallization under stable, uniform conditions.

Precipitation of unzoned blocky calcite cement has typically been assigned to the fresh water phreatic zone (Longman, 1980; Flugel, 1982; James and Choquette, 1984). However, more recently precipitation of unzoned blocky calcite has also been documented from the deep burial diagenetic environment (Choquette and James, 1987).

Zoned Blocky Calcite Cement

Description: The zoned blocky calcite (Plate 10A) occurs in mosaics of coarse crystals (0.1-3.5 mm diameter) which are light brown colored in hand sample. The zoning is the result of alternation of bands of ferroan and nonferroan calcite and can be detected in thin section by use of potassium ferricyanide stain (Plate 10A). According to Evamy (1969) the amount of ferrous iron needed to generate a response to potassium ferricyanide stain is in the order of 100 ppm.

The zoned blocky calcite occurs most commonly in facies C8 where it typically occludes 15% of the porosity. In this facies it generally fills or partly fills growth-framework,

interparticle, intraparticle, and channel porosity. Zoned blocky calcite cement can also occlude shelter porosity, interparticle porosity, and intraparticle porosity in the other facies of the Kakisa Formation.

Timing of formation: The cement stratigraphic relationship outlined in the preceding section indicates that the zoned blocky calcite was precipitated after the unzoned blocky calcite (Fig. 8). Furthermore, the presence of the medium grained quartzarenites of facies C1 can fill the center of pores that have not been totally occluded by zoned blocky calcite. This indicates that the zoned blocky calcite was precipitated before the emplacement of the Trout River Formation-derived quartzarenites (Fig. 8).

Mechanism of formation: The very coarse texture of the zoned blocky calcite cement probably reflects a slow rate of crystallization under stable, uniform conditions. It is generally agreed that ferroan calcite is formed under reducing conditions (Evamy, 1969; Meyers, 1974; Richter and Fuchtbauer, 1978; Wong and Oldershaw, 1981; James and Choquette, 1984). Reducing conditions are typically created by the bacterial decomposition of organic matter (Richter and Fuchtbauer, 1978; Wong and Oldershaw, 1981; Scholle and Halley, 1985) and can occur anywhere below the water table (Evamy, 1969; Meyers, 1974; James and Choquette, 1984). This means that reducing conditions can occur in the meteoric, mixed water, and deep burial diagenetic environments.

The zoning in the zoned blocky calcite cement records changes in the precipitational environment during the time of crystal growth. Each zone in zoned calcite cement is deemed to represent a different diagenetic time horizon (Givamy, 1969; Meyers, 1974; Wong and Oldershaw, 1981). Wong and Oldershaw (1981) noted that these changes can result from fluctuations in either the Fe^{2+}/Ca^{2+} ratio of the pore fluids or the amount of ferrous iron supplied to those fluids. Zoning has been documented from both the fresh water phreatic zone (Meyers, 1974) and the deep burial environment (Wong and Oldershaw, 1981). In the case of the zoned blocky calcite of the Kakisa Formation, zoning probably occurred in the fresh water phreatic zone. This is based on the observation that precipitation of this calcite occurred before the emplacement of the facies C9 quartzarenites and, hence, before the deposition of the lower part of the Trout River Formation. The lower part of the Trout River Formation was deposited after the resubmergence of the subaerially exposed Kakisa Formation. Prior to this resubmergence the Kakisa limestones resided in the meteoric diagenetic environment. Thus, the zoned blocky calcite must have been formed in the fresh water phreatic zone as the Kakisa limestones did not reside in the deep burial diagenetic environment until long after the deposition of the lower part of the Trout River Formation. The fact that the zoned blocky calcite was precipitated after the unzoned blocky calcite indicates that the unzoned calcite was also formed

in the fresh water phreatic zone, rather than the deep burial environment.

Syntaxial Rim Cement

Description: Syntaxial rim cement (Plate 10A) is a special form of unzoned blocky calcite. In the Kakisa Formation this cement typically occurs as a crystal surrounding an echinoderm nucleus. The rim was developed in optical continuity with its nucleus. Syntaxial rim cement is most common in facies B1 and C1 where it fills interparticle porosity (Plate 10B). It is much more abundant and coarsely crystalline in facies B1 than it is in facies C1. In facies B1 it comprises 25% of the bioclastic packstone matrix, and its crystals range up to 1.5 mm in width. Meanwhile in facies C1 syntaxial rim cement comprises only 10% of the bioclastic packstone matrix and its crystals range up to 0.5 mm in width.

Timing of formation: The relative timing of formation of the syntaxial rim cement cannot be determined from petrographic observation. However, by examining its mechanism of formation a good estimation of its relative timing of formation can be made.

Mechanism of formation: It is generally agreed that precipitation of syntaxial rim cement occurs under the influence of meteoric waters in the fresh water phreatic zone (Longman, 1980; Flügel, 1982; James and Choquette, 1984; Walkden and Berry, 1984). Therefore, the occurrence of

syntaxial rim cement in facies B1 and C2 requires that these two facies were exposed to meteoric waters.

There has been some disagreement on the precise mechanism of formation of syntaxial rim cement in rocks that contain significant quantities of lime mudstone. The brecciated wackestone matrices of facies B1 and C2 fall into this category. In this case the model of passive precipitation into primary pore space adopted by Evamy and Shearman (1969, 1967) to explain the formation of syntaxial rim cement in mudstone free carbonates such as grainstones cannot be used. Bathurst (1958, 1975) and Orme and Browne (1963) claimed that in mudstone rich carbonates syntaxial rim cement was formed as a neomorphic replacement of the adjacent lime mudstone. Each rim was formed by the simultaneous dissolution of the mudstone and precipitation of calcite cement. According to Bathurst (1958) this process occurred across a very thin solution film. More recently, however, a new mechanism of formation was proposed by Walkden and Berry (1984). Through the use of cathodoluminescence petrography these authors determined that selective meteoric dissolution of lime mud occurred around the echinoderm fragments and that this was followed by the precipitation of syntaxial rim cement in the newly created void spaces around the fragments.

Since chemical dissolution preceded the precipitation of syntaxial rim cement and because it has been determined that chemical dissolution occurred in the meteoric

environment. It is assumed that precipitation of the syntaxial rim cement also occurred in this diagenetic environment. In fact, this cement was probably precipitated prior to the zoned blocky calcite cement (Fig. 8). This is indicated by the nonferroan nature of the syntaxial rim cement which implies that it was precipitated before the establishment of reducing conditions in the fresh water phreatic zone.

Saddle Dolomite Cement

Description: Ferroan saddle dolomite (Plate 10C) occurs in mosaics of very coarse crystals (0.5-4.5 mm long) which are commonly orange brown colored in hand sample. The crystals in these mosaics commonly have curved faces, curved cleavage planes, scimitar shaped terminations, zig zag crystal boundaries (Plate 10C), and sweeping extinction in cross polarized light.

Saddle dolomite is most common in facies C8 where it typically fills 10% of the porosity. In this facies it partly fills growth-framework, interparticle, and channel porosity. It rarely fills intraparticle porosity. Saddle dolomite also occurs in facies A1, A2, A3, B1, B5, B6, C2, C4, and C7 where it occludes 5% of the interparticle, shelter, and, more rarely, intraparticle porosity.

Timing of formation: The saddle dolomite typically occurs near the center of the pore space and is commonly flanked by zoned and/or unzoned blocky calcite cement (Plate

luc). This relationship suggests that the saddle dolomite was precipitated after these two blocky calcite cements (Fig. 8).

Mechanism of formation: Saddle dolomite has been widely interpreted as a late phase cement precipitated in the burial diagenetic environment (Choquette, 1971; Mattes and Mountjoy, 1980; Radke and Mathis, 1980; Wong and Oldershaw, 1981; Krebs and Macqueen, 1984; Smosna, 1984; Choquette and James, 1987). Zenger (1983) argued that the elevated temperature, greater stability, and lack of time constraints in the burial environment promote dolomite crystallization despite the lower flow rate and lower Mg^{2+} concentration in this environment. Saddle dolomite is generally considered to have formed at high temperatures (Fritz, 1969; Choquette, 1971; Radke and Mathis, 1980; Krebs and Macqueen, 1984). Radke and Mathis (1980) concluded that saddle dolomite was precipitated at temperatures of 60-150°C and that its precipitation was commonly contemporaneous with sulphate reduction and hydrocarbon migration and accumulation.

The precise mechanism of saddle dolomite formation is still unknown. The high temperatures necessary for its precipitation may have been caused by either deep burial (Wong and Oldershaw, 1981; Smosna, 1984; Choquette and James, 1987) and/or the flow of hydrothermal fluids (Fritz, 1969; Choquette, 1971; Krebs and Macqueen, 1984).

E. REPLACEMENT

Introduction

The distinction between cement and crystals formed by replacement of previous material can be difficult. Unlike cement, replacement fabrics rarely reduce porosity in a carbonate sequence. Thus, when assessing how much porosity has been destroyed by diagenesis it is important to be able to distinguish between replacement fabrics and cement. Anhedral dolomite is the only replacement fabric that will be discussed in this section.

Anhedral Dolomite

Description: Anhedral dolomite (Plate 10D) occurs in mosaics of finely to coarsely crystalline (0.04-0.3 mm diameter), cloudy, inclusion-rich crystals which exhibit undulose extinction in cross-polarized light. According to Gregg and Sibley (1984) anhedral dolomite crystals which exhibit undulose extinction are commonly of replacement origin. The cloudy, inclusion-rich nature of the anhedral dolomite crystals is also suggestive of such an origin.

Anhedral dolomite is widely distributed in the Kakisa Formation. It occurs in facies A1, A2, B4, B5, C1, C2, C3, C4, C5, C6, C7, and D1 where it replaces argillaceous lime mudstone (Plate 10D).

Timing of formation: The timing of formation of the anhedral dolomite cannot be determined by petrographic

observation. Yet, by examining its mechanism of formation the relative timing of formation of this dolomite can be accurately estimated.

Mechanism of formation: The common association of dolomite with argillaceous carbonates or shales has been recognized by several authors (e. g. Kahle, 1965; Irwin, 1980; Mattes and Mountjoy, 1980; McHargue and Price, 1982; Smosma, 1984). According to Kahle (1965), Mattes and Mountjoy (1980), Wong and Olderghaw (1981), and McHargue and Price (1982) argillaceous sediments can supply the Mg²⁺ necessary for dolomitization. Wong and Olderghaw (1981) suggested that the transformations of kaolinite to Ca montmorillonite and Mg-montmorillonite to carbonate at the elevated temperatures typically associated with burial will favor dolomitization. McHargue and Price (1982) concluded that the conversion of smectite to illite in the deep burial diagenetic environment is also a viable mechanism for the formation of ferroan dolomite. Furthermore, Gregg and Sibley (1984) determined that anhedral dolomite with undulose extinction forms at temperatures of about 50°C and higher. Thus, the high temperature deep burial diagenetic environment is also favored by this data.

According to McHargue and Price (1982) the smectite-illite conversion takes place at burial temperatures of 50-125°C and this process is commonly synchronous with hydrocarbon migration and accumulation.

This temperature range is similar to that required for saddle dolomite precipitation. Thus, the anhedral and saddle dolomites in the Kakisa Formation were probably formed at approximately the same time in the deep burial diagenetic environment (Fig. 8).

F. DIAGENETIC HISTORY

Introduction

The diagenetic history will be recounted in two parts. The diagenetic framework will be outlined first. This will be followed by a reconstruction of the succession of events responsible for the diagenesis of the Kakisa limestones.

The diagenetic history of a carbonate sequence can have important implications with regard to its reservoir potential. The Kakisa Formation provides an excellent example of this. In the Trout River area the Kakisa limestones exhibit virtually no porosity and, hence, have poor reservoir potential. Yet prior to its diagenesis the tabular stromatoporoid framestone of facies C8 possessed excellent porosity. Thus, if we can understand the events in the diagenetic history of the Kakisa Formation that were responsible for the elimination the facies C8 porosity in the Trout River area we may be able to delineate other areas where these events were less effective. In these areas the Kakisa Formation should have good reservoir potential.

Diagenetic Framework

Diagenesis of the Kakisa Formation occurred in three main diagenetic environments: 1) the sea floor environment, 2) the meteoric environment, and 3) the deep burial environment. Diagenesis took place first in the sea floor environment, then in the meteoric environment, and finally in the deep burial environment.

This environmental succession was influenced by sea level fluctuations. The Kakisa Formation resided in the sea floor diagenetic environment during its deposition. Following the eustatic sea level drop which subaerially exposed its upper part, the Kakisa Formation moved from the sea floor environment into the meteoric diagenetic environment. A subsequent eustatic rise in sea level resubmerged the Kakisa Formation. The Trout River Formation was then deposited unconformably above the Kakisa Formation. The deposition of the Trout River Formation and overlying formations moved the Kakisa Formation into the deep burial diagenetic environment.

Succession of Events

In order to make a coherent reconstruction of the diagenetic history of the Kakisa Formation what is known about the relative timing of formation of the main diagenetic features and the diagenetic environment in which each feature was formed must be integrated with what is known about the depositional history of the formation. The

abundance of diagenetic features in the Kakisa limestones and their intricate interrelationships suggests that the diagenetic history was complex.

The diagenesis of the Kakisa Formation began while the formation was still being deposited. The isopachous calcite cement of facies C8 was precipitated syndepositionally in the sea floor diagenetic environment (Fig. 8). This cement occluded up to 35% of the primary porosity in facies C8 and was the only diagenetic feature that was formed during the deposition of the Kakisa limestones. The rest of the diagenetic features were formed after the termination of Kakisa deposition.

A widespread sea level drop was responsible for the subaerial exposure of the Kakisa limestones and the termination of Kakisa deposition. As a result of this subaerial exposure, meteoric waters were permitted to percolate down into the Kakisa Formation. This caused the establishment of a new diagenetic regime, the meteoric diagenetic environment. In this new regime the sea floor environment was replaced by the vadose, fresh water phreatic, and mixed water zones.

Fracturing was the first significant post-depositional event to occur in this new suite of diagenetic zones (Fig. 8). After fracturing occurred, meteoric waters flowed down from the vadose zone into the fresh water phreatic zone via the fractures. As they flowed these waters dissolved limestone (Fig. 8). The dissolution resulted in the creation

of channel and vuggy porosity in the upper part of the formation. Dissolution of lime mudstone around some of echinoderm fragments in the bioclastic packstone matrices of facies B1 and C2 probably also occurred in the fresh water phreatic zone. This created the void spaces that were later to be filled with syntaxial rim cement (Fig. 8).

Dissolution was succeeded by the precipitation of unzoned blocky calcite and syntaxial rim cements (Fig. 8). This was followed by the precipitation of zoned blocky calcite cement (Fig. 8). All three of these calcite cements were formed in the fresh water phreatic zone (Fig. 8); the zoned blocky calcite being precipitated after reducing conditions were established in this zone. Together the unzoned and zoned blocky calcite cements generally fill 40% of the primary porosity in facies C8 and much of the secondary porosity.

Precipitation of the zoned blocky calcite was followed by the resubmergence of the Kakisa Formation by a eustatic sea level rise and the deposition of the marine sands of the lower part of the Trout River Formation. The Trout River Formation-derived facies C9 quartzarenites serve to occlude much of the porosity in facies C8. They commonly fill 15% of the primary porosity and much of the channel porosity in this facies.

Deposition of the Trout River Formation and the overlying formations gradually moved the Kakisa Formation into the deep burial diagenetic environment. Saddle dolomite

precipitated in this environment (Fig. 8). It occluded most of the remaining porosity in the formation.

At about the same time anhedral dolomite replaced much of the lime mudstone in the mudstone-rich facies (Fig. 8). This replacement also occurred in the deep burial diagenetic environment.

Pressure solution is another diagenetic process that took place in the deep burial environment (Fig. 8). It succeeded precipitation of the saddle and anhedral dolomite, occurring after the overburden stress exceeded some critical value. This critical value was probably exceeded due to additional burial.

Hydrocarbon migration, at least in part, accompanied the formation of stylolites in the Kakisa Formation. Unfortunately by this time most of the porosity in the Kakisa Formation had been eliminated in the Trout River area, thus precluding the existence of a viable hydrocarbon reservoir in the area.

IV. SUMMARY AND CONCLUSIONS

1. The Upper Devonian Kakisa Formation was deposited on a depositional margin near the western edge of the north northeast-south-southwest trending Great Slave Shelf margin during latest Frasnian time. Overall this formation represents a shallowing-upward sequence formed during a period of rising sea level.
2. In the Trout River area the Kakisa Formation can be divided into four informal members designated, from bottom to top, A, B, C, and D. Members A and B are characterized by storm-influenced shelf slope sedimentation. Three shallowing-upward sequences comprise member A while member B is formed of a single deepening-upward sequence. Several small reef mounds occur near the base of member B. These mounds grew on an irregular, thin debris flow deposit. The lower part of member C is formed of an irregular, relatively thick debris flow deposit. This deposit was laid down on the shelf slope. It is overlain by the carbonate bank deposits that form the upper part of member C. Most of member D was deposited in a restricted lagoon that existed above the member C carbonate bank. Isolated patch reefs grew in the lagoon. The lagoonal deposits are capped by a thin paleosol.
3. The debris flow deposits that occur at the bases of

members B and C are important depositional elements of the Kakisa Formation. Deposition of these deposits significantly altered the Kakisa depositional regime. These deposits were also important precursors for reef growth. The sudden shallowing and stable substrate they provided promoted reef growth. The type of reef growth that occurred can be related to the thickness of the underlying, precursor debris flow deposit.

4. The upper part of the member C carbonate bank was cemented syndepositionally in the sea floor diagenetic environment by isopachous calcite.
5. The Kakisa Formation was subaerially exposed after a eustatic drop in sea level. At this time the Kakisa limestones were removed from the sea floor diagenetic environment and placed in the meteoric diagenetic environment. The paleosol which caps the Kakisa Formation in the Trout River area and the solution-enlarged vertical fractures which transect the upper part of the formation were formed in this environment. Precipitation of the unzoned blocky, syntaxial rim, and the zoned blocky calcite cements also occurred in the meteoric diagenetic environment.
6. Following a eustatic sea level rise the marine sands of the lower part of the Trout River Formation were deposited unconformably on top of the Kakisa Formation limestones. As they were being deposited, some of these sands percolated down the solution-enlarged vertical

fractures into the upper part of the Kakisa Formation.

7. With the deposition of the overlying formations the Kakisa Formation was eventually submerged into the deep burial diagenetic environment. In this environment anhydral and saddle dolomite were precipitated and pressure solution occurred.
8. Hydrocarbon migration accompanied pressure solution in the Kakisa Formation. However, by this time virtually all of the porosity and permeability in the formation had been destroyed.

PLATES




Plate 1

1A) Field photograph of facies A1 sharply overlying facies A2. Black arrow denotes the vertically burrowed hardground surface that separates these two facies. Note the more recessive weathering character, slightly darker color, and lensoid bedded nature of facies A1. Scale bar=1.5 m

1B) Field photograph showing close-up of the vertically burrowed hardground surface separating facies A1 (above dashed white line) from facies A2 (below dashed white line). Note the lensoid bedded nature of facies A1. Scale bar=10 cm

1C) Field photograph of a planar laminated bioclastic wackestone lens from facies A3. Scale bar=2 cm

1D) Polished hand sample the nodular bioclastic wackestone of facies A2. Note the subhorizontal alignment of the bioclastic wackestone nodules and the differential compaction displayed by the argillaceous mudstone matrix that surrounds the nodules. Scale bar=2 cm

1E) Field photograph of facies A2 truncated by a trough-shaped bed of facies A3 (a). Note the flaggy bedded nature of facies A2 and the sharp base and somewhat gradational upper contact of the facies A3 bed. Scale bar=30 cm

1F) Field photograph of three dome-shaped massive corals in growth position on a facies A2 bedding plane surface. Note the alignment of these corals along a linear trend. Scale bar=15 cm

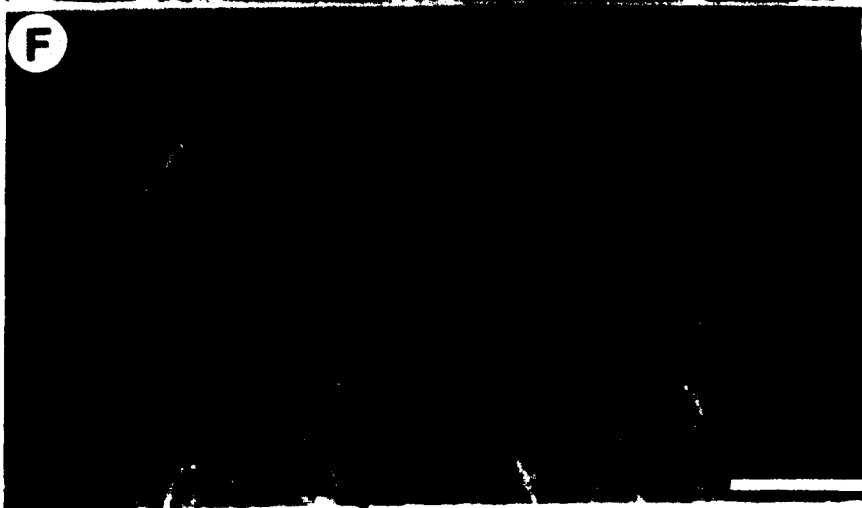
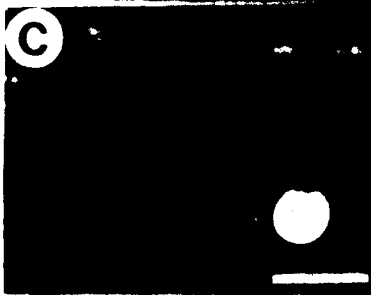
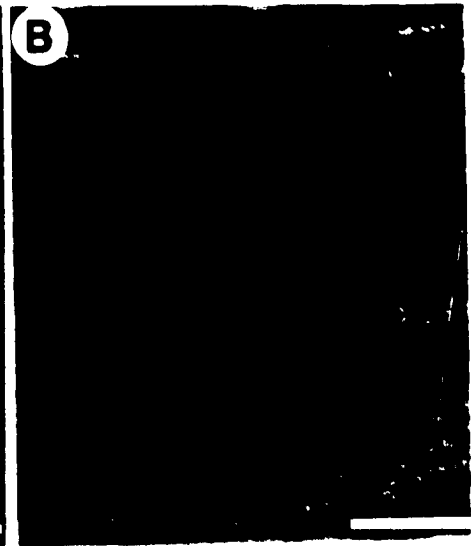
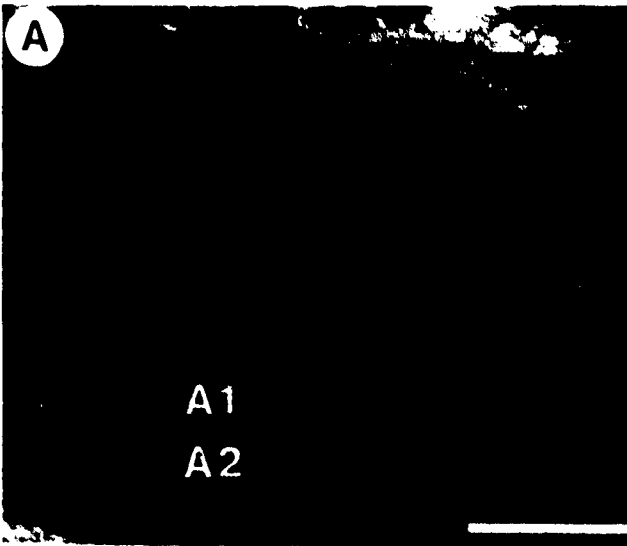


Plate 2

2A) Field photograph of a nearly intact crinoid on a bedding plane in facies A2. Scale bar=5 cm

2B) Field photograph of the underside of a heavily bioturbated bedding plane surface. These burrows belong to the deposit-feeding members of the *Cruziana* ichnofacies. Scale bar=10 cm

2C) Polished hand sample of a facies A3 lens erosionally overlying facies A2. Black arrow denotes the erosional contact between two facies. Note the lag-type deposit at the base of the facies A3 lens and the *Skolithos* burrows transecting the upper part of the lens. Scale bar=2 cm

2D) Field photograph of a cliff face illustrating differences in weathering character between facies A1 and facies A2. Note the more recessive, concave-inward weathering nature of facies A1. The large black arrows denote the sharp contact between facies A2 and A1. The small black arrows mark areas of maximum recessiveness in facies A1. Top of the white measuring stick in the center of the photograph approximates the location of the gradational contact between facies A1 and A2. Scale bar=2 m

2E) Polished hand sample of facies B1 sharply overlying facies A2. Note the manner in which the contact between these two facies truncates branching corals in facies A2. This suggests an erosive depositional mechanism for facies B1. Scale bar=2 cm

2F) Field photograph of facies B1 illustrating its subhorizontal alignment of low profile massive corals and massive weathering character. Scale bar=20 cm

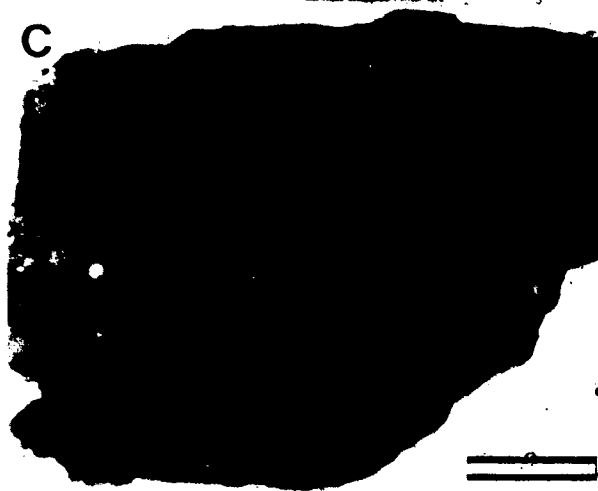


Plate 3

3A) Polished hand sample of the coarse grained bioclastic packstone matrix of facies B1. Black arrow denotes a mudstone lithoclast. Scale bar=2 cm

3B) Field photograph of two large dome-shaped massive corals in facies B3. Scale bar=20 cm

3C) Field photograph of four facies B2 coral bioherms (denoted by black arrows). These bioherms are aligned along a linear trend. Note the draping relationship of the facies B4 nodular bioclastic wackestones over these bioherms. Scale bar=50 cm

3D) Field photograph of a facies B2 bioherm draped by the coral bafflestones of facies B3. Facies B3 is gradationally overlain and interfingers with the flaggy bedded, nodular bioclastic wackestones of facies B4. Black arrow denotes a bed of facies B4 which pinches out against the bioherm. Scale bar=10 cm

3E) Field photograph close-up of a colony of the branching coral *Phacellophyllum tructense* in facies B3. Scale bar=5 cm

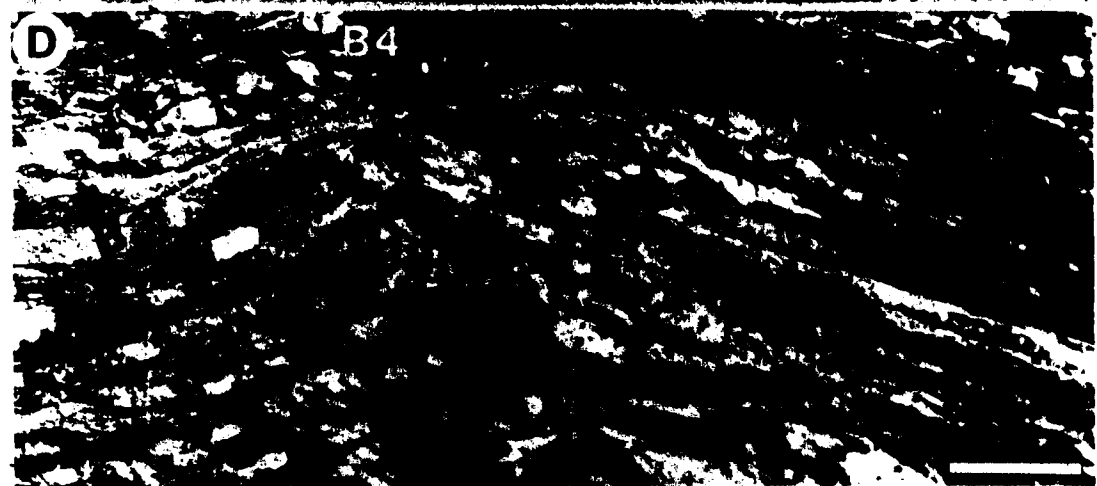
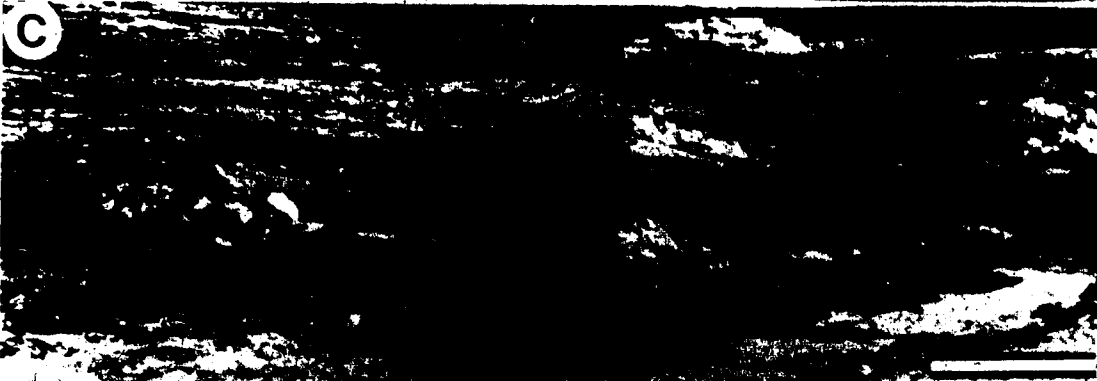


Plate 4

Field photograph of a facies C1 coral bafflestone block overlain by the bedded coral/echinoderm rudstone of facies C2 and underlain by facies B5. Note the crudely bedded nature of the bafflestone blocks (bedding dipping to the left or south side of the photograph), the manner in which the base of the block truncates as well as slightly downwarps beds in the underlying facies B5 limestones, and the way the bedded coral/echinoderm rudstone of facies C2 surrounds the block. Black arrow denotes a large dome-shaped massive coral in the bafflestone block. Scale bar=0.5 m



Plate 5

5A) Field photograph of a facies C1 coral bafflestone block overlain by the bedded coral/echinoderm rudstone of facies C2. This is a sectional view exposed on an eastward protruding promontory of a cliff face at Trout River. Scale bar=25 cm

5B) Polished hand sample of the coarse grained bioclastic packstone matrix of facies C2. Note the dolomitic mudstone partings and lithoclasts in the packstone. Scale bar=3 cm

5C) Field photograph of the vertical and lateral relationships between facies C1, C2, C3, C4, C5, and C6 as exposed on a north-south trending cliff face at Trout River. Facies C1, C2, and C4 are exposed on an eastward protruding promontory on this cliff face while facies C3, C5, and C6 are exposed in the recessive area adjacent to this promontory. Scale bar= 3 m

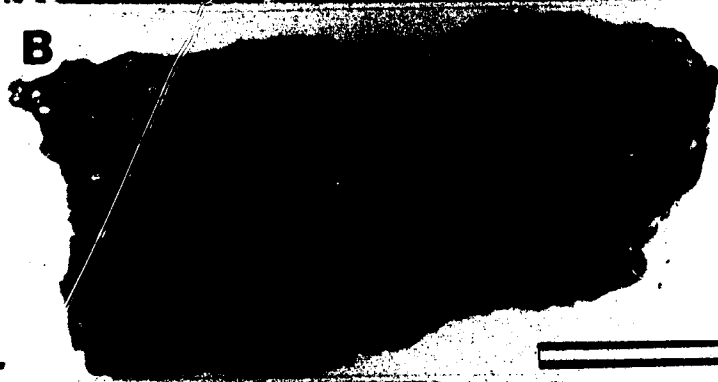


Plate 6

6A) Field photograph of the coral bafflestone of facies C5. Note the growth position of both the branching and solitary corals and the mudstone matrix. Scale bar=5 cm

6B) Field photograph of the coral/stromatoporoid bindstone of facies C6. Note the growth position of the low profile massive corals and wafer stromatopofoids. Also note the coarsely layered texture of this facies. Scale bar=5 cm

6C) Field photograph of the irregular contact between the massive coral bioherms of facies C4 and the coral/stromatoporoid bindstone of facies C6. Note the abundance and growth position of the massive corals in facies C4 and the more mudstone-rich character of facies C6.

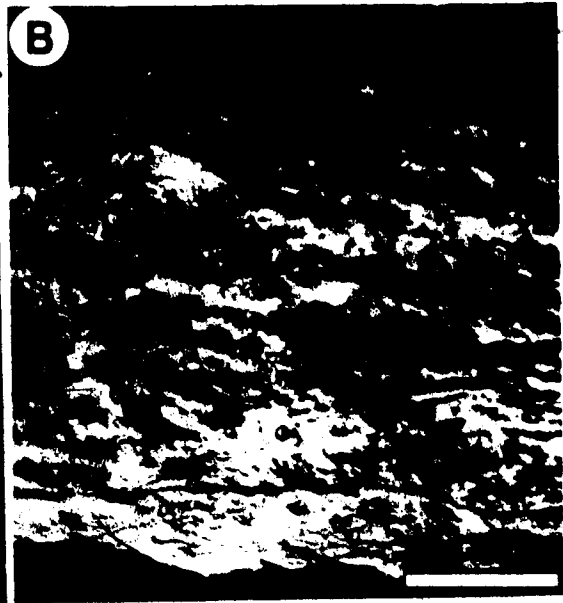


Plate 7

7A) Field photograph of the massive weathering tabular stromatoporoid framestone of facies C8 overlying the semi-recessive weathering massive coral bindstone of facies C7. Note the abrupt increase in thickness of facies C8 from the left side of the photograph to the right side. Scale bar=10 m

7B) Field photograph of the medium grained quartzarenite of facies C9 filling a lens-shaped cavity in facies C8. The solid black arrow indicates a stromatoporoid fragment contained in the quartzarenite lens while the hollow black arrow denotes a black charcoal-like fragment set in another facies C9 cavity-fill. Scale bar=5 cm

7C) Field photograph of a facies C8 bedding plane surface. Black arrow denotes medium grained quartzarenite of facies C9 filling a vertical fracture in facies C8. Scale bar=5 cm

7D) Field photograph close-up of the tabular stromatoporoid framestone of facies C8. Note the vertically stacked nature of the stromatoporoids which give this facies a coarsely layered texture. Scale bar=10 cm

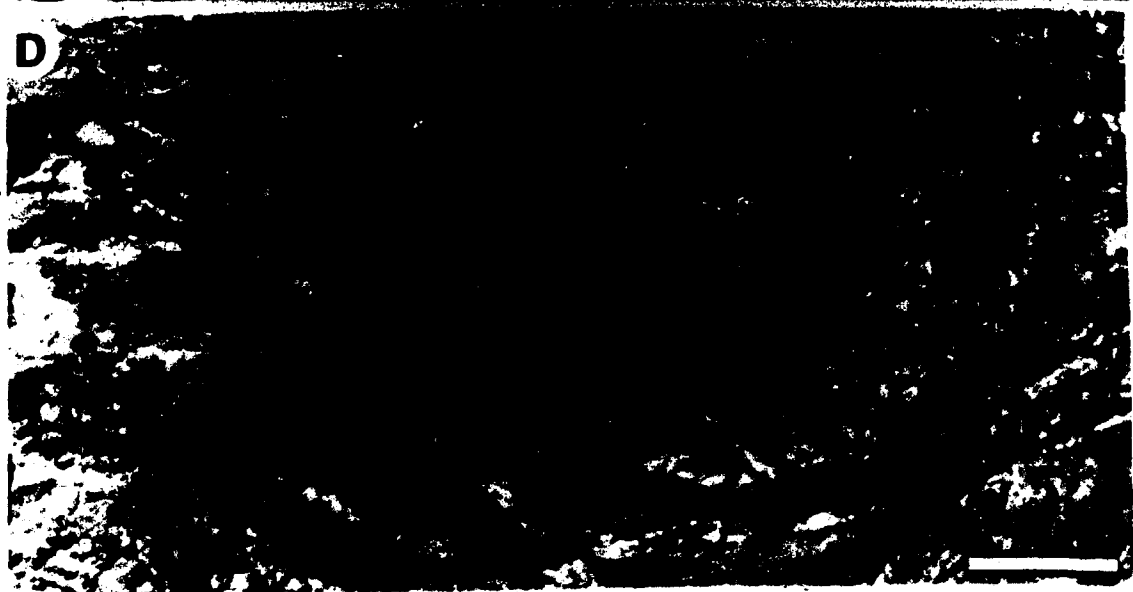
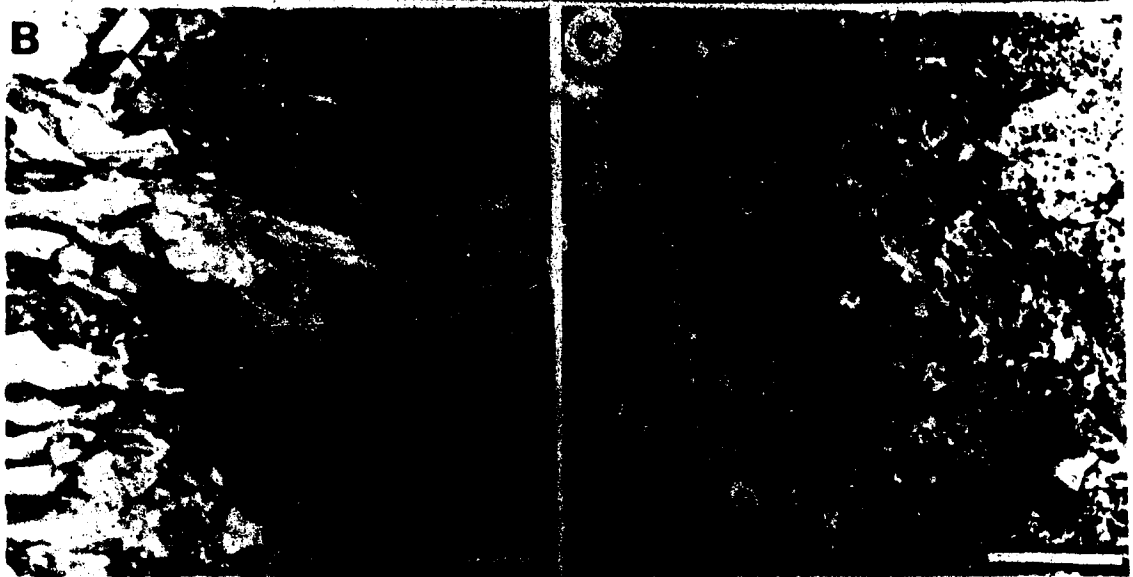


Plate 8

8A) Field photograph of the mottled bioclastic wackestone of facies D1. Note the blocky to rubbly weathering character of this facies and its abundance of vertical fractures. Scale bar=2 m

8B) Polished hand sample of the mottled bioclastic wackestone of facies D1. Note the tabular and wafer stromatoporoids at the base of the sample, the branching coral fragments (black arrows), and the vertical fractures. Scale bar=2 cm

8C) Field photograph of a facies D2 stromatoporoid/coral bioherm. Solid black arrow denotes the irregular basal contact of the bioherm while the hollow black arrow marks its curved upper contact. Note the vertical fractures in this bioherm. Scale bar=25 cm

8D) Field photograph of the sharp contact (dashed white line) between the calcereous claystone of facies D3 and the medium grained quartzarenite of the lower part of the Trout River Formation. Note the recessive, rubbly weathering character of facies D3. Black arrow denotes the irregular, gradational basal contact of facies D3. Scale bar=10 cm

8E) Field photograph illustrating the Trout River Formation overlying the Kakisa Formation. Black arrow marks the contact between these two formations. Note the difference in the weathering characters of these two formations as well as the slightly curved nature of the contact. Scale bar=2 m

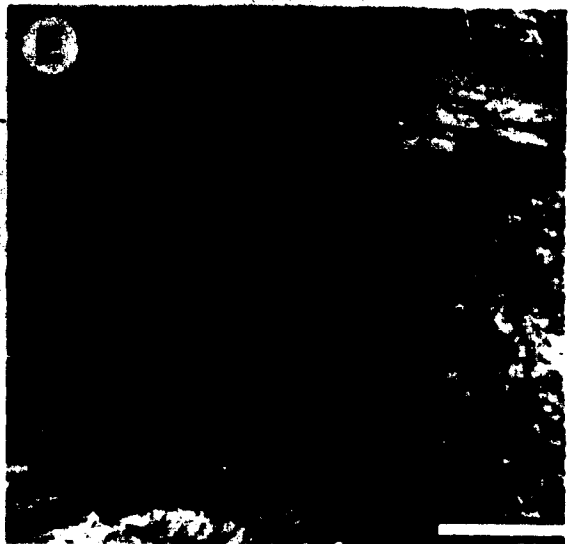
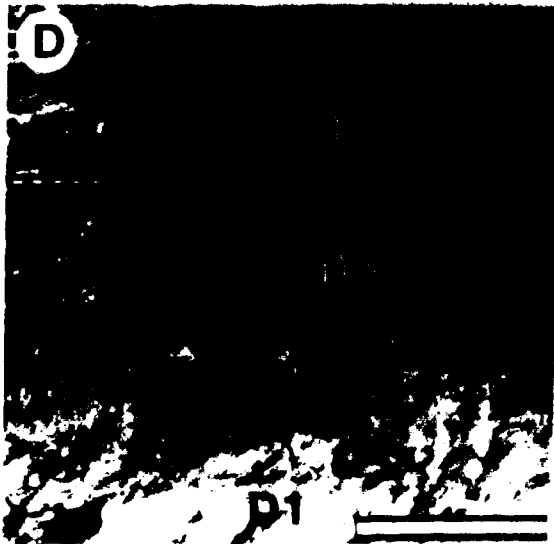
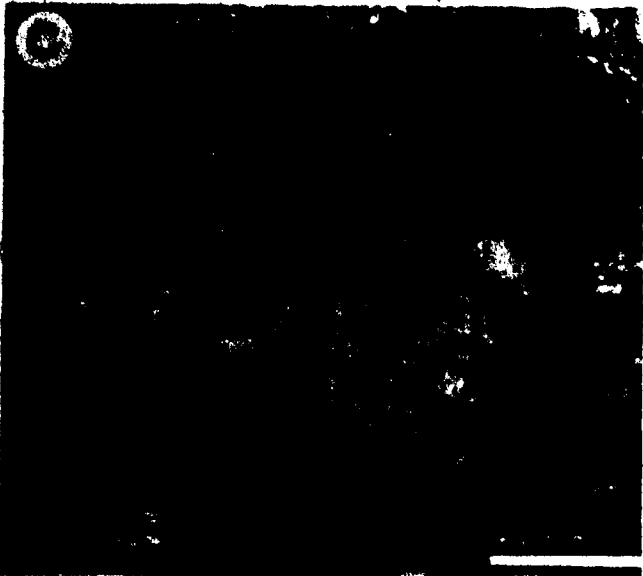
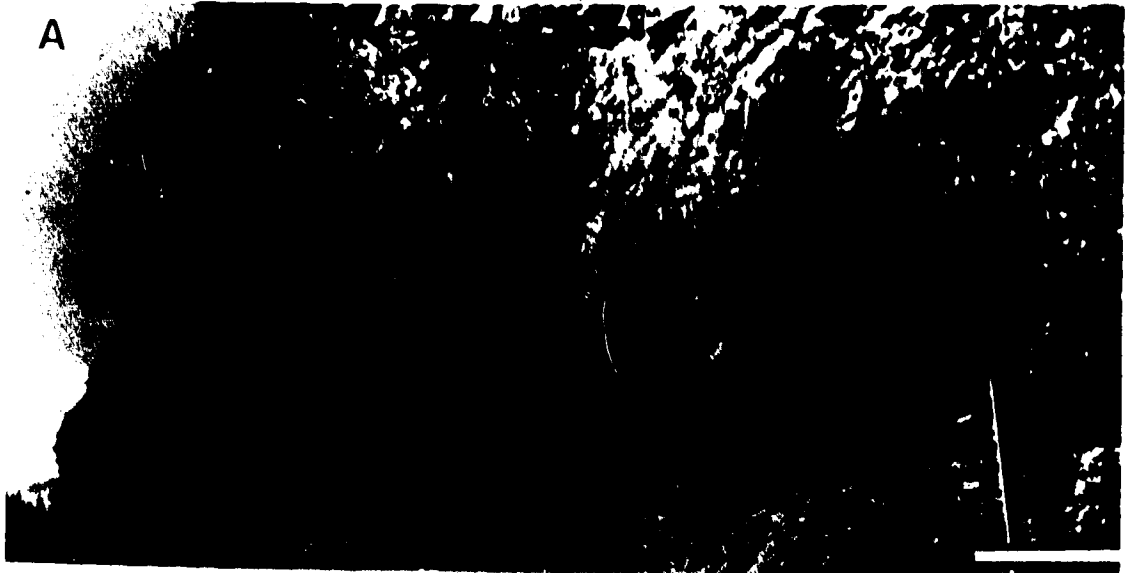


Plate 9

9A) Photomicrograph of a blocky calcite cement-filled vertical fracture in facies C8. Plane polarized light. Scale bar=0.55 mm

9B) Polished hand sample of horizontal stylolite (black arrow) transecting facies C8' tabular stromatoporoid framestone. Note also the fractures in this sample. Scale bar=2 cm

9C) Photomicrograph of stylolitic boundary between ferroan saddle dolomite cement (D) and its tabular stromatoporoid framestone substrate (S) in facies C8. This section has been artificially stained by potassium ferricyanide. Plane polarized light. Scale bar=0.55 mm

9D) Polished hand sample illustrating the irregular distribution of isopachous calcite cement (i) in facies C8. Unzoned blocky calcite cement (b) is also denoted. Black arrow indicates a vertical fracture which has truncated isopachous calcite cement and has been filled by unzoned blocky calcite cement. Scale bar=2 cm

9E) Photomicrograph of isopachous calcite cement in facies C8. The tabular stromatoporoid framestone substrate (S) is also denoted. Cross polarized light. Scale bar=0.55 mm

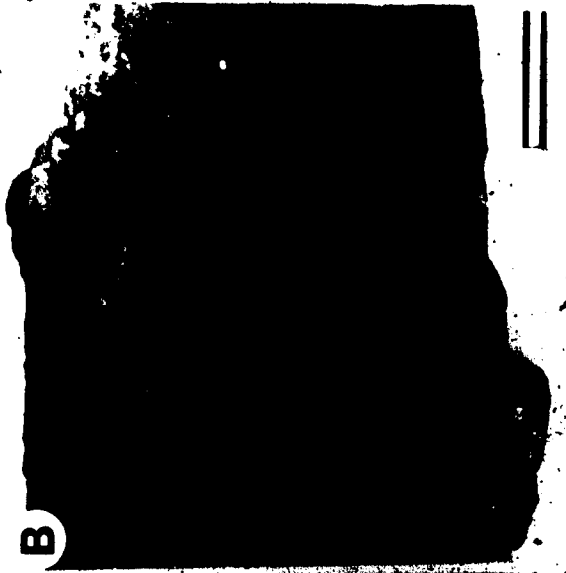


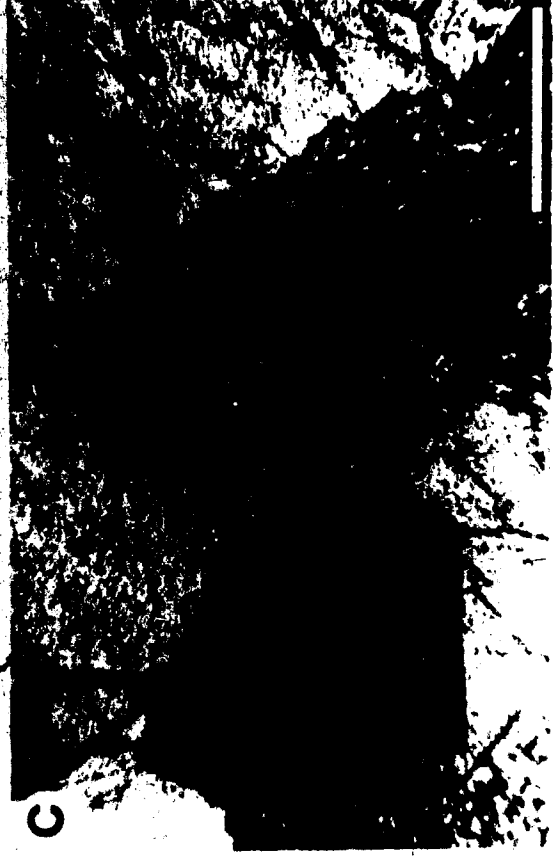
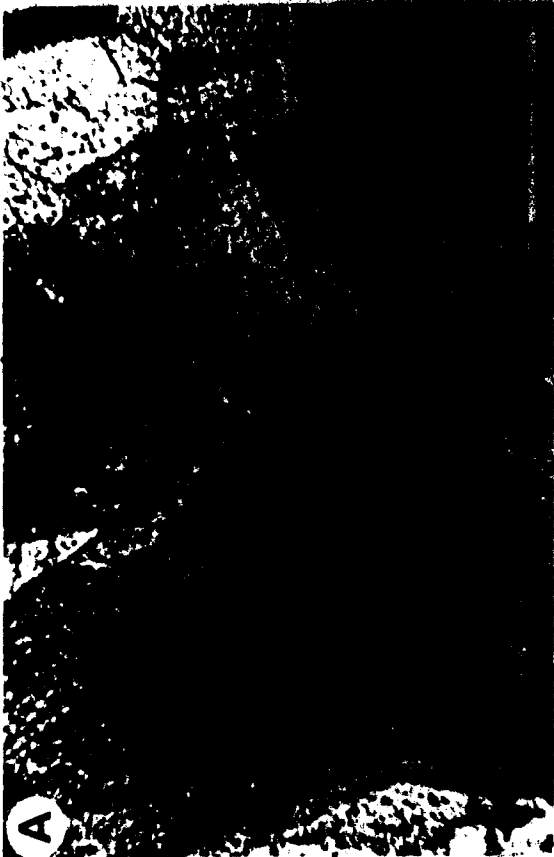
Plate 10

10A) Photomicrograph of zoned blocky calcite cement in facies C8. Thin section has been artificially stained by potassium ferricyanide. Plane polarized light. Scale bar=0.22 mm

10B) Photomicrograph of syntaxial rim cement (S) surrounding echinoderm fragments (E) in facies B1. Plane polarized light. Scale bar=0.5 mm

10C) Photomicrograph of ferroan saddle dolomite cement (dark grey) surrounded by unzoned blocky calcite cement in facies C8. Note the curved crystal faces and cleavage planes, scimitar-shaped crystal terminations, and zig-zag crystal boundaries of the saddle dolomite. Thin section has been artificially stained by potassium ferricyanide. Plane polarized light. Scale bar=0.2 mm

10D) Photomicrograph of anhedral dolomite (white rhombs) in an argillaceous mudstone burrow-filling in facies A3. Plane polarized light. Scale bar=0.5 mm



REFERENCES CITED

- Apon, J. F. 1980. Upper Devonian conodonts from Hay River-Fort Simpson area. Unpublished M.Sc. thesis, University of Alberta, 116p.
- Bassett, H. G. and Stout, J. G. 1967. Devonian of western Canada. *In*: Oswald, D. H. (Ed.), International Symposium on the Devonian System, v. 1. Alberta Society of Petroleum Geologists, p. 717-752.
- Bathurst, R. G. C. 1958. Diagenetic fabrics in some British Dinantian limestones. *Liverpool and Manchester Geological Journal*, v. 2, p. 11-36.
- Bathurst, R. G. C. 1975. Carbonate Sediments and their Diagenesis. Elsevier Scientific Publishing Company, Amsterdam, 658p.
- Belyea, H. R. 1964. Upper Devonian, part 2, Woodbend, Winterburn and Wabamun groups. *In*: McCrossan, R. G. and Glaister, R. P. (Eds.), Geological History of Western Canada. Alberta Society of Petroleum Geologists, p. 66-86.
- Belyea, H. R. 1971. Middle Devonian tectonic history of the Tathlina Uplift, southern District of Mackenzie and northern Alberta, Canada. Geological Survey of Canada, Paper 70-14.
- Belyea, H. R. and McLaren, D. J. 1962. Upper Devonian formations, southern part of Northwest Territories, northeastern British Columbia, and northwestern Alberta. Geological Survey of Canada, Paper 61-29.
- Bosellini, A. 1984. Progradation geometrics of carbonate platforms: examples from the Triassic of the Dolomites, northern Italy. *Sedimentology*, v. 31, p. 1-24.
- Braun, R. K. and Lethiers, F. 1982. A new Late Devonian ostracode fauna and its bearing on the Frasnian-Famennian boundary in western Canada. *Canadian Journal of Earth Sciences*, v. 19, p. 1952-1963.
- Burchette, T. P. 1981. European Devonian reefs: a review of current concepts and models. *In*: Tqomey, D. G. (Ed.), European Fossil Reef Models. Society of Economic Paleontologists and Mineralogists, Special Publication 30, p. 85-142.
- Cant, D. J. 1980. Storm-dominated shallow marine sediments of Arisaig Group (Silurian-Devonian) of Nova Scotia. *Canadian Journal of Earth Sciences*, v. 17, p. 120-131.

- Choquette, P. W. 1971. Late ferroan dolomite cement, Mississippian carbonates, Illinois Basin, U. S. A. In: Bricker, O. P. (Ed.), Carbonate Cements. The Johns Hopkins Press, Baltimore, p. 339-346.
- Choquette, P. W. and James, N. P. 1987. Diagenesis 12. Diagenesis in limestones-3. The deep burial environment. Geoscience Canada, v. 14, p. 3-35.
- Choquette, P. W. and Pray, L. C. 1970. Geologic nomenclature and classification of porosity in sedimentary carbonates. American Association of Petroleum Geologists Bulletin, v. 54, p. 207-250.
- Cook, H. E., McDaniel, P. N., Mountjoy, E. W. and Pray, L. C. 1972. Allochthonous carbonate debris flows at Devonian bank ("reef") margins, Alberta, Canada. Bulletin of Canadian Petroleum Geology, v. 20, p. 439-497.
- Cook, H. E. and Mullins, H. T. 1983. Basin margin environment. In: Scholle, P. A., Bebout, D. G., and Moore C. H. (Eds.), Carbonate Depositional Environments, American Association of Petroleum Geologists, Memoir 33, p. 539-617.
- Copper, P. 1977. Paleolatitudes in the Devonian of Brazil and the Frasnian-Famennian mass extinction. Paleogeography, Paleoclimatology, Paleoecology, v. 21, p. 165-207.
- Crevello, P. D. and Schlager, W. 1980. Carbonate debris sheets and turbidites, Exuma Sound, Bahamas. Journal of Sedimentary Petrology, v. 50, p. 1121-1148.
- Crickmay, C. H. 1953. New Spiriferidae from the Devonian of western Canada. Published by author, Imperial Oil Limited, Calgary, 11p.
- Crickmay, C. H. 1957. Elucidation of some western Canada Devonian formations. Published by author, Imperial Oil Limited, Calgary, 17p.
- Davies, G. R. 1977. Turbidites, debris sheets and truncation structures in upper Paleozoic deep-water carbonates of the Sverdrup Basin, Arctic Archipelago. In: Cook, H. E. and Enos, P. (Eds.), Deep-water Carbonate Environments. Society of Economic Paleontologists and Mineralogists, Special Publication 25, p. 221-249.
- Davies, G. R. 1986. Table of formations of Alberta. AGAT Laboratories.
- de Wit, R., Gronberg, E. C. and Richmond, W. O. 1973.

- Tathlina area, District of Mackenzie. *In*: McCrossan, R. G. (Ed.), *The Future Petroleum Provinces of Canada-Their Geology and Potential*. Canadian Society of Petroleum Geologists, Memoir 1, p. 187-212.
- Dickson, J. A. D. 1966. Carbonate identification and genesis as revealed by staining. *Journal of Sedimentary Petrology*, v. 36, p. 491-505.
- Dott, R. H. Jr. and Bourgeois, J. 1982. Hummocky stratification: significance of its variable bedding sequences. *Geological Society of America Bulletin*, v. 93, p. 663-680.
- Douglas, R. J. W. 1974. *Geology, Trout River, District of Mackenzie*. Geological Survey of Canada, Map 1371A.
- Druckman, Y. and Moore, C. H. 1985. Late subsurface secondary porosity in a Jurassic grainstone reservoir, Smackover Formation, Mt. Vernon field, southern Arkansas. *In*: Roehl, P. O. and Choquette, P. W. (Eds.), *Carbonate Petroleum Reservoirs*. Springer-Verlag, New York, p. 787-793.
- Embry, A. F., III and Klovan, J. E. 1971. A Late Devonian reef tract on northeastern Banks Island, N. W. T. *Bulletin of Canadian Petroleum Geology*, v. 19, p. 730-781.
- Esteban, M. and Klappa, C. F. 1983. Subaerial exposure. *In*: Scholle, P. A., Bebout, D. G. and Moore, C. H. (Eds.), *Carbonate Depositional Environments*, American Association of Petroleum Geologists, Memoir 33, p. 1-54.
- Evamy, B. D. 1969. The precipitational environment and correlation of some calcite cement deduced from artificial staining. *Journal of Sedimentary Petrology*, v. 39, p. 787-793.
- Evamy, B. D. and Shearman, D. J. 1965. The development of overgrowths from echinoderm fragments. *Sedimentology*, v. 5, p. 211-233.
- Evamy, B. D. and Shearman, D. J. 1969. Early stages in development of overgrowths on echinoderm fragments in limestones. *Sedimentology*, v. 12, p. 317-322.
- Flügel, E. 1982. *Microfacies Analysis of Limestones*. Springer-Verlag, New York, 633p.
- Folk, R. L. 1959. Practical petrographic classification of limestones. *American Association of Petroleum Geologists Bulletin*, v. 43, p. 1-38.

- Folk, R. L. 1968. *Petrology of Sedimentary Rocks*. Hemphill Publishing Company, Austin, Texas, 170p.
- Friedman, B. M. 1965. Terminology of crystallization textures and fabrics in sedimentary rocks. *Journal of Sedimentary Petrology*, v. 35, p. 643-655.
- Fritz, P. 1969. The oxygen and carbon isotopic composition of carbonates from the Pine Point lead-zinc deposits. *Economic Geology*, v. 64, p. 733-742.
- Goodwin, P. W. and Anderson, E. J. 1985. Punctuated aggradational cycles: a general hypothesis of episodic stratigraphic accumulation. *Journal of Geology*, v. 93, p. 515-533.
- Gregg, J. M. and Sibley, D. F. 1984. Epigenetic dolomitization and the origin of epigenetic dolomite texture. *Journal of Sedimentary Petrology*, v. 54, p. 908-931.
- Hamblin, A. P. and Walker, R. G. 1979. Storm dominated shallow marine deposits: the Fernie-Kootenay (Jurassic) transition, southern Rocky Mountains. *Canadian Journal of Earth Sciences*, v. 16, p. 1673-1690.
- Harms, J. C., Southard, J. B. and Walker, R. G. 1982. Structures and sequences in clastic rocks. Society of Economic Paleontologists and Mineralogists, Short Course 9.
- Harrison, R. S. 1977. Caliche profiles, indicators of near-surface subaerial diagenesis, Barbados, West Indies. *Bulletin of Canadian Petroleum Geology*, v. 25, p. 123-173.
- Havard, C. J. and Oldershaw, A. E. 1976. Early diagenesis in back-reef sedimentary cycles, Snipe Lake reef complex, Alberta. *Bulletin of Canadian Petroleum Geology*, v. 24, p. 27-69.
- Heckel, P. H. 1974. Carbonate buildups in the geologic record: a review. In: Laporte, L. F. (Ed.), *Reefs in Time and Space*. Society of Economic Paleontologists and Mineralogists, Special Publication 18, p. 90-154.
- Hein, F. J. 1982. Depositional mechanisms of deep-sea coarse clastic sediments, Cap Enragé Formation, Quebec. *Canadian Journal of Earth Sciences*, v. 19, p. 267-287.
- Hendry, H. E. 1973. Sedimentation of deep water conglomerates in Lower Ordovician rocks of Quebec composite bedding produced by progressive lithification of sediment? *Journal of Sedimentary Petrology*, v. 43, p.

125-136.

- Hills, L. V., Sangster, E. V. and Suneby, L. B. 1981. *Lexicon of Canadian Stratigraphy Volume 2, Yukon Territory and District of Mackenzie*. Canadian Society of Petroleum Geologists, 240p.
- Hopkins, J. C. 1977. Production of foreslope breccias by differential submarine cementation and downslope displacement of carbonate sands, Miette and Ancient Wall buildups. *In: Cook, H. E. and Enos, P. (Eds.), Deep water Carbonate Environments*, Society of Economic Paleontologists and Mineralogists, Special Publication 25, p. 155-170.
- House, M. R. 1975. Facies and time in Devonian tropical areas. *Proceedings of the Yorkshire Geological Society*, v. 40, p. 233-288.
- House, M. R. and Pedder, A. E. H. 1963. Devonian goniatites and stratigraphical correlations in western Canada. *Paleontology*, v. 6, p. 491-539.
- Hubbard, J. A. E. B. and Pocock, Y. P. 1972. Sediment rejection by recent scleractinian corals: a key to paleoenvironment reconstruction. *Geologische Rundschau*, v. 61, p. 598-626.
- Ingram, R. L. 1954. Terminology for the thickness of stratification and parting units in sedimentary rocks. *Geological Society of America Bulletin*, v. 65, p. 937-938.
- Irwin, H. 1980. Early diagenetic carbonate precipitation and pore-fluid migration in the Kimmeridge Clay of Dorset, England. *Sedimentology*, v. 27, p. 577-591.
- James, N. P. 1972. Holocene and Pleistocene calcereous crust (caliche) profiles: criteria for subaerial exposure. *Journal of Sedimentary Petrology*, v. 42, p. 817-836.
- James, N. P. 1983. Reefs. *In: Scholle, P. A., Bebout, D. G. and Moore, C. H. (Eds.), Carbonate Depositional Environments*, American Association of Petroleum Geologists, Memoir 33, p. 345-440.
- James, N. P. 1984. Shallowing-upward sequences in carbonates. *In: Walker, R. G. (Ed.), Facies Models*. Geoscience Canada, Reprint Series 1, p. 213-228.
- James, N. P. and Choquette, P. W. 1983a. Diagenesis 5. Limestones: Introduction. *Geoscience Canada*, v. 10, p. 159-161.

- James, N. P. and Choquette, P. W. 1983b. Diagenesis of Limestones-the sea-floor diagenetic environment. *Geoscience Canada*, v. 10, p. 162-179.
- James, N. P. and Choquette, P. W. 1984. Diagenesis of Limestones-the meteoric diagenetic environment. *Geoscience Canada*, v. 11, p. 161-194.
- James, N. P., Ginsburg, R. N., Marszalek, D. S. and Choquette, P. W. 1976. Facies and fabric specificity of early subsea cements in shallow Belize (British Honduras) reefs. *Journal of Sedimentary Petrology*, v. 46, p. 523-544.
- James, N. P. and Mountjoy, E. W. 1983. Shelf-slope break in fossil carbonate platforms: an overview. In: Stanley, D. J. and Moore, G. T. (Eds.), *The Shelfbreak: Critical Interface on Continental Margins*, Society of Economic Paleontologists and Mineralogists, Special Publication 33, p. 186-206.
- Jamieson, E. R. 1971. Paleogeology of Devonian reefs of western Canada. *North American Paleontological Convention Proceedings*, pt. J, p. 1300-1340.
- Jenik, A. J. and Lerbekmo, J. F. 1968. Facies and geometry of Swan Hills reef member of Beaverhill Lake Formation (Upper Devonian), Goose River field, Alberta, Canada. *American Association of Petroleum Geologists Bulletin*, v. 52, p. 21-56.
- Johnson, J. G., Klapper, G. and Sandberg, C. A. 1985. Devonian eustatic fluctuations in Euramerica. *Geological Society of America Bulletin*, v. 96, p. 567-587.
- Jones, B., Oldershaw, A. E. and Narbonne, G. M. 1979. Nature and origin of rubbly limestone in the Upper Silurian Read Bay Formation of Arctic Canada. *Sedimentary Geology*, v. 24, p. 227-252.
- Kahle, C. F. 1965. Possible roles of clay minerals in the formation of dolomite. *Journal of Sedimentary Petrology*, v. 35, p. 448-453.
- Kahle, C. F. 1977. Origin of subaerial Holocene crusts: role of algae, fungi, and sparmicritization. *Sedimentology*, v. 24, p. 413-436.
- Kendall, C. G. St. C. and Schlager, W. 1981. Carbonates and relative changes in sea level. *Marine Geology*, v. 44, p. 181-212.
- Klapper, G. and Lane, H. R. 1985. Upper Devonian (Frasnian) conodonts of the *Polygnathus* biofacies, N. W. T.;

- Canada. *Journal of Paleontology*, v. 59, p. 904-951.
- Element, K. W. 1967. Practical classification of reefs and banks, bioherms and biostromes. *American Association of Petroleum Geologists Bulletin*, v. 51, p. 167-168.
- Elovan, J. E. 1964. Facies analysis of the Redwater reef complex, Alberta. *Bulletin of Canadian Petroleum Geology*, v. 12, p. 1-100.
- Frause, F. F. 1984. Nisku reef: Devonian lithoherms. *In: Elnik, L. (Ed.), Carbonates in Subsurface and Outcrop. Canadian Society of Petroleum Geologists, Core Conference 1984*, p. 171-189.
- Friess, W. 1969. Early void filling cementation in Devonian fore reef limestones (Germany). *Sedimentology*, v. 12, p. 279-299.
- Friess, W. and Macqueen, R. W. 1984. Sequence of diagenetic and mineralization events, Pine Point lead-zinc property, Northwest Territories, Canada. *Bulletin of Canadian Petroleum Geology*, v. 32, p. 434-464.
- Kriess, R. D. 1981. Storm-generated sedimentary structures in subtidal marine facies with examples from the Middle and Upper Ordovician of southwestern Virginia. *Journal of Sedimentary Petrology*, v. 51, p. 823-848.
- Law, J. 1971. Regional Devonian geology and oil and gas possibilities, upper Mackenzie River area. *Bulletin of Canadian Petroleum Geology*, v. 19, p. 437-486.
- Leavitt, E. M. 1968. Petrology, paleontology, Carson Creek North reef complex, Alberta. *Bulletin of Canadian Petroleum Geology*, v. 16, p. 298-413.
- Longman, M. W. 1980. Carbonate diagenetic textures from nearsurface diagenetic environments. *American Association of Petroleum Geologists Bulletin*, v. 64, p. 461-487.
- Lowe, D. R. 1976. Grain flow and grain flow deposits. *Journal of Sedimentary Petrology*, v. 46, p. 188-199.
- Machel, H. G. 1983. Facies and diagenesis of some Nisku buildups and associated strata, Upper Devonian, Alberta, Canada. *In: Harris, P. M. (Ed.), Carbonate Buildups. Society of Economic Paleontologists and Mineralogists, Core Workshop No. 4*, p. 144-181.
- Machel, H. G. and Mountjoy, E. W. 1987. General constraints on extensive pervasive dolomitization and their application to the Devonian carbonates of western

- Canada. Bulletin of Canadian Petroleum Geology, v. 35, p. 143-158.
- Machielse, S. 1972. Devonian algae and their contribution to the western Canada sedimentary basin. Bulletin of Canadian Petroleum Geology, v. 20, p. 187-237.
- MacIntyre, I. G. 1977. Distribution of submarine cements in a modern Caribbean fringing reef, Galeta Point Panama. Journal of Sedimentary Petrology, v. 47, p. 503-516.
- Mattes, B. W. and Mountjoy, E. W. 1980. Burial dolomitization of the Upper Devonian Miette buildup, Jasper National Park Alberta. In: Zenger, D. H., Dunham, J. B. and Ethington, R. L. (Eds.), Concepts and Models of Dolomitization. Society of Economic Paleontologists and Mineralogists, Special Publication 28, p. 259-297.
- McGillivray, J. G. and Mountjoy, E. W. 1975. Facies and related reservoir characteristics, Golden Spike reef complex, Alberta. Bulletin of Canadian Petroleum Geology, v. 23, p. 753-809.
- McHargue, T. R. and Price, R. C. 1982. Dolomite from W clay in argillaceous or shale-associated marine carbonates. Journal of Sedimentary Petrology, v. 52, p. 873-886.
- McIlreath, I. A. and James, N. P. 1984. Carbonate slopes. In: Walker, R. G. (Ed.), Facies Models. Geoscience Canada, Reprint Series 1, p. 245-257.
- McLaren, D. J. 1959. The role of fossils in defining rock units with examples from Devonian of Science, v. 57, p. 734-751.
- McLaren, D. J. 1970. Time, life, and boundaries. Journal of Paleontology, v. 44, p. 801-815.
- McLaren, D. J. 1982. Frasnian-Famennian extinctions. Geological Society of America, Special Paper 190, p. 477-484.
- McLaren, D. J. and Mountjoy, E. W. 1962. Alexo equivalents in the Jasper region, Alberta. Geological Survey of Canada, Paper 62-23.
- McLaren, D. J., Norris, A. W. and McGregor, D. C. 1962. Illustrations of Canadian fossils; Devonian of western Canada. Geological Survey of Canada, Paper 62-4.
- McLean, R. A. 1982. *Ceciliaphyllum*, a new charactophyllid coral genus from the Upper Devonian (Late Frasnian) of British Columbia. Geological Survey of Canada, Paper 82-1C, p. 95-98.

- Meyers, W. J. 1974. Carbonate cement stratigraphy of the Lake Valley Formation (Mississippian), Sacramento Mountains, New Mexico. *Journal of Sedimentary Petrology*, v. 44, p. 837-861.
- Middleton, G. V. and Hampton, M. A. 1973. Sediment gravity flows; mechanics of flow and deposition. *In: Middleton, G. V. and Bouma, A. H. (Eds.), Turbidites and Deep Water Sedimentation. Society of Economic Paleontologists and Mineralogists, Short Course*, p. 1-38.
- Mountjoy, E. W. 1980. Some questions about the development of Upper Devonian carbonate buildups (reefs), western Canada. *Bulletin of Canadian Petroleum Geology*, v. 28, p. 315-344.
- Mountjoy, E. W. and Jull, R. K. 1978. Fore-reef carbonate mud bioherms and associated reef-margin, Upper Devonian, Ancient Wall reef complex, Alberta. *Canadian Journal of Earth Sciences*, v. 15, p. 1304-1325.
- Mountjoy, E. W. and Riding, R. 1981. Foreslope stromatoporeid renalcid bioherm with evidence of early cementation, Devonian Ancient Wall reef complex, Rocky Mountains. *Sedimentology*, v. 28, p. 299-319.
- Mullins, H. T., Gardulski, A. G. and Hine, A. C. 1986. Catastrophic collapse of the west Florida carbonate platform margin. *Geology*, v. 14, p. 167-170.
- Murray, J. W. 1966. An oil-producing reef-fringed carbonate bank in the Upper Devonian Swan Hills Member, Judy Creek, Alberta. *Bulletin of Canadian Petroleum Geology*, v. 14, p. 1-103.
- Orme, G. R. and Brown, W. W. M. 1963. Diagenetic fabrics in the Avonian limestones of Derbyshire and North Wales. *Proceedings of the Yorkshire Geological Society*, v. 34, p. 51-66.
- Pedder, A. E. H. 1982. The rugose coral record across the Frasnian/Famennian boundary. *Geological Society of America, Special Paper 190*, p. 485-489.
- Pemberton, S. G. and Frey, R. W. 1984. Ichnology of storm-influenced shallow marine sequence: *Cardium* Formation (Upper Cretaceous) at Seebe, Alberta. *In: Stott, D. F. and Glass, D. J. (Eds.), The Mesozoic of Middle North America. Canadian Society of Petroleum Geologists, Memoir 9*, p. 281-304.
- Prather, B. E. 1984. An Upper Pennsylvanian desert paleosol in the D-zone of the Lansing-Kansas City Groups, Hitchcock County, Nebraska. *Journal of Sedimentary*

- Smosna, R. 1984. Diagenesis of a stromatoporoid patch reef. *Journal of Sedimentary Petrology*, v. 54, p. 1000-1011.
- Stearn, C. W. 1966. Upper Devonian stromatoporoids from southern Northwest Territories and northern Alberta. *Geological Survey of Canada, Bulletin 133*, p. 35-68.
- Swift, D. J. P., Figueiredo, A. G., Freeland, G. L. and Oertel, G. F. 1983. Hammocky cross stratification and megaripples: a geological double standard. *Journal of Sedimentary Petrology*, v. 53, p. 1295-1317.
- Tsien, H. H. 1971. The Middle and Upper Devonian reef complexes of Belgium. *Petroleum Geology of Taiwan*, v. 8, p. 119-173.
- Vail, P. R., Mitchum, R. M. Jr. and Thompson, S. III. 1977. Seismic stratigraphy and global changes of sea level, part 4. *In: Payton, C. E. (Ed.), Seismic Stratigraphy Applications to Hydrocarbon Exploration*. American Association of Petroleum Geologists, Memoir 26, p. 83-97.
- Wafkden, G. M. and Berry, J. R. 1984. Syntaxial overgrowths in muddy crinoidal limestones: cathodoluminescence sheds new light on an old problem. *Sedimentology*, v. 31, p. 251-268.
- Walker, R. G. 1984. Shelf and shallow marine sands. *In: Walker, R. G. (Ed.), Facies Models*. Geoscience Canada, Reprint Series 1, p. 141-170.
- Walker, K.R. and Alberstadt, L. P. 1975. Ecological succession as an aspect of structure in fossil communities. *Paleobiology*, v. 1, p. 238-257.
- Walls, R. A. and Burrowes, G. 1985. The role of cementation in the diagenetic history of Devonian reefs, western Canada. *In: Schneidermann, N. and Harris, P. M. (Eds.), Carbonate Cements*. Society of Economic Paleontologists and Mineralogists, Special Publication 36, p. 185-220.
- Walls, R. A., Harris, W. B. and Nunan, W. E. 1975. Calcareous crust (caliche) profiles and early subaerial exposure of Carboniferous carbonates, northeastern Kentucky. *Sedimentology*, v. 22, p. 417-440.
- Walls, R. A., Mountjoy, E. W. and Fritz, P. 1979. Isotopic composition and diagenetic history of carbonate cements in Devonian Golden Spike reef, Alberta. *Geological Society of America Bulletin*, v. 90, p. 963-982.
- Wanless, H. R. 1979. Limestone response to stress: pressure solution and dolomitization. *Journal of Sedimentary*

Petrology, v. 49, p. 437-462.

- Warren, P. S. and Stelck, C. R. 1956. Reference fossils of Canada, part 1, Devonian faunas of western Canada. Geological Association Canada, Special Paper 17, p. 1-15.
- Wendt, J. C. and Stoakes, F. A. 1982. Evolution and corresponding porosity of the Judy Creek complex, Upper Devonian, central Alberta. In: Cutler, W. G. (Ed.), Canada's Giant Hydrocarbon Reservoirs. Canadian Society of Petroleum Geologists, Core Conference 1982, p. 63-81.
- Wentworth, C. K. 1922. A scale of grade and class terms for clastic sediments. Journal of Geology, v. 30, p. 377-392.
- Whittaker, E. J. 1922. Mackenzie River district between Great Slave Lake and Simpson. Geological Survey of Canada, Summary Report 1921, part B, p. 45-55.
- Whittaker, E. J. 1923. Mackenzie River district between Providence and Simpson. Geological Survey of Canada, Summary Report, part B, p. 88-100.
- Wilkinson, B. R. 1982. Cyclic cratonic carbonates and Phanerozoic calcite seas. Journal of Geological Education, v. 30, p. 189-203.
- Wilson, J. L. 1975. Carbonate Facies in Geologic History. Springer-Verlag, New York, 471p.
- Wong, P. K. and Oldershaw, A. E. 1981. Burial cementation in the Devonian Kaybob reef complex, Alberta, Canada. Journal of Sedimentary Petrology, v. 51, p. 507-520.
- Zenger, D. H. 1983. Burial dolomitization in the Lost Burro Formation (Devonian), east-central California, and the significance of late diagenetic dolomitization. Geology, v. 11, p. 519-522.
- Ziegler, P. A. 1967. Guidebook for Canadian Cordillera Field Trip. Alberta Society of Petroleum Geologists, 80p.

- Petrology, v. 55, p. 213-221.
- Radke, R. M. and Mathis, R. L. 1980. On the formation of saddle dolomite. *Journal of Sedimentary Petrology*, v. 54, p. 1149-1168.
- Reineck, H. E. and Singh, I. B. 1972. Genesis of laminated sand and graded rhythmites in storm sand layers of shell mud. *Sedimentology*, v. 18, p. 123-128.
- Richter, D. K. and Fuchtbauer, H. 1978. Ferroan calcite replacement indicates former magnesian calcite skeletons. *Sedimentology*, v. 25, p. 843-860.
- Rodine, J. D. and Johnson, A. M. 1976. The ability of debris, heavily freighted with coarse clastic materials, to flow on gentle slopes. *Sedimentology*, v. 23, p. 213-234.
- Różkowska, M. 1980. On Upper Devonian habitats of rugose corals. *Acta Palaeontologica Polonica*, v. 25, p. 597-611.
- Ruhe, R. U., Cady, J. G. and Gomez, R. S. 1961. Paleosols of Bermuda. *Geological Society of America Bulletin*, v. 72, p. 1121-1142.
- Runnels, D. D. 1969. Diagenesis, chemical sediments, and the mixing of natural waters. *Journal of Sedimentary Petrology*, v. 39, p. 1188-1201.
- Scholle, P. A. and Halley, R. B. 1985. Burial diagenesis: out of sight out of mind! *In*: Schneiderman, N. and Harris, P. M. (Eds.), *Carbonate Cements*. Society of Economic Paleontologists and Mineralogists, Special Publication 36, p. 309-334.
- Schroeder, J. H. 1972. Fabrics and sequences of submarine carbonate cements in Holocene Bermuda cup reefs. *Geologisches Rundschau*, v. 61, p. 708-730.
- Scotese, C. R., Van der Voo, R. and Barrett, S. F. 1985. Silurian and Devonian base maps. *Philosophical Transactions of the Royal Society of London*, v. 309, p. 57-77.
- Shinn, E. A. 1969. Submarine lithification of Holocene carbonate sediments in the Persian Gulf. *Sedimentology*, v. 12, p. 109-144.
- Smith, S. 1945. Upper Devonian corals of the Mackenzie River region, Canada. *Geological Society of America, Special Paper* 59.